



Search for new phenomena with top-quark pairs and large missing transverse momentum using 140 fb^{-1} of pp collision data at $\sqrt{s} = 13 \text{ TeV}$ with the ATLAS detector

The ATLAS Collaboration

A search is conducted for new phenomena in events with a top quark pair and large missing transverse momentum, where the top quark pair is reconstructed in final states with one isolated electron or muon and multiple jets. The search is performed using the Large Hadron Collider proton–proton collision data sample at a centre-of-mass energy of $\sqrt{s} = 13 \text{ TeV}$ recorded by the ATLAS detector that corresponds to an integrated luminosity of 140 fb^{-1} . An analysis based on neural network classifiers is optimised to search for directly produced pairs of supersymmetric partners of the top quark (stop), and to search for spin-0 mediators, produced in association with a pair of top quarks, that decay into dark-matter particles. In the stop search, the analysis is designed to target models in which the mass difference between the stop and the neutralino from the stop decay is close to the top quark mass. This new search is combined with previously published searches in final states with different lepton multiplicities. No significant excess above the Standard Model background is observed, and limits at 95% confidence level are set. Models with neutralinos with masses up to 570 GeV are excluded, while for small neutralino masses models are excluded for stop masses up to 1230 GeV. Scalar (pseudoscalar) dark matter mediator masses as large as 350 (370) GeV are excluded when the coupling strengths of the mediator to Standard Model and dark-matter particles are both set to one. At lower mediator masses, models with production cross-sections as small as 0.15 (0.16) times the nominal predictions are excluded. Results of this search are also used to set constraints on effective four-fermion contact interactions between top quarks and neutrinos.

1 Introduction

The top quark, as the heaviest particle in the Standard Model (SM), is a key probe in the search for new particles predicted by several extensions of the SM. Prominent examples of such extensions are Supersymmetry (SUSY) [1–7] and models with Dark Matter (DM) particles that interact with top quarks via a spin-0 mediator [8, 9]. In proton–proton (pp) collisions at the Large Hadron Collider (LHC), both scenarios would produce final states with a pair of top quarks and missing transverse momentum (E_T^{miss}) from undetected new particles ($t\bar{t} + E_T^{\text{miss}}$), the signature investigated in this paper. The $t\bar{t}$ pair is selected in final states with exactly one isolated charged lepton (electron or muon,¹ henceforth referred to as ‘lepton’ or ‘ ℓ ’) from the decay of an on-shell W boson, and jets. Significant missing transverse momentum (\vec{p}_T^{miss} , with magnitude E_T^{miss}), is also required.

Since the discovery of the Higgs boson at the LHC [10, 11], SUSY has been searched for with particular interest as it may offer a solution to the hierarchy problem [12–15]. SUSY extends the SM by introducing a supersymmetric partner (sparticle) for each SM particle. The particle and sparticle quantum numbers are identical apart from a half-unit difference in spin. The underlying supersymmetry is broken, so particle and sparticle masses differ. In this theory, the hierarchy problem may be solved by the presence of a light supersymmetric partner of the top quark, referred to as the top squark or ‘stop’, which largely cancels the divergent loop corrections to the Higgs boson mass [16–23]. The superpartners of the left- and right-handed top quarks mix to form the mass eigenstates \tilde{t}_1 and \tilde{t}_2 , where \tilde{t}_1 is defined as the lighter of the two. A generic R -parity-conserving² minimal SUSY extension of the SM (MSSM) [7, 16, 24–26] predicts pair production of SUSY particles and the existence of a stable lightest SUSY particle (LSP). In the MSSM models considered in this search the LSP is assumed to be the lightest mass eigenstate of the superpartners of the Higgs boson and neutral electroweak gauge bosons. This LSP, also referred to as the lightest neutralino or $\tilde{\chi}_1^0$, may be a DM candidate as it is stable and only interacts weakly with SM particles [27, 28]. This paper presents a search for direct pair production of \tilde{t}_1 particles ($\tilde{t}_1\tilde{t}_1$)³ in events with significant E_T^{miss} from the two weakly interacting LSPs that escape detection and the decay products of two on- or off-shell top quarks. The search for a spin-0 mediator produced in association with top quarks that decays into a pair of DM particles ($t\bar{t}+\text{DM}$) is motivated by SM extensions that respect the principle of minimal flavour violation, which results in the interaction strength between the spin-0 mediator and the SM quarks being proportional to the quark masses via Yukawa-like couplings [29].

Previous searches for direct \tilde{t}_1 pair production and for spin-0 mediators produced in association with top quarks and decaying into DM particles were reported by the ATLAS [30–33] and CMS [34–37] Collaborations using the full LHC Run 2 pp recorded data sample. This paper presents a new search in final states with exactly one lepton, which were already analysed by the ATLAS Collaboration [31] using the same data sample. Compared with Ref. [31], this analysis employs improved object reconstruction and identification algorithms, improved background simulations, and new neural-network-based classifiers for the reconstruction of the hadronically decaying top quark and for event discrimination. In the $\tilde{t}_1\tilde{t}_1$ search, this analysis focuses on improving the sensitivity in the challenging scenario where the mass difference between the stop and the lightest neutralino is close to the top quark mass. The results are statistically combined with those from an independent analysis of the $t\bar{t} + E_T^{\text{miss}}$ final state with no leptons [30] to provide improved sensitivity for scenarios with a heavy stop and a very light neutralino. In the $t\bar{t}+\text{DM}$ search, this

¹ Electrons and muons from τ -lepton decays are included.

² A multiplicative quantum number, referred to as R -parity, is introduced to conserve baryon and lepton numbers, where R -parity is $1(-1)$ for all SM (SUSY) particles.

³ When denoting pair production of a stop and an anti-stop, the charge-conjugation notation is omitted for notational simplicity.

analysis is designed to improve the sensitivity across the full range of mediator masses considered and is statistically combined with independent analyses in $t\bar{t} + E_T^{\text{miss}}$ final states with zero and two leptons. The data analysed in this search are also used to test for the presence of new interactions between top quarks and neutrinos that can be described by a four-fermion contact interaction (CI) in an Effective Field Theory (EFT) approach.

2 Signal models and search strategy

Leading-order diagrams of the signal processes targeted in this search are shown in Figure 1.

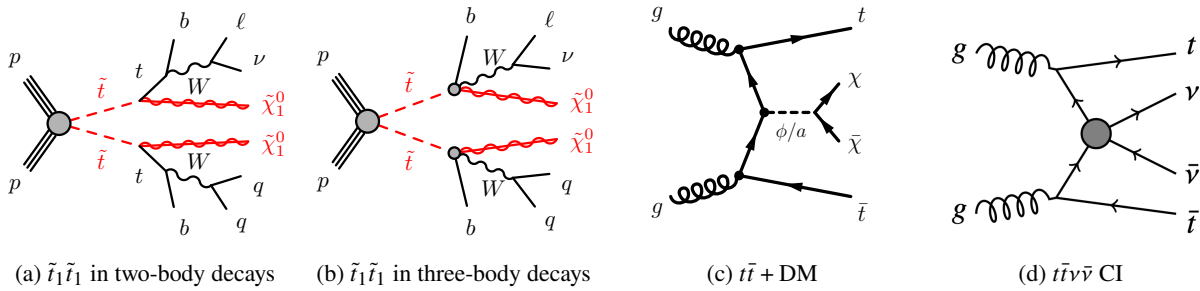


Figure 1: Diagrams illustrating direct \tilde{t}_1 pair production with (a) two-body ($\tilde{t}_1 \rightarrow t\tilde{\chi}_1^0$) or (b) three-body ($\tilde{t}_1 \rightarrow bW\tilde{\chi}_1^0$) decays, (c) the production of DM fermions (χ) in association with a pair of top quarks via a [pseudo] scalar mediator ϕ [a] and (d) the production of a $t\bar{t}\nu\bar{\nu}$ final state via an effective four-fermion contact interaction. In the SUSY diagrams, the charge-conjugate symbols are omitted for simplicity.

The $\tilde{t}_1\bar{\tilde{t}}_1$ production is considered in a simplified SUSY model [38, 39] where the only light sparticles are \tilde{t}_1 and $\tilde{\chi}_1^0$. Each stop can decay promptly either via the two-body process $\tilde{t}_1 \rightarrow t\tilde{\chi}_1^0$, which produces an on-shell top quark, or via a three-body decay $\tilde{t}_1 \rightarrow bW\tilde{\chi}_1^0$ with an intermediate off-shell top quark. These are assumed to be the only possible stop decays. The \tilde{t}_1 is modelled to decay only in the two-body mode when $\Delta m(\tilde{t}_1, \tilde{\chi}_1^0) = m(\tilde{t}_1) - m(\tilde{\chi}_1^0) > m(t)$, and only in the three-body mode when $m(W) < \Delta m(\tilde{t}_1, \tilde{\chi}_1^0) < m(t)$. Decays at smaller $\Delta m(\tilde{t}_1, \tilde{\chi}_1^0)$ values, where both the top quark and the W boson are off-shell were explored in Ref. [31]. In this search, the $\tilde{t}_1\bar{\tilde{t}}_1$ production is tested with a two-dimensional scan of the parameter space $(m(\tilde{t}_1), m(\tilde{\chi}_1^0))$.

The simplified benchmark model for the $t\bar{t}$ +DM production [29, 40] assumes the existence of a (pseudo) scalar mediator ϕ (a), which can be produced in association with two top quarks and decay into a pair of SM-singlet DM particles (χ). The interactions of the mediator with SM particles are Yukawa-like. This model has four parameters: the mass of the mediator $m(\phi/a)$, the mass of the DM particle $m(\chi)$, the strength of the DM–mediator interaction g_χ , and a universal scaling factor of the interactions of the mediator with SM fermions g_q . To reduce the number of free parameters, g_χ and g_q are assumed to have the same value, $g = g_\chi = g_q$. The results are presented as one dimensional scans of either $m(\phi/a)$ or $m(\chi)$. The $t\bar{t} + E_T^{\text{miss}}$ final state is mainly sensitive to the mediator mass range $m(\phi/a) < 2m(t)$, where the $\phi/a \rightarrow t\bar{t}$ decay is kinematically forbidden.

Going beyond simplified models, the search for new phenomena in $t\bar{t} + E_T^{\text{miss}}$ final states is generalised by searching for an effective $t\bar{t}\nu\bar{\nu}$ four-fermion CI. Following the model developed in Refs. [41–44], the CI is implemented via four-fermion operators acting on SM fields within the SMEFT theoretical

framework [45–49]. When considering SM left-handed neutrinos, out of the possible scalar, vector and tensor operators, only vector operators can be implemented at dimension six. The resulting effective Lagrangian is composed of two terms:

$$\mathcal{L}_{t\bar{t}\nu\bar{\nu}} = \frac{1}{\Lambda^2} \left[V_{LL}(\bar{\nu}\gamma_\mu P_L\nu)(\bar{t}\gamma^\mu P_L t) + V_{LR}(\bar{\nu}\gamma_\mu P_L\nu)(\bar{t}\gamma^\mu P_R t) \right] ,$$

where Λ is the energy scale of new physics, $P_{L,R} = (1 \mp \gamma_5)/2$ and V_{LL} and V_{LR} are the dimensionless Wilson coefficients of the vector four-fermion interactions with left-handed and right-handed top quarks, respectively. Operators of higher dimension, including tensor or scalar operators, are neglected⁴. Results are presented by considering either the LL or LR operators separately. The interference between the CI and the SM $t\bar{t}Z(\rightarrow \nu\bar{\nu})$ process is tested by considering the impact of both constructive and destructive interference hypotheses.

The search strategy is designed to retain sensitivity to a wide region of the signal parameter space by partitioning the $t\bar{t} + E_T^{\text{miss}}$ final state into orthogonal event categories and by using neutral networks (NNs) to classify events. Event categories are designed to target a specific final state, rather than a signal parameter region. They differ in the multiplicity of jets with b -hadrons and in the presence or absence of jets produced by hadronic decays of high- p_T top quarks. Events from signals in different regions of the parameter space populate these categories at different rates. For instance, events with a pair of top squarks with high mass are predominantly accepted in categories with high- p_T top quarks. Moreover, events accepted in the same category from different signal models feature similar kinematic properties. Background processes also populate event categories at different rates, leading to a varying background composition across categories. These features are exploited by employing several NNs to discriminate between signal and background events.

A key strategy implemented in this analysis is to avoid training different discriminators for different regions of the signal parameter space. This simplifies the fit, the validation of the background modelling and future reinterpretations of these data using new signal models while retaining good sensitivity for the parameter regions studied. In each event category, one dedicated NN is trained with $\tilde{t}_1\tilde{t}_1$ or $t\bar{t}$ +DM signal events from the full parameter space accepted in that category. The corresponding NN output distributions in each category are used as input to template fits across the full model parameter space.

The most important background processes for this search are top-quark pair production ($t\bar{t}$), the associated production of a top quark and a W boson (tW), W +jets production and the production of a Z boson in association with a pair of top quarks and decaying into neutrinos ($t\bar{t}Z(\rightarrow \nu\bar{\nu})$). Except for the irreducible $t\bar{t}Z$ background, which has a small production cross-section and cannot be easily discriminated from signal, all other major backgrounds are determined in situ in each event category using events classified at low NN output values. The resulting background model is then validated with events classified using an intermediate range in NN output values where no significant potential signal contribution is expected. Each event category is therefore split into three regions via orthogonal selections on the NN output value: a Control Region (CR) at low values, a Validation Region (VR) at intermediate values, and a Signal Region (SR) at high values. A combined binned fit to the data in all CRs and SRs is then used to assess the presence of signal events. In this fit, the distributions of the observed data and of the expected backgrounds remain the same, while the signal templates change according to the point of the parameter space under test. Separate NNs are used in the search for top squarks and in the search for DM particles.

⁴ In this EFT approach with only SM fields, the couplings of the operators to left-handed neutrinos and to left-handed charged leptons are the same, so results of this search can be combined with results from searches for $t\bar{t}\ell\bar{\ell}$ CIs. If right-handed neutrinos were to be included, scalar and tensor operators could have been implemented at dimension six. These additional operators could be sensitive to new physics not coupled to SM fields.

3 ATLAS detector and data collection

The ATLAS experiment [50] at the LHC uses a multipurpose particle detector with a forward–backward–symmetric cylindrical geometry and a near 4π coverage in solid angle.⁵ The detector consists of an inner tracking detector (ID) surrounded by a thin superconducting solenoid that provides a 2 T axial magnetic field, electromagnetic (EM) and hadron calorimeters, and a muon spectrometer (MS). The ID covers the pseudorapidity range $|\eta| < 2.5$. The high-granularity silicon pixel detector covers the vertex region and typically provides four measurements (hits) per track, the first hit normally being in the insertable B-layer (IBL) that was installed before Run 2 [51, 52]. It is surrounded by a silicon microstrip detector and a straw tube transition-radiation tracking detector. Lead/liquid-argon (LAr) sampling calorimeters provide EM energy measurements with high granularity. A steel/scintillator-tile hadron calorimeter covers the central pseudorapidity range ($|\eta| < 1.7$). The endcap and forward regions are instrumented with LAr calorimeters for both EM and hadronic energy measurements up to $|\eta| = 4.9$. The MS surrounds the calorimeters and is based on three large superconducting air-core toroidal magnets with eight coils each. The field integral of the toroids ranges between 2.0 and 6.0 Tm across most of the detector. The MS includes a system of precision tracking chambers and fast detectors for triggering. A two-level trigger system is used to select events [53]. The first-level trigger is implemented in hardware and uses a subset of the detector information to accept events at a rate up to 100 kHz. This is followed by a software-based trigger that reduces the accepted event rate to 1 kHz on average, depending on the data-taking conditions. An extensive software suite [54] is used in data simulation, in the reconstruction and analysis of real and simulated data, in detector operations, and in the trigger and data acquisition systems of the experiment.

The analysis uses the full Run 2 pp data sample delivered by the LHC at $\sqrt{s} = 13$ TeV in the period between 2015 and 2018. After the application of data-quality requirements [55], the total integrated luminosity is $(140.1 \pm 1.2) \text{ fb}^{-1}$. The luminosity is measured with an accuracy of 0.83% [56] using the LUCID-2 detector [57], complemented by measurements using the inner detector and calorimeters. All analysed events were recorded by triggers that accepted events with large $E_{\text{T}}^{\text{miss}}$ [58] or with an electron [59] or muon [60]. The primary vertex in these events, defined as the reconstructed vertex with the highest $\sum_{\text{tracks}} p_{\text{T}}^2$, must have at least two associated tracks with $p_{\text{T}} > 500$ MeV.

4 Simulated events

Samples of Monte Carlo (MC) simulated events are used for the description of SM processes and for the hypothesized signals. Details of the simulation samples used, including the matrix element (ME) event generator, its accuracy in the strong coupling constant (QCD accuracy), the parton distribution function (PDF) set used, the parton shower (PS) and hadronisation model, and the accuracy of the cross-section calculation, are summarised in Table 1.

The samples produced with the MADGRAPH5_AMC@NLO [61] and POWHEG BOX [87–90] generators used the EVTGEN [98] software to model b -hadron decays. In these samples, the PYTHIA [91] library was used for the parton shower and hadronisation with the A14 tune [99] and the NNPDF2.3LO set of PDFs [100].

⁵ ATLAS uses a right-handed coordinate system with its origin at the nominal interaction point (IP) in the centre of the detector and the z -axis along the beam pipe. The x -axis points from the IP to the centre of the LHC ring, and the y -axis points upwards. Cylindrical coordinates (r, ϕ) are used in the transverse plane, ϕ being the azimuthal angle around the z -axis. The pseudorapidity is defined in terms of the polar angle θ as $\eta = -\ln \tan(\theta/2)$. Angular distance is measured in units of $\Delta R \equiv \sqrt{(\Delta\eta)^2 + (\Delta\phi)^2}$.

Table 1: Overview of the configurations used to simulate signal and background processes.

Process	ME event generator	ME QCD accuracy	ME PDF	Parton shower and hadronisation	Cross-section calculation
SUSY signals	MADGRAPH 2.8.1, 2.9.9 [61]	0,1,2j@LO	NNPDF2.3LO	PYTHIA 8.240, 8.307	NNLO+NNLL [62–66]
DM signals	MADGRAPH 2.7.3	0,1j@LO	NNPDF2.3LO	PYTHIA 8.244	NLO [67, 68]
CI signals	MADGRAPH 2.9.9	0,1j@LO	NNPDF2.3LO	PYTHIA 8.307	
$t\bar{t}$	SHERPA 2.2.12 [69]	0,1j@NLO +2,3,4j@LO [83–86]	NNPDF3.0NNLO [70]	SHERPA [71–75]	NNLO+NNLL [76–82]
Single-top					
tW	POWHEG BOX v2 [87–90]	NLO	NNPDF3.0NLO	PYTHIA 8.307 [91]	NLO+NNLL [92, 93]
s- and t-channel	POWHEG BOX v2	NLO	NNPDF3.0NLO	PYTHIA 8.230	NLO [94, 95]
V+jets ($V = Z, W$)	SHERPA 2.2.11	0,1,2j@NLO +3,4,5j@LO	NNPDF3.0NNLO	SHERPA	NNLO [96]
$t\bar{t}V$	MADGRAPH5_AMC@NLO 2.3.3 [61]	NLO	NNPDF3.0NLO	PYTHIA 8.210	NLO QCD+EW [97]
VV'	SHERPA 2.2.1, 2.2.2	0,1j@NLO+2,3j@LO	NNPDF3.0NNLO	SHERPA	

In all samples, the effect of multiple interactions in the same and neighbouring bunch crossings (pile-up) was modelled by overlaying the simulated hard-scattering event with inelastic pp collisions generated with PYTHIA 8.186 [101] using the NNPDF2.3LO set of PDFs and the A3 set of tuned parameters [102]. All samples were processed using the full simulation of the ATLAS detector [103] based on the GEANT4 [104] software.

The $\tilde{t}_1\tilde{t}_1$ production was simulated with the MADGRAPH [61] package at leading order (LO) with up to two additional partons. The simplified SUSY model used was the same as in Ref. [31]. Stop decays were simulated with the MADSPIN [105] software, which emulates kinematic distributions without calculating the full ME. The $\tilde{t}_1\tilde{t}_1$ production cross-sections were calculated to approximate next-to-next-to-leading order in QCD, adding the resummation of soft gluon emission at next-to-next-to-leading-logarithm accuracy (approximate NNLO+NNLL) [62–66]. The nominal cross-section and its uncertainty were derived using the PDF4LHC15_mc PDF set, following the recommendations of Ref. [106].

The $t\bar{t}$ +DM production was simulated with $g = g_\chi = g_q = 1$ using MADGRAPH at LO with up to one additional parton and with MADSPIN for the decay of top quarks. The kinematics of the mediator decay were found to not depend strongly on the values of the couplings; however, the particle kinematic distributions are sensitive to the scalar or pseudoscalar nature of the mediator and to the mediator and DM particle masses. The cross-sections were computed at next-to-leading order (NLO) in QCD [67, 68].

The $t\bar{t}v\bar{\nu}$ CIs with either LL and LR operators were simulated with two samples, one for the pure contribution from new physics ('NP') and one for the interference with the SM ('Int'), so that the total contribution is estimated as

$$\sigma_{t\bar{t}v\bar{\nu}} = \frac{V_{ij}}{\Lambda^2} \sigma_{\text{Int}} + \frac{V_{ij}^2}{\Lambda^4} \sigma_{\text{NP}} ,$$

where the sign of V_{ij} determines whether the interference is constructive or destructive. These samples were simulated with MADGRAPH at LO with up to one additional parton using the model provided by the authors of Ref. [41]. In simulation the model parameters were set to $\Lambda = 1$ TeV and $V_{ij} = 1$. These values scale the predicted cross-section, but not the kinematics of the simulated events. The LL and LR operators were simulated separately. Assuming $\Lambda = 1$ TeV, $V_{ij} = \pm 4\pi$ and considering all three generations of neutrinos, the cross-sections of the NP and interference contributions for the LL (LR) operator were computed to be 384 fb (365 fb) and ± 17 fb (∓ 6.4 fb), respectively.

The $t\bar{t}$ and W +jets processes were simulated with the SHERPA 2.2.12 and SHERPA 2.2.11 [69] generators, respectively. The simulation of $t\bar{t}$ production used NLO MEs with up to one additional parton, and LO MEs with up to four additional partons calculated using the Comix [83] and OPENLOOPS [84–86] libraries. Similarly, the W +jets production used NLO MEs with up to two additional partons, and LO MEs with up to five additional partons. Approximate NLO EW corrections were included through event weights using the electroweak virtual approximation and the additive prescription. These simulations were interfaced to the SHERPA parton shower [71] using the MEPS@NLO prescription [72–75] with the set of tuned parameters developed by the SHERPA authors. The tW production was modelled by the POWHEG Box v2 [87–90] generator at NLO in QCD using the five-flavour scheme. The diagram removal scheme [107] was used to remove interference and overlap with $t\bar{t}$ production. The uncertainty related to this scheme was estimated by comparison with an alternative sample generated using the diagram subtraction scheme [107, 108]. The production of a gauge boson with a top quark pair ($t\bar{t}W$ and $t\bar{t}Z$) was modelled using the MADGRAPH5_AMC@NLO 2.3.3 [61] generator at NLO. Other sources of background events that are considered in this search are diboson production (VV' , where $V = W, Z$), Higgs boson production in association with a top quark pair, tZ and tWZ production, and the production of three and four top quarks.

Further details of the simulation are provided in Table 1. A major difference from the simulations used in Ref. [31] is the use of SHERPA instead of POWHEG Box v2 for $t\bar{t}$ production, which provides improved modelling of events in the high transverse momentum region relevant for this search. Another difference is the use of dynamic rather than fixed scales in the MEs used for the simulation of the tW production.

5 Event reconstruction

The event categorisation and discrimination is based on reconstructed objects: leptons, jets (including those containing b -hadrons) and E_T^{miss} . Depending on object quality and kinematic requirements, reconstructed electrons and muons are labelled as either *baseline* or *signal*, where the latter is a subset of the former that passes tighter selection criteria. Baseline leptons are used to classifying overlapping objects, to compute the missing transverse momentum, and for background rejection. Signal leptons are used to select events and construct discriminating variables. Hadronically decaying top quarks are reconstructed using dedicated algorithms.

Electron candidates are reconstructed from an isolated electromagnetic calorimeter energy deposit matched to a track in the ID [109]. The pseudorapidity of the calorimeter energy cluster must satisfy $|\eta_{\text{cluster}}| < 2.47$. Baseline electrons are required to have $p_T > 4.5$ GeV and to satisfy loose likelihood identification criteria. Furthermore, their longitudinal impact parameter (z_0), defined as the distance along the beam direction between the primary vertex and the point of closest approach of the track to the beam axis, must satisfy $|z_0 \sin \theta| < 0.5$ mm, where θ is the polar angle of the track. Signal electrons must satisfy, in addition to the baseline requirements, $p_T > 20$ GeV and $|d_0|/\sigma_{d_0} < 5$, where d_0 is the transverse impact parameter with uncertainty σ_{d_0} . Signal electrons are also required to be isolated and satisfy tighter identification criteria. The isolation is defined as the sum of the transverse energy or momentum reconstructed in a cone of size $\Delta R = \sqrt{(\Delta\eta)^2 + (\Delta\phi)^2}$ around the electron, excluding the energy of the electron itself. The isolation criteria depend on the electron p_T .

Muon candidates are reconstructed either by combining tracks in the ID with tracks in the MS or as stand-alone MS tracks [110, 111], and are required to have $|\eta| < 2.7$. Baseline muons are required to have $p_T > 4$ GeV, $|z_0 \sin \theta| < 0.5$ mm, and to satisfy the ‘Medium’ identification criterion. In addition to all

baseline requirements, signal muons must have $p_T > 20$ GeV and $|d_0|/\sigma_{d_0} < 3$. Signal muons must also be isolated, based on criteria similar to those used for electrons.

Particle-flow (PFlow) jets in the region $|\eta| < 4.5$ are reconstructed using the anti- k_t algorithm [112] with a radius parameter $R = 0.4$ [113], using neutral PFlow constituents and charged constituents associated with the primary vertex as input [114]. They are referred to hereafter as ‘small- R jets’. These jets are calibrated to the particle level by applying a jet energy scale derived from simulation with in situ corrections based on data [115]. Jets with $p_T > 20$ GeV are selected. A cleaning procedure is used to identify and remove jets arising from calorimeter noise or non-collision backgrounds. To suppress pile-up jets with $|\eta| < 2.4$, a discriminant called the ‘jet vertex tagger’ (JVT) is constructed using a likelihood method [116]. A similar discriminant, the ‘forward JVT’ (fJVT), is used for jets with $|\eta| > 2.5$ [117]. PFlow jets with $|\eta| < 2.5$ identified as containing b -hadrons are referred to as b -tagged jets. This identification is based on the DL1r b -tagging algorithm [118, 119] with a working point that corresponds to a b -tagging efficiency of 77% as measured in a sample of simulated $t\bar{t}$ events. The corresponding rejection factors are approximately 200 and 6 for light-quark or gluon jets and c -jets, respectively.

To reconstruct high- p_T hadronic top quark decays, ‘large- R jets’ are used [120]. These jets are reconstructed using the anti- k_t algorithm with $R = 1.0$, taking as input topological clusters of calorimeter cells calibrated to the hadronic scale [121]. These jets are trimmed [122] to remove energy deposits from pile-up and the underlying event. The energy and mass of the large- R jets are calibrated using data [123, 124]. Large- R jets with $|\eta| < 2$ are selected if they have a transverse momentum in the range [600, 2500] GeV and a mass in the range [40, 600] GeV. Large- R jets with $p_T < 600$ GeV are not considered, since low- p_T hadronic top quark decays are reconstructed from small- R jets, as described in Section 5.1. A multivariate classifier is used to identify the large- R jets from hadronic top decays using a working point with a top-tagging efficiency of 80% [125, 126]. This classifier uses jet substructure observables as input. To improve the identification of hadronic top decays, jets containing b -hadrons are reconstructed inside the large- R jet using a track-based jet reconstruction with a variable cone size [127] and are tagged with the DL1r b -tagging algorithm.

Hadronically decaying τ -leptons are reconstructed and used to veto background. The reconstruction of jets from these τ decays ($\tau_{\text{had-vis}}$) [128, 129] is seeded from jets reconstructed from topological clusters using the anti- k_t algorithm with $R = 0.4$. Tracks that originate from the primary vertex and satisfy requirements on the impact parameter and on a multivariate discriminant are associated with the $\tau_{\text{had-vis}}$ if they lie within a cone of angle $\Delta R < 0.2$ around the jet axis. Reconstructed $\tau_{\text{had-vis}}$ candidates must have one or three associated tracks with a total charge equal to ± 1 . They must satisfy $p_T > 20$ GeV and be reconstructed in the pseudorapidity ranges $|\eta| < 1.37$ or $1.52 < |\eta| < 2.5$. Furthermore, reconstructed $\tau_{\text{had-vis}}$ need to satisfy loose identification criteria aimed at rejecting jets that originate from quarks, gluons or electrons.

The missing transverse momentum \vec{p}_T^{miss} [130] is reconstructed as the negative vector sum of the \vec{p}_T of all selected electrons, muons and small- R jets. An extra track-based ‘soft term’ is built using additional tracks associated with the primary vertex, but not with any reconstructed object, to improve the performance of the \vec{p}_T^{miss} reconstruction at high pile-up. An object-based missing transverse momentum significance [131] is used to identify events in which the reconstructed \vec{p}_T^{miss} comes from undetected or weakly interacting particles rather than from detected particles with mis-measured energies.

Correction factors are applied to reconstructed objects to take account of differences in energy scale and resolution and in trigger, reconstruction, identification and isolation efficiencies between data and simulation. Ambiguities among selected objects are resolved via an overlap removal procedure similar to the one used in Ref. [31]. Given a set of baseline objects, the procedure checks for overlaps based on

shared tracks, ghost-matching [132], or a minimum distance ΔR_y between pairs of objects.⁶ Small- R jets with $\Delta R < 1.1$ from a large- R jet are discarded and no overlap removal is performed between leptons and large- R jets.

5.1 Resolved hadronic top decays

Jets in signal events can arise from top quark decays, additional radiation, pile-up and the underlying event. A NN-based algorithm, hereafter referred to as the ‘top-NN’, is used to identify sets of small- R jets associated with the hadronic decay of a top quark. This algorithm targets resolved decays, in which the jets from the top-quark decay are spatially separated and can be reconstructed as individual small- R jets. The target p_T range is below the 600 GeV threshold used for the large- R -jet reconstruction of hadronically decaying top candidates. The momentum reconstructed using the top-NN algorithm is used in the event classification.

The top-NN evaluates all two- and three-jet combinations in an event. While a fully reconstructed resolved decay would result in three jets, jet pairs are also considered to allow for cases in which one jet is outside acceptance or where the two jets from a high- p_T W boson are reconstructed as a single small- R jet. The two- and three-jet combinations are formed from a set of jets that includes up to two b -tagged jets and up to four not- b -tagged jets (referred to as ‘light jets’ hereafter) in the event. Each candidate jet combination must contain exactly one b -tagged jet. To facilitate the use of jet four-momentum components in the top-NN and remove spurious degrees of freedom a set of transformations is used. These transformations include a Lorentz boost into the rest frame of the jet combination and a rotation such that the b -tagged jet is aligned along the z -axis and the leading- p_T light jet lies in the xz -plane with a positive p_x component. After these transformations, six non-trivial jet momentum components together with the p_T of the original jet combination are used as NN inputs. The top-NN is a binary feed-forward NN trained with KERAS [133] with the Tensorflow backend. It is trained using SUSY signal events drawn from all simulated points of the parameter space in order to include a large range of top quark p_T . Jet combinations that are kinematically matched to the partons from the top-quark decay are labelled signal and all other combinatorics of jets are labelled background. In the training, weights are assigned so that both signal and background candidates are uniformly distributed in p_T . In each event the top-NN assigns an output value to all combinations of selected jets.

The combination with the highest top-NN output value in each event is chosen as the hadronic top quark candidate. According to simulation, the top-NN reaches the highest efficiency in finding the correct jet combination for top quark p_T between 200 and 600 GeV. In this p_T range, the top-NN identifies the right daughter jets in about 70% of the events in which a correctly tagged b -tagged jet and at least one light jet are kinematically matched to the hadronically decaying top quark. Above this range the performance worsens, as the decay products are less likely to be reconstructed as individual small- R jets. These high p_T decays are better reconstructed using large- R jets. Therefore the top-NN is used to reconstruct the hadronic top candidate only in events that have no large- R jet with $p_T > 600$ GeV. Events selected by the top-NN are further required to have an output value above a minimum threshold to ensure the presence of a good hadronic top quark candidate.

⁶ Rapidity $y \equiv \frac{1}{2} \ln \frac{E+p_z}{E-p_z}$ is used instead of pseudorapidity (η) when computing the distance ΔR_y .

6 Event classification

Events are collected using both E_T^{miss} and single lepton triggers, and different thresholds on the reconstructed E_T^{miss} and signal lepton p_T are applied to select events in the kinematic range where these triggers reach high efficiency. Reconstructed events with $E_T^{\text{miss}} > 230$ GeV are required to have satisfied the E_T^{miss} trigger. Events with E_T^{miss} in the range $[70, 230]$ GeV are instead required to have satisfied a single lepton trigger. For these events, the signal electron (muon) associated with the lepton selected at trigger level must have $p_T > 27$ (27.5) GeV and $|\eta| < 2.47$ (2.4). All events are required to have exactly one or three signal leptons and no additional baseline lepton or $\tau_{\text{had-vis}}$ candidate. Events with three signal leptons are only used for the validation of the $t\bar{t}Z$ background.

Events that satisfy the selection are classified into mutually exclusive categories: high- E_T^{miss} events with $E_T^{\text{miss}} > 230$ GeV, and ‘boosted’ events with a large- R jet. If an event satisfies the criteria for both categories, it is assigned to the boosted category. These categories target events with top-quark decays at different transverse momenta. Events are further categorised according to the number of b -tagged jets and the presence of a top-tagged large- R jet. The requirements for these categories are summarised in Table 2. Events not accepted in any of these categories are not further considered.

Table 2: Summary of the selections for each event category together with the definitions of the hadronic and leptonic top quark candidates. Trigger, lepton and E_T^{miss} selections are described in the text. Large- R jets are referred to as ‘ lR ’ for brevity.

Analysis Category	High- E_T^{miss}		Boosted					
	1b	2b	1b-lep-0t	1b-had-0t	2b-0t	1b-lep-1t	1b-had-1t	2b-1t
$N(lR \text{ jet}, p_T > 600 \text{ GeV})$	0		≥ 1					
$N(\text{top-tagged } lR \text{ jet})$	-		0			≥ 1		
$N_{b\text{-jet with } \Delta R(b, lR \text{ jet}) < 1.1}$	-		0	≥ 1	≥ 1	0	≥ 1	≥ 1
$N_{b\text{-jet with } \Delta R(b, lR \text{ jet}) > 1.1}$	-		≥ 1	0	≥ 1	≥ 1	0	≥ 1
top-NN-tagged multiplet	✓		-					
$N_{b\text{-jet}}$	1	≥ 2	-					
$N_{\text{light-jet}}$	≥ 2	≥ 1	-					
top _{had} candidate	top-NN multiplet		lR jet					
top _{lep} candidate	$\ell + j$	$\ell + b$	$\ell + b$	$\ell(+j)$	$\ell + b$	$\ell + b$	$\ell(+j)$	$\ell + b$
Event NN selection	See Table 3							

High- E_T^{miss} events are placed in ‘1b’ or ‘2b’ categories according to the number of b -tagged jets. A minimum number of light jets is required so that a top-NN-tagged jet combination can be defined by at least two jets and an additional jet can be used for the reconstruction of the leptonically decaying top quark. In the 2b (1b) categories, the hadronic top quark candidate is formed by the combination of jets that give the highest top-NN output value, while the leptonic top quark candidate comprises the lepton and the b -tagged (light) leading- p_T jet that is not associated with the hadronic top quark candidate. In the 1b category, the leading- p_T jet is used to build the leptonic top quark candidate to retain a good kinematic description of the events in which the jet from the b -quark in the leptonic top-quark decay is not correctly tagged.

Boosted events must have at least one large- R jet. In events with more than one, only the leading- p_T large- R jet is considered for event selection and classification. These boosted events are first categorised according to whether the large- R jet is top-tagged (‘1t’) or not (‘0t’), and then according to the numbers of b -tagged jets inside and outside the large- R jet. The ‘2b’ events have at least one b -tagged jet inside the

large- R jet ($\Delta R(b, \text{large-}R \text{ jet}) < 1.1$) and at least one b -tagged jet outside. The ‘1b-had’ events have at least one b -tagged jet inside the large- R jet and none outside. Finally, the ‘1b-lep’ events have at least one b -tagged jet outside the large- R jet and none inside. This classification defines six orthogonal boosted categories. In these events, the hadronic top quark candidate is defined by the large- R jet momentum, while the leptonic top quark momentum is the vectorial sum of the momenta of the lepton and the leading- p_T b -tagged jet outside the large- R jet. In cases where this b -tagged jet is not present, the leading- p_T light jet, if present, is used.

Overall, eight orthogonal categories (two high- E_T^{miss} and six boosted) in different kinematic regimes and with different reconstructed objects are used to maximise the signal acceptance. In each high- E_T^{miss} category, two NN-based event classifiers, one for the $\tilde{t}_1\tilde{t}_1$ search (‘stop-NN’) and one for the $t\bar{t}$ +DM search (‘DM-NN’), are employed to discriminate signal from background events. In each boosted category, only a dedicated stop-NN is employed. This is because $t\bar{t}$ +DM signals in the mediator mass range targeted in this search are not expected to yield sizeable fractions of events in the boosted regions. Each NN is trained with all simulated events accepted in a given category, including background processes and signals from across the parameter space. For the stop-NNs, only signal events from two-body decays are used in the training. For the DM-NNs, signal events with both scalar and pseudoscalar mediators are used together. Each event is weighted by the predicted cross-section of the parent process. The distribution of the output value of either the stop-NN or the DM-NN in each category is used in a fit to the observed data to assess the presence of signal events across the parameter space. Events generated from different signal model parameters populate different event categories at different rates, but events accepted into a particular category have similar kinematic properties. For instance, $\tilde{t}_1\tilde{t}_1$ events with large $\Delta m(\tilde{t}_1, \tilde{\chi}_1^0)$ are accepted at similar rates in the boosted and high- E_T^{miss} categories, while events with small $\Delta m(\tilde{t}_1, \tilde{\chi}_1^0)$ are accepted almost exclusively in the high- E_T^{miss} categories. When compared with more complex approaches, in which NNs are trained for specific signal model parameters, this approach retains high classification power across the parameter space with the simplicity of having only one distribution per event category to fit.

The stop- and DM-NNs are binary feed-forward NNs. In each event category the sets of inputs are the same for the stop- and DM-NNs, but these sets differ across categories. A set of ‘low-level’ inputs is used by all NNs in all categories. It includes the momentum components of the hadronic and leptonic top quark candidates, the momentum components of \vec{p}_T^{miss} , and the momentum components of the lepton and of the b -tagged jets associated with the two top quark candidates.⁷ Transformations in the plane transverse to the beam direction are used to remove rotational symmetries and reduce the input dimensionality. Additional ‘high-level’ variables include the E_T^{miss} significance, the top-NN output value (only for the high- E_T^{miss} categories), and kinematic variables such as the transverse mass

$m_T(\vec{p}_T^\ell, \vec{p}_T^{\text{miss}}) = \sqrt{2|\vec{p}_T^\ell||\vec{p}_T^{\text{miss}}|(1 - \cos \Delta\phi(\vec{p}_T^\ell, \vec{p}_T^{\text{miss}}))}$ and the stransverse mass [134]:

$$m_{T2}(\vec{p}_T^1, \vec{p}_T^2, \vec{p}_T^{\text{miss}}) = \min_{\vec{q}_T^1 + \vec{q}_T^2 = \vec{p}_T^{\text{miss}}} \left\{ \max [m_T(\vec{p}_T^1, \vec{q}_T^1), m_T(\vec{p}_T^2, \vec{q}_T^2)] \right\} ,$$

where \vec{p}_T^i is the transverse momentum of a visible particle and \vec{q}_T^i is the transverse momentum of an undetected particle, assumed to be massless, which contributes to E_T^{miss} . The variants of m_{T2} used in this search are $m_{T2}(b, b, E_T^{\text{miss}})$ and $m_{T2, \text{min}}(b + \ell, b, E_T^{\text{miss}}) = \min [m_{T2}(b_1 + \ell, b_2, E_T^{\text{miss}}), m_{T2}(b_1, b_2 + \ell, E_T^{\text{miss}})]$, where b indicates the b -tagged (or light) jet associated with one of the two top quark candidates. The distributions of these variables are expected to have endpoints around $m(W)$ or $m(t)$ in $t\bar{t}$ events, while

⁷ In the high- E_T^{miss} 1b category, the momentum components of the light jet associated with the leptonic top candidate are used. In the boosted 1b-lep categories, the b -tagged jet associated with the hadronic top quark candidate is omitted.

reaching higher values in signal events with more undetected particles. The m_{T2} variables are not used as NN inputs in the boosted categories. In total, depending on the event category, the number of NN inputs varies from 19 to 26.

The classification power in each event category depends on the signal source. SUSY signals at large stop masses have the largest classification power, with output values close to unity, while signals with small $\Delta m(\tilde{t}_1, \tilde{\chi}_1^0)$ or from the three-body regime have lower classification power. Among DM signals, events with a pseudoscalar mediator have higher classification power than events with a scalar mediator for the same mediator mass. Moreover, when considering mediators with the same parity, signals with small $m(\phi/a)$ have a lower classification power than signals with large $m(\phi/a)$. To illustrate these features, Figure 2 shows the expected distributions of events as a function of the NN output value in the high- E_T^{miss} 2b category for SM background processes and for classes of signal models. The analysis retains sensitivity to all classes of signal events by performing a binned fit to the data distribution of the NN output value, as described in Section 7.

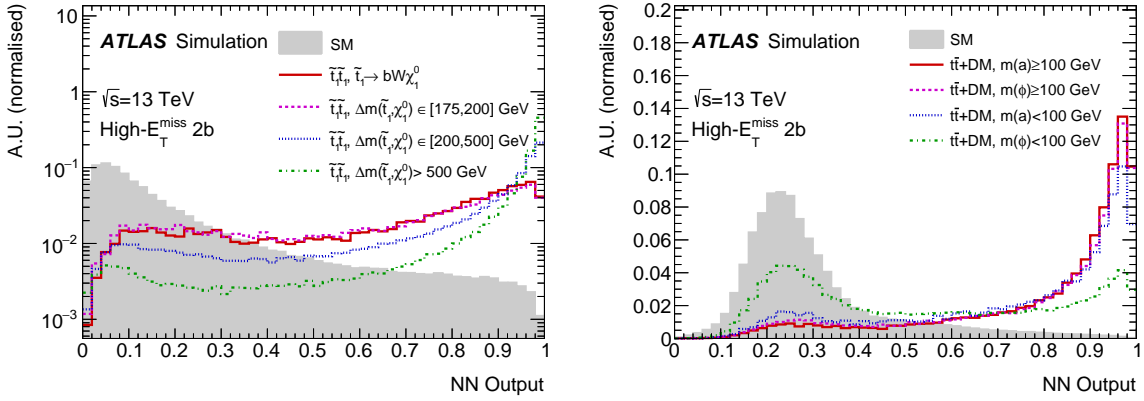


Figure 2: Expected distributions of events as a function of the output value of the stop-NN (left) and of the DM-NN (right) in the high- E_T^{miss} 2b category. The distribution of the SM background processes is compared with classes of signal models. In the left plot, $\tilde{t}_1\tilde{t}_1$ models are grouped according to $\Delta m(\tilde{t}_1, \tilde{\chi}_1^0)$ and the \tilde{t}_1 decay mode. In the right plot, $t\bar{t}+\text{DM}$ models with a scalar ϕ or pseudoscalar a mediator are shown for mediator masses larger or smaller than 100 GeV and $m(\chi) = 1$ GeV. Distributions are normalised to the same integral.

The stop-NN and DM-NN output values are used to split each event category into an SR, a CR and a VR. The SR contains events at high output values with the highest purity of signal events. The CR contains events at low output values with negligible contributions from potential signals. These CR events are used to improve the modelling of the background normalisations and templates in situ in each event category. The VR contains events in the intermediate range which are used to check the validity of the background model, derived at low output values, when applied to background events at higher values. For each SR, the lower threshold on the NN output value is set based on its binned distribution and on the maximum of the signal-to-background ratio ($s/b_{\text{bin}}^{\text{max}}$) expected in each bin for all signals not excluded by Ref. [31].⁸ As the $s/b_{\text{bin}}^{\text{max}}$ increases monotonically, the minimum threshold for the SR is chosen as the maximum output value below which all bins have $s/b_{\text{bin}}^{\text{max}} < 0.1$. The lower threshold for the VR is chosen in the same way with $s/b_{\text{bin}}^{\text{max}} < 0.05$. In case the resulting expected number of events in the VR is less than 40, this threshold is lowered in order to reach a number of events suitable to validate the background model. Events with

⁸ For the DM signals, given the previously excluded cross-sections, the expected $s/b_{\text{bin}}^{\text{max}}$ in each bin is evaluated assuming $g = 0.5$.

NN output values below the VR lower threshold are accepted into the CR. In some categories, a lower threshold is set for the CR, and events below that threshold are rejected and not used for further analysis. These rejected events have background compositions that are not representative of the background events in the SR and may contain multijet events, which are not simulated. With this approach, all CRs, VRs and SRs are orthogonal and span the full range of the NN output value above a minimum threshold. Table 3 reports a summary of these selections, together with the signal acceptance efficiencies in the SRs.

Table 3: Summary of the selections on the stop-NN and DM-NN output values that define CRs, VRs and SRs. Signal efficiencies, computed as the fraction of signal events in a given category with a NN output value in the range accepted in the SR, are also reported. The quoted range encompasses efficiencies estimated for all signals across the simulated parameter space. In boosted categories, only efficiencies for $\tilde{t}_1\tilde{t}_1$ signals with $\Delta m(\tilde{t}_1, \tilde{\chi}_1^0) > 500$ GeV are quoted.

Category	stop-NN				DM-NN			
	CR Range	VR Range	SR Range	Eff.	CR Range	VR Range	SR Range	Eff.
High- E_T^{miss} 1b	[0.2, 0.64)	[0.64, 0.79)	[0.79, 1.0]	0.4-0.9	[0.3, 0.69)	[0.69, 0.87)	[0.87, 1.0]	0.3-0.4
High- E_T^{miss} 2b	[0.1, 0.56)	[0.56, 0.70)	[0.70, 1.0]	0.5-0.9	[0.3, 0.60)	[0.60, 0.76)	[0.76, 1.0]	0.6-0.8
Boosted 1b-lep-1t	[0.0, 0.65)	[0.65, 0.80)	[0.80, 1.0]	0.5-0.9				
Boosted 1b-had-1t	[0.0, 0.65)	[0.65, 0.85)	[0.85, 1.0]	0.6-0.9				
Boosted 2b-1t	[0.0, 0.75)	[0.75, 0.95)	[0.95, 1.0]	0.6-0.8				
Boosted 1b-lep-0t	[0.0, 0.70)	[0.70, 0.85)	[0.85, 1.0]	0.6-0.8				
Boosted 1b-had-0t	[0.0, 0.75)	[0.75, 0.95)	[0.95, 1.0]	0.4-0.8				
Boosted 2b-0t	[0.0, 0.65)	[0.65, 0.80)	[0.80, 1.0]	0.6-0.9				

7 Background estimation and statistical model

The dominant sources of background events are processes that produce $t\bar{t}$, single-top (including tW) and W +jets. Despite its small cross-section, $t\bar{t}Z(\rightarrow \nu\bar{\nu})$ production constitutes another important background as it yields events with signal-like kinematic properties. All these backgrounds, along with other minor contributions, are estimated from simulation and corrected based on a fit to CRs in data. According to simulation, the fraction of background events in which the selected signal lepton is not a real prompt lepton from a W boson or τ lepton decay is small. This contribution is estimated from simulation with a conservative systematic uncertainty. Multijet events are expected to yield negligible contributions in all categories after the selection on the minimum NN output value and are therefore neglected in the background estimate.

Events from $t\bar{t}$ production are modelled via two classes: the semileptonic $t\bar{t}$ events with up to one prompt lepton ($t\bar{t}$ -1L) and the fully leptonic $t\bar{t}$ events with at least two prompt leptons ($t\bar{t}$ -2L). The $t\bar{t}$ -1L events have the same final state as the signal events, but a lower E_T^{miss} due to the presence of only one neutrino from W -boson decays. The $t\bar{t}$ -2L events, in which only one lepton is selected, have a similar level of E_T^{miss} to signal events, but differ in the properties of the hadronic top quark candidate, which is built from the additional jet activity in the event. Given the different kinematics and the higher sensitivity of the $t\bar{t}$ -2L events to the modelling of additional radiation, the $t\bar{t}$ -1L and the $t\bar{t}$ -2L backgrounds are estimated separately. Their prediction is based on the same simulation, but their in situ estimates are independent.

The predicted event yields from $t\bar{t}$, single-top and W +jets are corrected in situ by fitting the observed events in CRs. This correction is determined jointly with the fit to the observed events in SRs to test the presence of signal events. This fit uses a binned maximum-likelihood approach implemented in the

statistical analysis packages RooFIT [135], RooSTATS [136] and HistFitter [137]. The statistical model is composed of observed and expected binned distributions in CRs and SRs. In SRs, events are binned by the output values of either the stop-NNs or the DM-NNs, depending on the type of signal being tested. In CRs, events are binned by m_T multiplied by the lepton electric charge ($m_T \times q(\ell)$) as this variable allows the individual contributions of the $t\bar{t}$ -1L, $t\bar{t}$ -2L, and W +jets backgrounds to be determined simultaneously. The m_T variable is used because events with one leptonically decaying W boson (eg, $t\bar{t}$ -1L and W +jets events) are distributed differently from events with more (eg, $t\bar{t}$ -2L) as the former feature an endpoint around m_W , while the latter extend to higher values. The lepton charge is used to discriminate between $t\bar{t}$ -1L and W +jets events by exploiting the difference in the production cross-section for W^+ and W^- bosons. The contribution from single-top events is determined mainly in dedicated CRs. The boosted-2b-1t and boosted-2b-0t CRs are split with a selection on $m_{T2, \min}(b + \ell, b, E_T^{\text{miss}})$ at 300 GeV into ‘low- m_{T2} ’ and ‘high- m_{T2} ’ regions, with the high- m_{T2} region being enhanced in single-top events. Given the small number of events in the high- m_{T2} regions, only their total event yields are considered in the fit.

Overall, the statistical model used for the $\tilde{t}_1\tilde{t}_1$ search includes ten CRs and eight SRs, as summarised in Table 4. In the $t\bar{t}$ +DM search, only the high- E_T^{miss} SRs are considered since no sizeable signal yield is expected in the boosted SRs. However, the boosted categories are still used to improve the determination of the single-top background. Therefore the statistical model for the $t\bar{t}$ +DM includes the two high- E_T^{miss} SRs with their associated CRs and the eight boosted CRs used in the $\tilde{t}_1\tilde{t}_1$ search. In these fits, the normalisations of the $t\bar{t}$ -1L, $t\bar{t}$ -2L, single-top and W +jets contributions are scaled by independent unconstrained fit parameters (normalisation factors or ‘NFs’), as reported in Table 4. Via these NFs and the experimental and theoretical systematic uncertainties described in Section 8, the background predictions based on simulation are corrected in situ with the data in CRs and then used to estimate the background contributions in VRs and SRs. The samples of events in VRs are useful to validate the background predictions since they have background compositions similar to those in SRs and only small potential signal contributions. The observed and predicted distributions in CRs, VRs and SRs are shown in Section 9.

Table 4: Summary of the statistical model in terms of event categories, category subdivisions, observables used in the template fit and normalisation factors (‘NFs’) applied to background contributions in each region. ‘NN’ stands for the NN output value. The background process to which a NF applies is indicated by the name of the NF. All ten CRs and eight SRs are used in the fit for the $\tilde{t}_1\tilde{t}_1$ search. The SRs in the boosted categories are not used in the statistical model for the $t\bar{t}$ +DM search.

Category	Fitted observable		Normalisation Factors						
	CR	SR	NF _{top-1L} ^{High-met}	NF _{top-1L} ^{Boosted}	NF _{top-2L} ^{High-met}	NF _{top-2L} ^{Boosted}	NF _W ^{High-met}	NF _W ^{Boosted}	NF _{singletop}
High- E_T^{miss} 1b	$m_T \times q(\ell)$	NN	✓		✓		✓		✓
High- E_T^{miss} 2b	$m_T \times q(\ell)$	NN	✓		✓		✓		✓
Boosted 1b-lep-1t	$m_T \times q(\ell)$	NN		✓		✓		✓	✓
Boosted 1b-had-1t	$m_T \times q(\ell)$	NN		✓		✓		✓	✓
Boosted 2b-1t	$m_T \times q(\ell)$ (low- m_{T2})	NN		✓		✓		✓	✓
	Yield (high- m_{T2})			✓		✓		✓	✓
Boosted 1b-lep-0t	$m_T \times q(\ell)$	NN		✓		✓		✓	✓
Boosted 1b-had-0t	$m_T \times q(\ell)$	NN		✓		✓		✓	✓
Boosted 2b-0t	$m_T \times q(\ell)$ (low- m_{T2})	NN		✓		✓		✓	✓
	Yield (high- m_{T2})			✓		✓		✓	✓

The validation of the predictions for the irreducible $t\bar{t}Z(\rightarrow \nu\bar{\nu})$ background is done using events enhanced in $t\bar{t}Z(\rightarrow \ell\ell)$. These events are subject to the selection described in Section 6, except that exactly three signal leptons and no additional baseline lepton are required. From these three leptons, two are required to be of the same flavour and have opposite electric charges. The invariant mass of these two leptons is required to be compatible with the leptonic decay of a Z boson, $m_{\ell\ell} \in [81, 101]$ GeV. To select $t\bar{t}Z(\rightarrow \ell\ell)$ events

with kinematic properties similar to those of the $t\bar{t}Z(\rightarrow \nu\bar{\nu})$ events accepted in the SRs, the three-lepton events are categorised and classified as one-lepton events using a modified missing transverse momentum which incorporates the vectorial sum of the two leptons from the Z -boson decay.⁹ As shown in Figure 3, the observed distributions of events as a function of the stop-NN output value in the high- E_T^{miss} three-lepton regions are in good agreement with predictions. These theoretical predictions do not include data-driven corrections. Similar agreement is observed for the DM-NN output values. The three-lepton selection in the boosted regions is not used as it does not yield enough events to provide a useful validation.

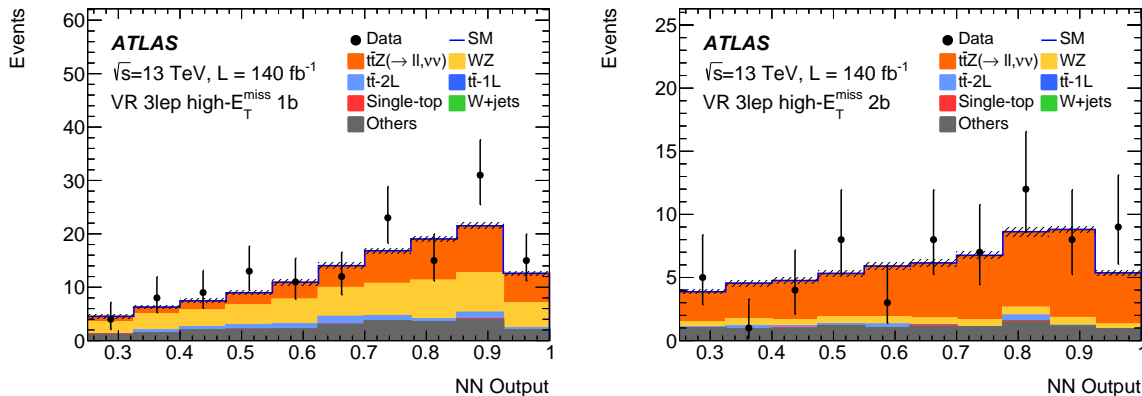


Figure 3: Observed and expected distributions of the stop-NN output values in the high- E_T^{miss} three-lepton events with one (left) and two or more (right) b -tagged jets. Only statistical uncertainties are shown and no data-driven correction is applied to background predictions.

The distributions of NN output values in the three-lepton categories are also useful to validate the NN modelling of signal-like events in the simulation.

8 Systematic uncertainties

The main experimental systematic uncertainties on the signal and background predictions include uncertainties on the determination of the energy scale and resolution of jets and of the E_T^{miss} soft-term, and on the modelling of the efficiencies of b -tagging, top-tagging and the (f)JVT selection. Other systematic uncertainties include uncertainties on the modelling of lepton energy scale and reconstruction, trigger, identification and isolation efficiencies. Uncertainties in the integrated luminosity and on the reweighting of the simulation as a function of the number of interactions per bunch crossing in data are also considered. The predicted yield of background events with a non-prompt lepton is assigned a 50% uncertainty, which has minimal impact on the results of the searches.

Theoretical uncertainties on the differential cross-sections of the main sources of background are also considered. For $t\bar{t}$ and W +jets events, these include uncertainties related to factorisation and renormalisation scales, PDF uncertainties, uncertainties on the matching of partons between ME and PS, uncertainties on the resummation scale, and uncertainties related to electroweak NLO corrections. For $t\bar{t}$, uncertainties on the fragmentation model are also considered. For W +jets, a relative uncertainty of 30% between the W +jets

⁹ The E_T^{miss} significance used to classify three-lepton events is not computed with the modified missing transverse momentum, but rather with the original \vec{p}_T^{miss} .

predictions in event categories with one and two or more b -tagged jets is assigned to cover uncertainties on the production of a W boson in association with heavy-flavour quarks [138]. To match the NF scheme used in the statistical model, these theoretical uncertainties are considered uncorrelated between $t\bar{t}$ -1L and $t\bar{t}$ -2L events, as well as between the predictions in the high- E_T^{miss} and boosted categories. Theoretical uncertainties on single-top production include uncertainties on the amount of initial-state radiation, on PDFs, and on factorisation and renormalisation scales. An uncertainty on the removal of the on-shell contributions in the tW process is estimated as the difference in predicted yields when using the diagram removal or the diagram subtraction prescriptions. For $t\bar{t}Z$, uncertainties related to PDFs and to factorisation and normalisation scales are considered. Other minor background contributions, mostly VV and ttV (apart from $t\bar{t}Z(\rightarrow \nu\bar{\nu}, \ell\bar{\ell})$), are predicted with a conservative uncertainty of 30% on the total cross-section [139, 140]. Theoretical uncertainties on signal predictions from factorisation and renormalisation scales and PDF uncertainties are also accounted for.

In the statistical model, systematic uncertainties are associated with nuisance parameters (NPs) whose values are constrained with Gaussian probability density functions. Statistical uncertainties on simulated events are also accounted for. The impact of these uncertainties on the sensitivity of the searches is discussed in Section 10.

9 Results

Multiple types of fits, either for the $\tilde{t}_1\tilde{t}_1$ or the $t\bar{t}$ +DM search, are performed to analyse the observed data. First a ‘background-only’ fit that uses only data in CRs is done to predict the background in the VRs. The data in the VRs is then used to validate the background modelling. A background-only fit using data from CRs and SRs is done to check the compatibility of the data in SRs with background-only contributions. Finally, ‘full’ fits, in which data in CRs and SRs are fitted with contributions from background processes and from a signal model, is done. These fits are performed separately for the $\tilde{t}_1\tilde{t}_1$ and $t\bar{t}$ +DM searches, with all associated regions fit simultaneously.

In the first background-only fit, background predictions were fitted to data in all CRs and then applied via the fit model to VRs, where predictions were found to agree with data. After this validation of the background modelling, the background-only fit including data from SRs was performed. Observed and expected distributions of $m_T \times q(\ell)$ and total yields in CRs and of the NN output values in VRs and SRs after this fit are shown in Figs. 4–9.¹⁰ The expected distributions in SRs from benchmark signal models are also shown. In the $\tilde{t}_1\tilde{t}_1$ search, the NFs of the $t\bar{t}$, W +jets and single-top contributions are generally compatible with unity within uncertainties. The NFs for the $t\bar{t}$ -1L (-2L) background are 1.02 ± 0.06 (1.09 ± 0.05) and 1.07 ± 0.06 (1.29 ± 0.13) in the high- E_T^{miss} and boosted regions, respectively. The NFs for the W +jets backgrounds are 1.30 ± 0.15 and 1.33 ± 0.11 in the same regions. The single-top NF is 1.4 ± 0.4 , with the large uncertainty due in part to the correlation with the uncertainty related to the removal of the on-shell tW contributions. Similar values are obtained in the fit for the $t\bar{t}$ +DM search. Compared with Ref. [31], the overall agreement between data and predictions is better due to improved background modelling, namely the simulation of the $t\bar{t}$ production with SHERPA and the simulation of the tW production with dynamic scales. The results of the background-only fits with and without data in SRs are statistically compatible with each other.

¹⁰ Distributions in the boosted CRs as determined in the fit for the $t\bar{t}$ +DM search are not shown as they are similar to those obtained in the fit for the stop search.

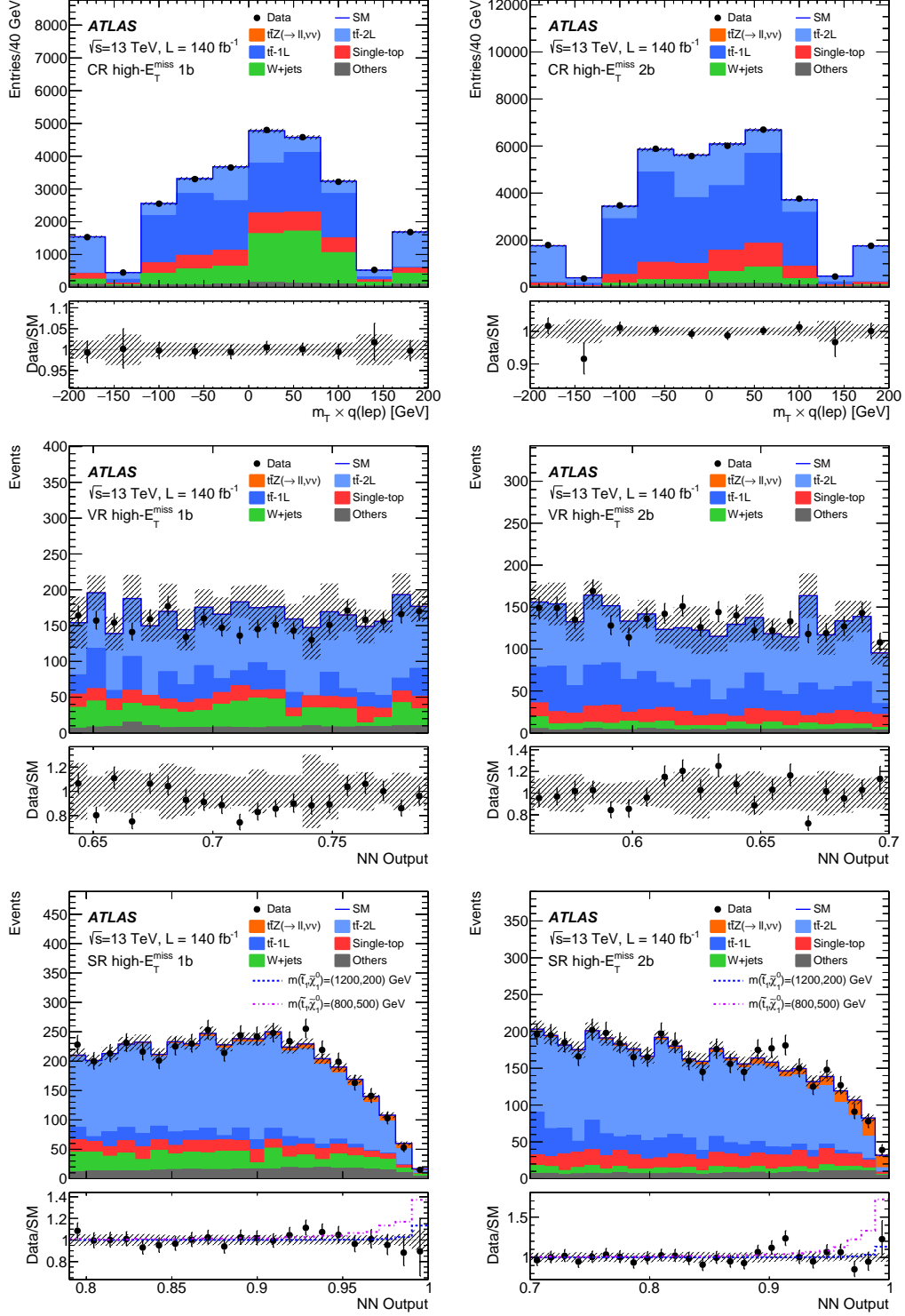


Figure 4: Observed and expected events as a function of $m_T \times q(\ell)$ in the CR (top) and of the stop-NN output value in the VR (middle row) and the SR (bottom) in the high- E_T^{miss} 1b (left) and 2b (right) stop regions. The expected distributions are as determined in the background-only fit with data in CRs and SRs for the $\tilde{t}_1\tilde{t}_1$ search. The hatched area around the total SM prediction includes statistical and systematic uncertainties. Uncertainties on predictions in VRs are dominated by statistical uncertainties on simulated samples. The lower panels show the ratio of the observed data to the expected SM events and the ratio of the sum of the SM and expected signal events to the SM events. In CRs, the last (first) bin contains overflows (underflows).

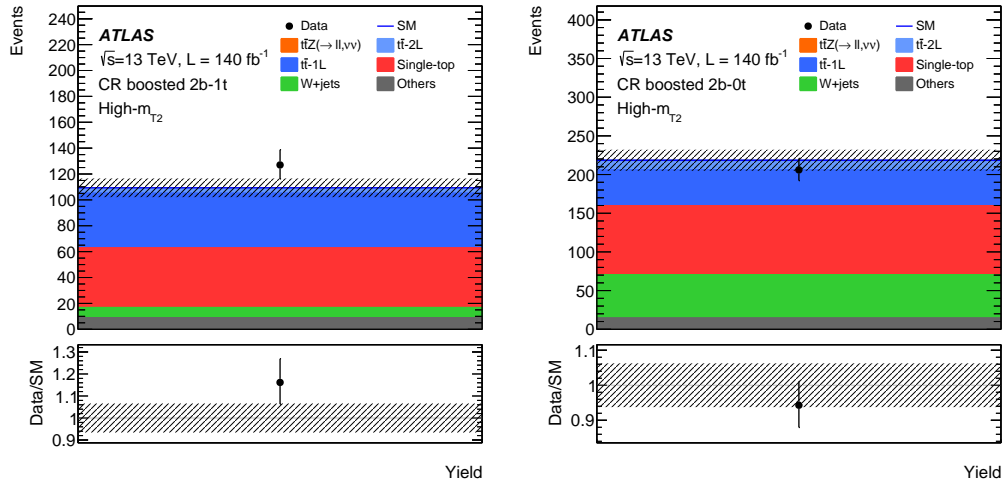


Figure 5: Observed and expected event yields in the high- m_{T2} CR in the boosted 2b-1t (left) and 2b-0t (right) stop regions. The expected distributions are as determined in the background-only fit with data in CRs and SRs for the $\tilde{t}_1\tilde{t}_1$ search. The hatched area around the total SM prediction includes statistical and systematic uncertainties. The lower panels show the ratio of the observed data to the expected SM events.

Good agreement between data and background predictions is seen in all CRs, VRs and SRs, although small excesses of events in data compared with predictions are seen in SRs with two b -tagged jets in bins at high NN output values. To quantify the level of agreement between data and predictions and the combined significance of any excesses, a profile-likelihood-ratio test [141] is performed on the result of the full fit, in which the statistical model includes signal predictions. In the $\tilde{t}_1\tilde{t}_1$ search, no point in the considered parameter space leads to a potential non-zero signal contribution by more than 2.1 standard deviations. The points with highest significance are those at high $m(\tilde{t}_1)$ and low $m(\tilde{\chi}_1^0)$ whose distributions are expected to be strongly peaked at high NN output values and to predominantly populate the boosted 2b-1t category (Figure 6). For the $t\bar{t}$ +DM search, no potential non-zero signal contribution is observed with a significance of more than 1.8 standard deviations. The significance for different models does not show a clear dependence on the mass or parity of the mediator.

The results of the $\tilde{t}_1\tilde{t}_1$ and $t\bar{t}$ +DM searches presented in this paper are statistically combined with those from previous searches in $t\bar{t} + E_T^{\text{miss}}$ final states performed by ATLAS. For the $\tilde{t}_1\tilde{t}_1$ search, results from this paper are combined with those from the search in the final state with no leptons [30], which has better sensitivity at high $m(\tilde{t}_1)$ and low $m(\tilde{\chi}_1^0)$. Of the SRs used in Ref. [30], only SRA and SRB, which target signals at high $m(\tilde{t}_1)$, are included in the combined fit, together with their associated CRs. For the $t\bar{t}$ +DM search, the combined fit performed in Ref. [33] with the zero-, one- and two-lepton final states is updated by replacing the results from the previous one-lepton analysis [31] with the results presented here. For both combined fits, it was checked that there is no overlap among the analysed sets of data events. Fit parameters associated with experimental systematic uncertainties are correlated across all the input analyses, while NFs and NPs associated with background modelling uncertainties are left uncorrelated. An alternative fit for the $\tilde{t}_1\tilde{t}_1$ search in which all fit parameters across the two analyses besides the parameter of interest were left uncorrelated was found to yield compatible results.

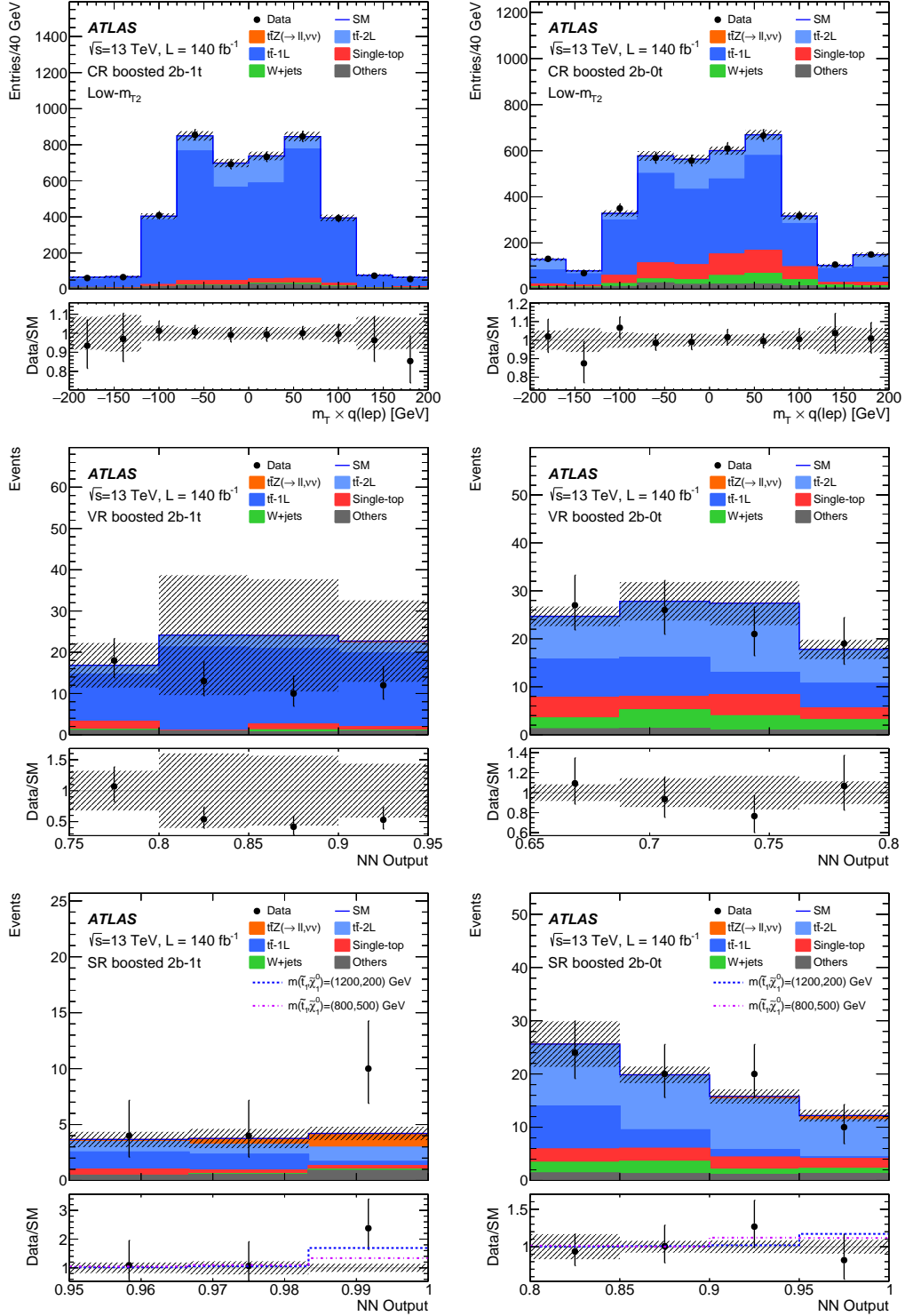


Figure 6: Observed and expected events distributed as a function of $m_T \times q(\ell)$ in the low- m_{T2} CR (top) and of the stop-NN output value in the VR (middle row) and SR (bottom) in the boosted 2b-1t (left) and 2b-0t (right) stop regions. The expected distributions are as determined in the background-only fit with data in CRs and SRs for the $\tilde{t}_1\tilde{t}_1$ search. The hatched area around the total SM prediction includes statistical and systematic uncertainties. Uncertainties on predictions in VRs are dominated by statistical uncertainties on simulated samples. The lower panels show the ratio of the observed data to the expected SM events and the ratio of the sum of the SM and expected signal events to the SM events. In CRs, the last (first) bin contains overflows (underflows).

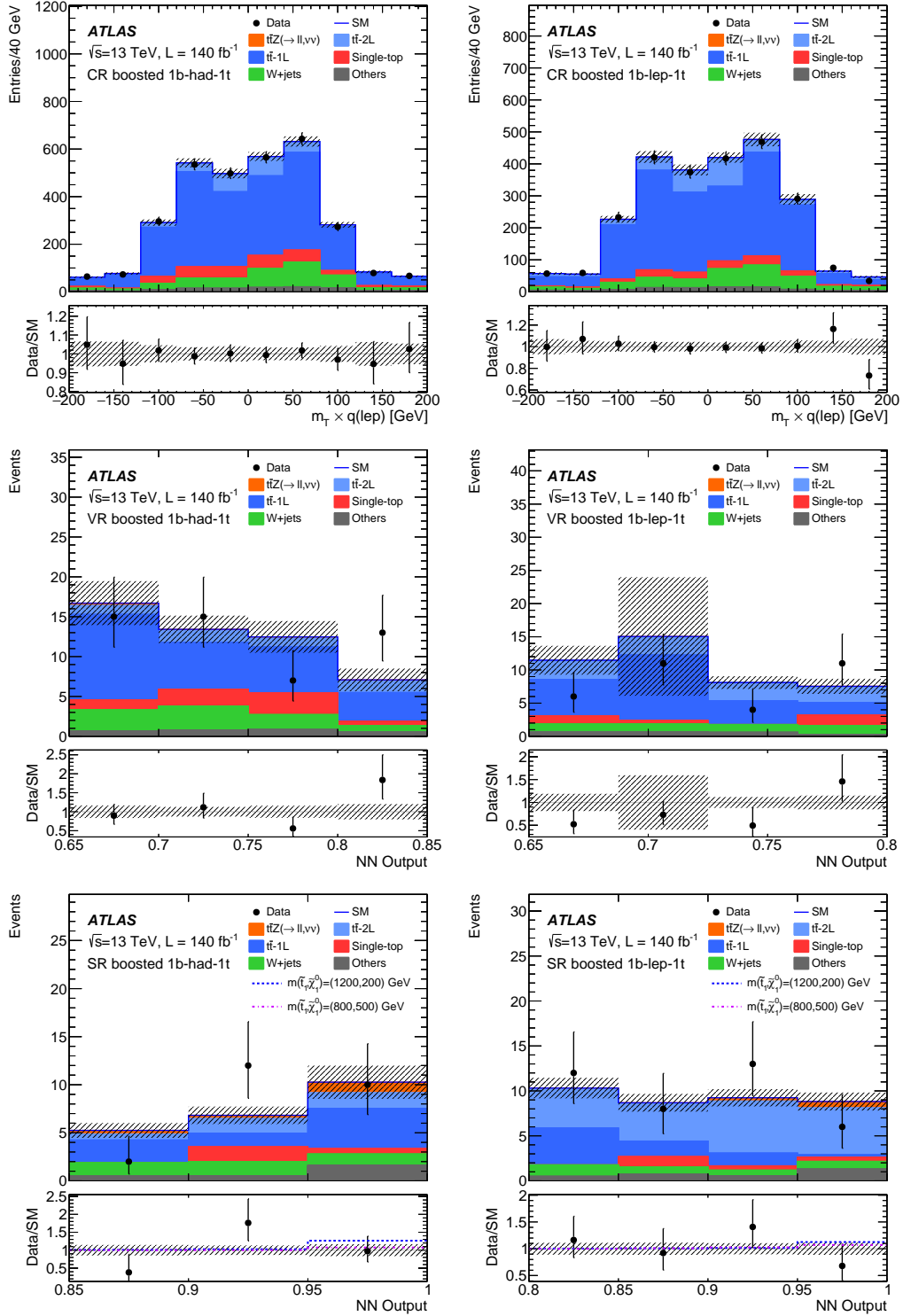


Figure 7: Observed and expected events as a function of $m_T \times q(\ell)$ in the CR (top) and of the stop-NN output value in the VR (middle row) and the SR (bottom) in the boosted 1b-had-1t (left) and 1b-lep-1t (right) stop regions. The expected distributions are as determined in the background-only fit with data in CRs and SRs for the $\tilde{t}_1\tilde{t}_1$ search. The hatched area around the total SM prediction includes statistical and systematic uncertainties. Uncertainties on predictions in VRs are dominated by statistical uncertainties on simulated samples. The lower panels show the ratio of the observed data to the expected SM events and the ratio of the sum of the SM and expected signal events to the SM events. In CRs, the last (first) bin contains overflows (underflows).

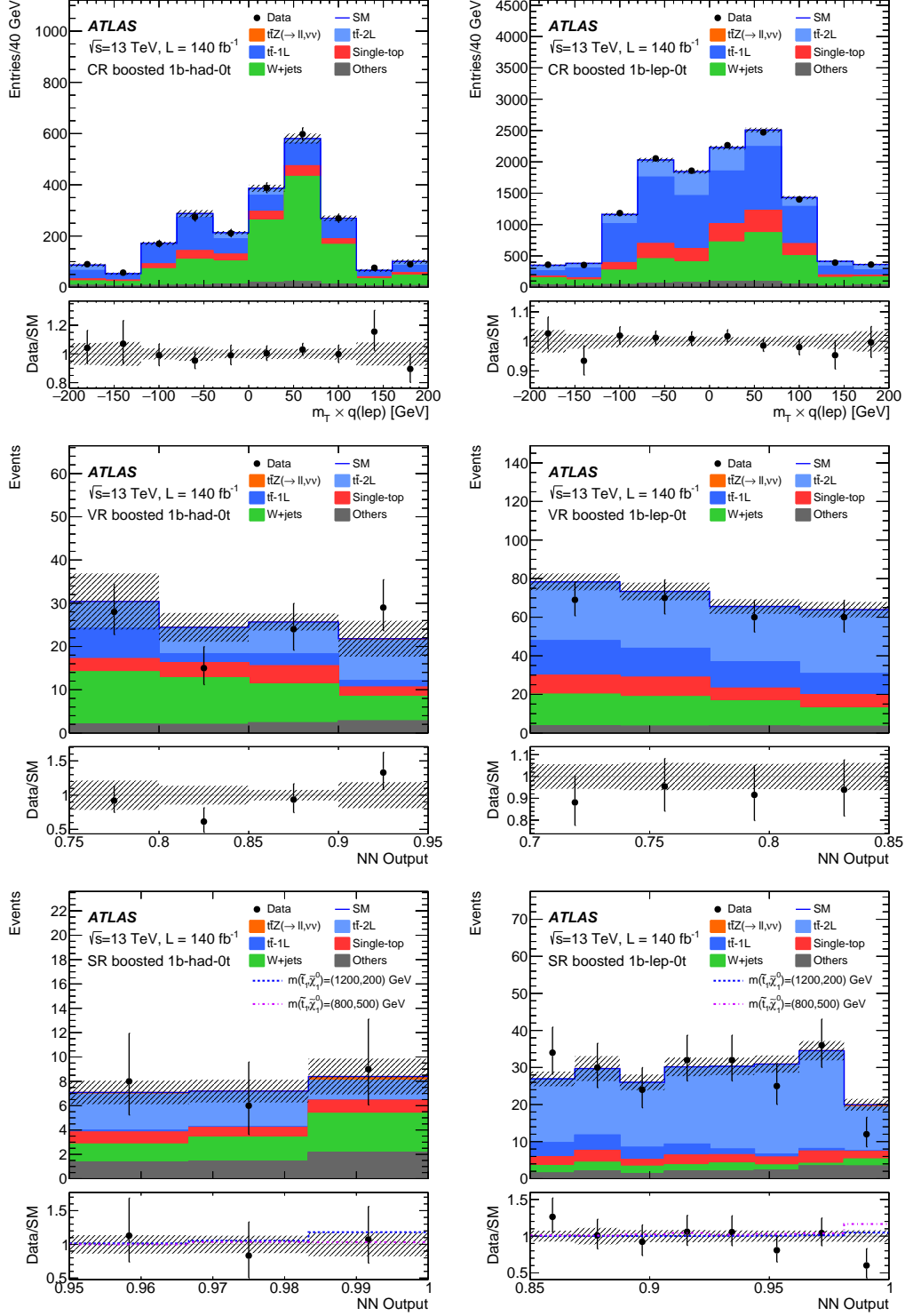


Figure 8: Observed and expected events as a function of $m_T \times q(\ell)$ in the CR (top) and of the stop-NN output value in the VR (middle row) and the SR (bottom) in the boosted 1b-had-0t (left) and 1b-lep-0t (right) stop regions. The expected distributions are as determined in the background-only fit with data in CRs and SRs for the $\tilde{t}_1\tilde{t}_1$ search. The hatched area around the total SM prediction includes statistical and systematic uncertainties. Uncertainties on predictions in VRs are dominated by statistical uncertainties on simulated samples. The lower panels show the ratio of the observed data to the expected SM events and the ratio of the sum of the SM and expected signal events to the SM events. In CRs, the last (first) bin contains overflows (underflows).

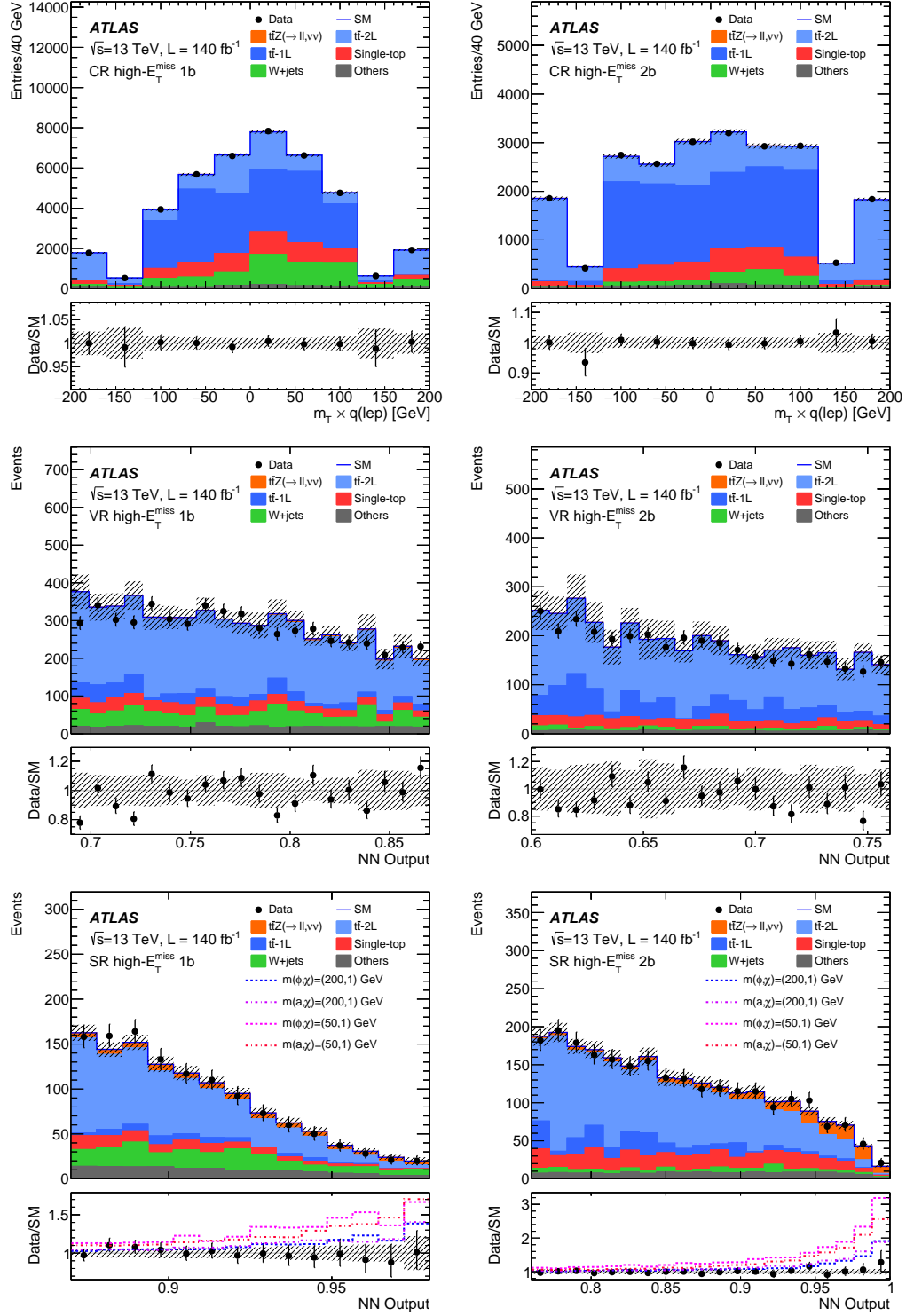


Figure 9: Observed and expected events as a function of $m_T \times q(\ell)$ in the CR (top) and of the DM-NN output value in the VR (middle row) and the SR (bottom) in the high- E_T^{miss} 1b (left) and 2b (right) DM regions. The expected distributions are as determined in the background-only fit with data in CRs and SRs for the $t\bar{t}$ +DM search. The hatched area around the total SM prediction includes statistical and systematic uncertainties. Uncertainties on predictions in VRs are dominated by statistical uncertainties on simulated samples. The lower panels show the ratio of the observed data to the expected SM events, and the ratio of the sum of the SM and expected signal events to the SM events. In CRs, the last (first) bin contains overflows (underflows).

10 Interpretations

As no significant excess is observed, exclusion limits are calculated using the CL_s prescription [142] at 95% confidence level (CL). Figure 10 shows the expected and observed exclusion contours as a function of $m(\tilde{t}_1)$ and $m(\tilde{\chi}_1^0)$ for the $\tilde{t} \rightarrow t\tilde{\chi}_1^0$ or $\tilde{t} \rightarrow bW\tilde{\chi}_1^0$ scenarios. The $\pm 1\sigma_{\text{exp}}$ uncertainty band indicates how much the expected limit is affected by systematic and statistical uncertainties. Compared with Ref. [31], this search significantly improves the sensitivity for high neutralino masses covering the parameter region at $\Delta m(\tilde{t}_1, \tilde{\chi}_1^0) \sim m(t)$ which was not probed by the previous search. At high stop masses where the sensitivity is driven by the statistical power of the recorded data sample, this analysis reaches a sensitivity close to the one from Ref. [31]. For signals with three-body decays ($m(W) < \Delta m(\tilde{t}_1, \tilde{\chi}_1^0) < m(t)$), this analysis has a sensitivity similar to the one from Ref. [31] even though the stop-NNs have not been trained for these signal events and in Ref. [31] an optimised event selection and an NN-based discriminant were used. Overall, the unified approach developed in this search without event categories targeting specific signal models achieves its design target. It provides more stringent constraints in the challenging signal parameter region at $\Delta m(\tilde{t}_1, \tilde{\chi}_1^0) \sim m(t)$ and is almost as sensitive as the approach with dedicated event categories used in the previous search in the other parameter regions. Table 5 shows the main sources of uncertainty on the determination of a potential signal contribution. Statistical uncertainties are the dominant source, followed by the theoretical uncertainties on the background predictions. The exclusion limits determined from the combination of the analysis presented in this paper with Ref. [30] are shown in Figure 11. This combination improves the sensitivity at high $m(\tilde{t}_1)$ and in the region around $m(\tilde{t}_1, \tilde{\chi}_1^0) \sim (1100, 500)$ GeV.

Table 5: Ratios of the signal cross-sections as determined in the fit to the expected signal cross-sections $\mu = \sigma_{\text{fit}}^{\text{sig}} / \sigma_{\text{Th}}^{\text{sig}}$ for different signal models in the $\tilde{t}_1\tilde{t}_1$ and $t\tilde{t}$ +DM searches. Components of the total uncertainty $\sigma(\mu)$ from statistical and major systematic uncertainties are also shown. The component from statistical uncertainties in data is estimated as the uncertainty on μ when all nuisance parameters in the fit are fixed. Components from systematic uncertainties are estimated as $\sigma_{\text{sys}}(\mu) = \sqrt{\sigma^2(\mu) - \sigma_{\text{fix}}^2(\mu)}$, where $\sigma_{\text{fix}}(\mu)$ is the uncertainty when the nuisance parameters associated with the systematic uncertainties are fixed. The components are reported as percentages relative to the total uncertainty $\sigma(\mu)$ only for positive variations of μ because uncertainties on negative variations may be biased by the requirement for μ to be positive. Correlations across components are not accounted for.

	$\tilde{t}_1\tilde{t}_1, m(\tilde{t}_1, \tilde{\chi}_1^0)$ GeV		$t\tilde{t}$ +DM, $m(a, \chi)$ GeV	
	(1000, 600)	(1200, 200)	(50, 1)	(150, 1)
$\mu \pm \sigma(\mu)$ (total uncertainty)	$0.25^{+0.42}_{-0.25}$	$0.8^{+0.7}_{-0.5}$	$0.08^{+0.10}_{-0.08}$	$0.12^{+0.13}_{-0.12}$
Data statistical uncertainty	82 %	74 %	67 %	69 %
Background modelling	45 %	62 %	51 %	48 %
MC statistical uncertainty	25 %	20 %	34 %	33 %
Jet energy scale and resolution	20 %	13 %	29 %	28 %
Flavour tagging efficiency	18 %	10 %	21 %	21 %

The exclusion limits for the $t\tilde{t}$ +DM search are shown in Figure 12. These limits are computed as upper limits at 95% CL on the ratio of the observed $t\tilde{t}$ +DM production cross-section for the spin-0 mediator model to the theoretical cross-section. Limits are shown either as a function of $m(\phi/a)$ assuming $m(\chi) = 1$ GeV,

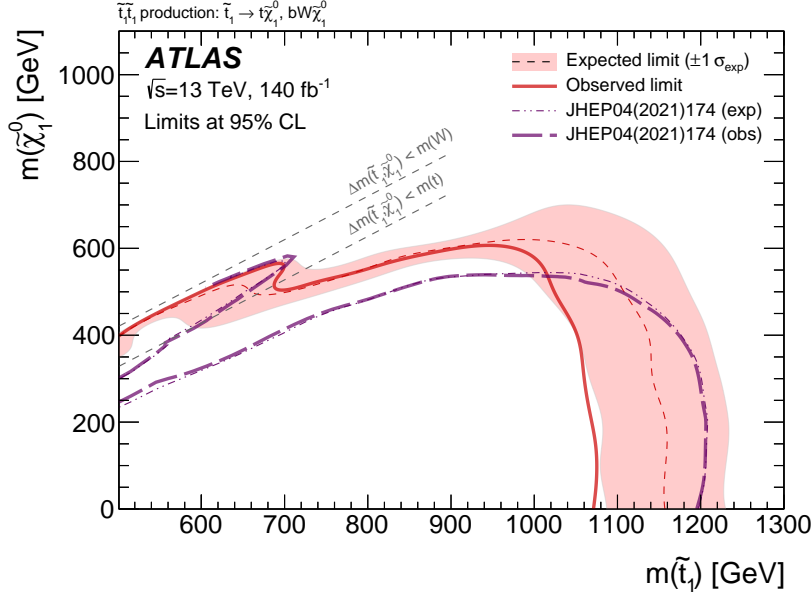


Figure 10: Expected and observed 95% CL excluded regions in the plane of $m(\tilde{\chi}_1^0)$ and $m(\tilde{t}_1)$ for $\tilde{t}_1\tilde{t}_1$ production assuming either a $\tilde{t} \rightarrow t\tilde{\chi}_1^0$ or $\tilde{t} \rightarrow bW\tilde{\chi}_1^0$ decay with a branching ratio of 100%. Models that lie within the contours are excluded. The red band indicates the $\pm 1\sigma$ variation of the expected limit. The diagonal dashed lines indicate the kinematic threshold of the stop decay modes. Also shown is the region excluded by Ref. [31], which targets a similar final state and uses the same data sample.

or as a function of $m(\chi)$ assuming $m(\phi/a) = 10$ GeV. All limits are computed under the hypothesis that $g = g_\chi = g_q = 1$. All signal uncertainties are included in the fit. The $\pm 1\sigma$ and $\pm 2\sigma$ uncertainty bands around the expected upper limits account for all statistical and systematic uncertainties. The upper limits plotted as a function of $m(\chi)$ show a sharp weakening at $m(\chi) = 5$ GeV as this corresponds to the transition from on-shell to off-shell pair production of DM from a mediator with $m(\phi/a) = 10$ GeV. The expected upper limits set by this search supersede those from the previous search in the one-lepton final state [31] and improve on the combined limits from Ref. [33], in which the sensitivity is largely dominated by the search in the two-lepton final state. As shown in Table 5, the impact of statistical and systematic uncertainties on the sensitivity of the $t\tilde{t}$ +DM search is similar to that of the $\tilde{t}_1\tilde{t}_1$ search. Figure 13 shows the combined limits obtained by updating the previous combination [33] and by replacing the previous analysis of the one-lepton final state with the analysis presented in this paper.

Results from the $\tilde{t}_1\tilde{t}_1$ fit are used to set constraints on effective $t\tilde{t}\nu\bar{\nu}$ contact interactions. Assuming the magnitude of the Wilson coefficients to be $|V_{ij}| = 4\pi$, lower limits on Λ are set at 95% confidence level depending on the chirality of the top quarks involved in the interaction and the sign of the Wilson coefficient, as reported in Table 6. To test the validity of the EFT approach, limits are also computed considering only subsets of the signal contributions selected by applying upper thresholds on the invariant mass of the two neutrinos involved in the CI ($m_{\nu\bar{\nu}}$).

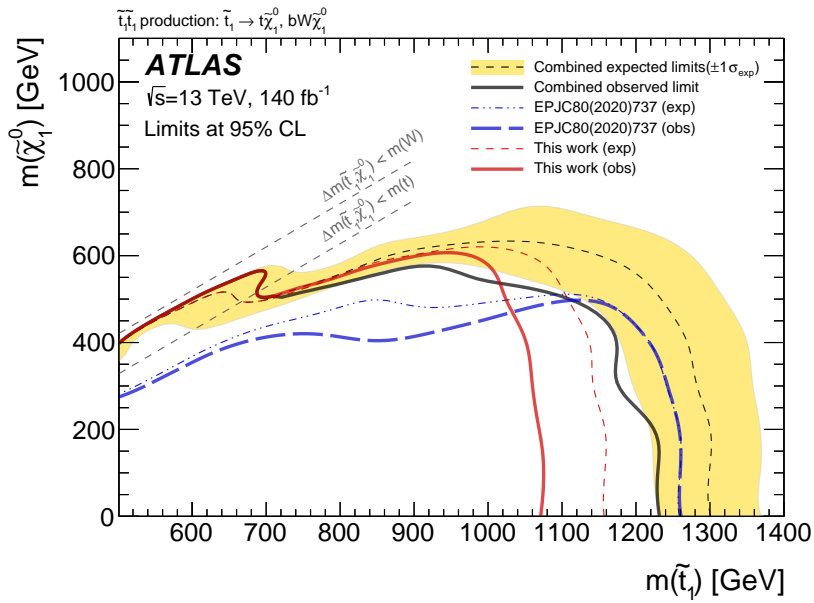


Figure 11: Expected and observed 95% CL excluded regions in the plane of $m(\tilde{\chi}_1^0)$ and $m(\tilde{t}_1)$ for $\tilde{t}_1 \tilde{t}_1$ production assuming either a $\tilde{t} \rightarrow t \tilde{\chi}_1^0$ or $\tilde{t} \rightarrow bW \tilde{\chi}_1^0$ decay with a branching ratio of 100% from the statistical combination of the analysis presented in this paper and Ref. [30]. Models that lie within the contours are excluded. Uncertainty bands corresponding to the $\pm 1\sigma$ variation of the combined expected limit (yellow band) are also indicated. The diagonal dashed lines indicate the kinematic threshold of the stop decay modes.

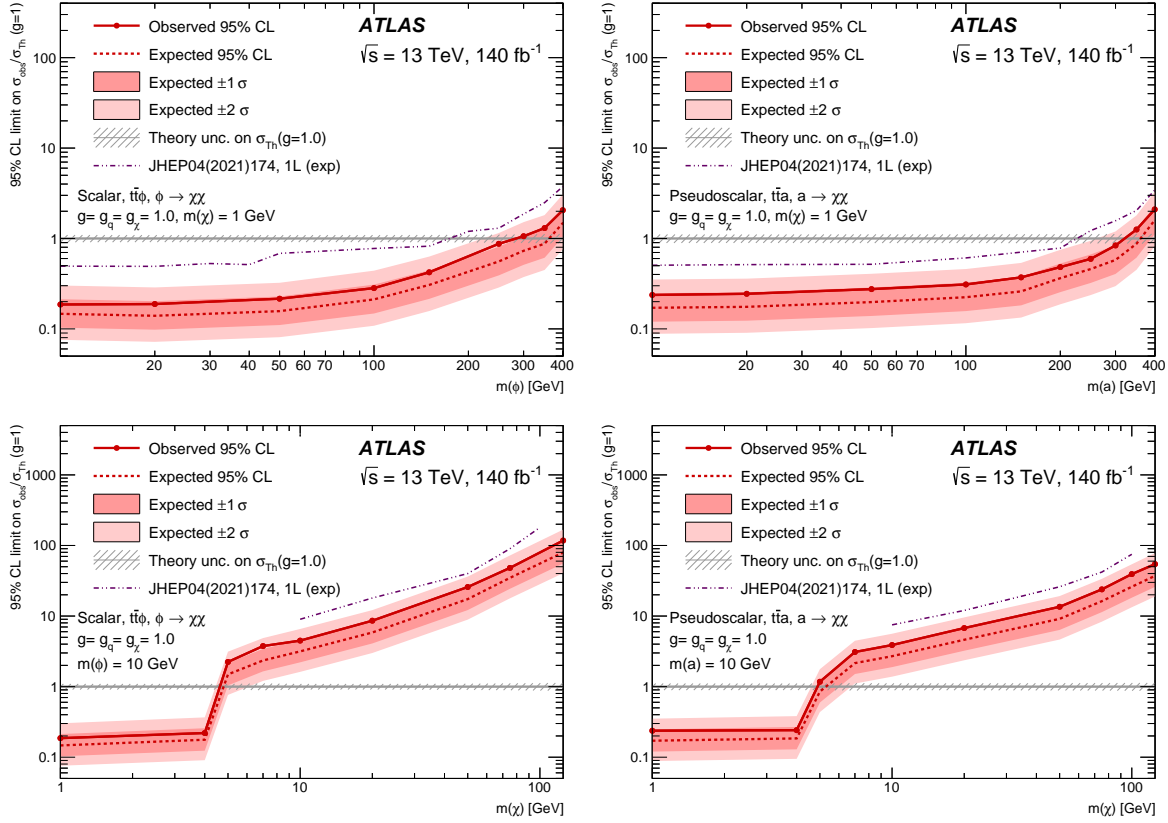


Figure 12: Upper limit at 95% CL on the ratio of the $t\bar{t} + \text{DM}$ production cross-section to the theoretical cross-section under the hypothesis of (left) a scalar or (right) a pseudoscalar mediator. Limits are shown as a function of $m(\phi/a)$ assuming $m(\chi) = 1 \text{ GeV}$ (top), or as a function of $m(\chi)$ assuming $m(\phi/a) = 10 \text{ GeV}$ (bottom). All limits are computed assuming $g = 1$. Limits from Ref. [31] are also shown.

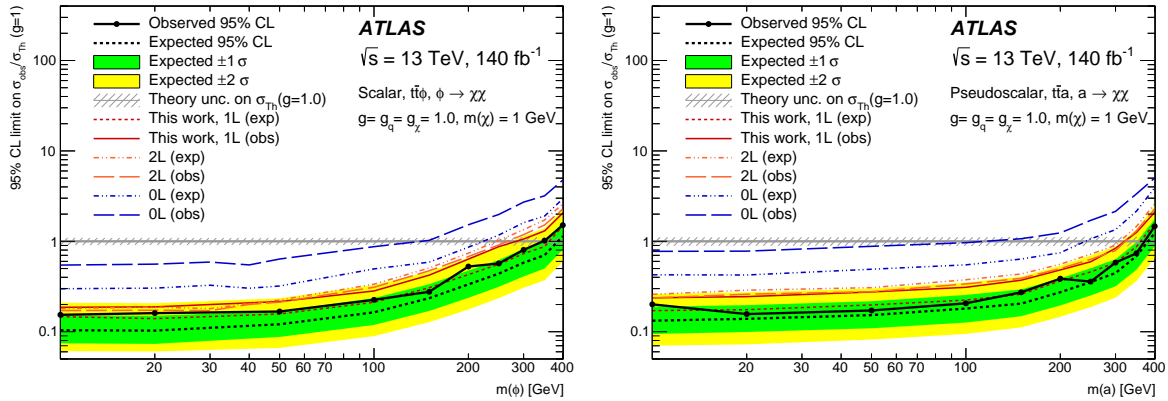


Figure 13: Upper limit at 95% CL on the ratio of the $t\bar{t} + \text{DM}$ production cross-section to the theoretical cross-section under the hypothesis of (left) a scalar or (right) a pseudoscalar mediator. Limits are shown as a function of $m(\phi/a)$ assuming $m(\chi) = 1 \text{ GeV}$. All limits are computed assuming $g = 1$. Combined limits from Ref. [33] are updated to include the analysis in the one-lepton final state presented in this paper. Limits from the individual analyses included in the combination are also shown.

Table 6: Constraints on effective $t\bar{t}\nu\bar{\nu}$ contact interactions involving all three generations of left-handed neutrinos based on the results of the $\tilde{t}_1\tilde{t}_1$ search. Constraints are set independently for different effective vector operators and for different hypotheses about the sign of the Wilson coefficient which leads to a constructive or destructive interference with $t\bar{t}Z(\rightarrow \nu\bar{\nu})$. Observed (expected) limits at 95% CL are reported for $\sqrt{|V_{ij}|}/\Lambda$ and for Λ , for the full phase space and for specified regions of the true invariant mass of the neutrino pair, assuming $|V_{ij}| = 4\pi$. Limits corresponding to $\pm 1\sigma$ variations of the expected limits are also reported.

Wilson coefficient	Observed (Expected) upper limit on $\sqrt{ V_{ij} }/\Lambda$ [TeV ⁻¹]	Observed (Expected) lower limit on Λ for $ V_{ij} = 4\pi$ [TeV]
$V_{LL} > 0$	1.59 (1.44 ^{1.58} _{1.31})	2.23 (2.47 ^{2.71} _{2.25})
$m_{\nu\bar{\nu}} < 1$ TeV	1.84 (1.66 ^{1.82} _{1.51})	1.93 (2.14 ^{2.35} _{1.95})
$m_{\nu\bar{\nu}} < 2$ TeV	1.62 (1.46 ^{1.61} _{1.36})	2.18 (2.42 ^{2.66} _{2.21})
$V_{LL} < 0$	1.66 (1.52 ^{1.66} _{1.40})	2.13 (2.33 ^{2.53} _{2.14})
$m_{\nu\bar{\nu}} < 1$ TeV	1.96 (1.80 ^{1.95} _{1.66})	1.81 (1.97 ^{2.13} _{1.82})
$m_{\nu\bar{\nu}} < 2$ TeV	1.70 (1.56 ^{1.69} _{1.44})	2.08 (2.28 ^{2.47} _{2.10})
$V_{LR} > 0$	1.67 (1.53 ^{1.66} _{1.40})	2.12 (2.32 ^{2.53} _{2.13})
$m_{\nu\bar{\nu}} < 1$ TeV	1.92 (1.78 ^{1.94} _{1.64})	1.84 (1.99 ^{2.16} _{1.82})
$m_{\nu\bar{\nu}} < 2$ TeV	1.70 (1.56 ^{1.70} _{1.44})	2.08 (2.27 ^{2.47} _{2.08})
$V_{LR} < 0$	1.63 (1.49 ^{1.63} _{1.36})	2.17 (2.38 ^{2.60} _{2.18})
$m_{\nu\bar{\nu}} < 1$ TeV	1.86 (1.72 ^{1.89} _{1.58})	1.91 (2.06 ^{2.25} _{1.88})
$m_{\nu\bar{\nu}} < 2$ TeV	1.66 (1.52 ^{1.67} _{1.40})	2.13 (2.33 ^{2.54} _{2.13})

11 Discussion and conclusions

This paper presents searches for the direct production of a pair of top squarks, for the production of a spin-0 mediator that decays into DM particles in association with a pair of top quarks, and for effective $t\bar{t}\nu\bar{\nu}$ contact interactions, using the full Run 2 pp data sample recorded by ATLAS at $\sqrt{s} = 13$ TeV. The searches are conducted with events compatible with the presence of one semileptonic and one hadronic top-quark decay and with large E_T^{miss} . The results are combined with previous searches in similar final states but with different lepton multiplicities.

The new searches employ an analysis approach based on neural networks and event categories designed to target final states rather than specific signal model parameter regions. Event categories are defined using the multiplicities and kinematic properties of jets, b -tagged jets and E_T^{miss} . In each category, neural networks are trained by considering potential signals across the parameter space under study, so that the resulting signal regions are sensitive to wide ranges of the parameter space. A novel approach using neural networks is also developed to reconstruct hadronic top-quark decays.

In the $\tilde{t}_1\tilde{t}_1$ search, the sensitivity to stop pair production for a mass splitting between the stop and the neutralino masses near the top quark mass is significantly improved compared with Ref. [31], which uses the same data sample. For models with heavy stops and light neutralinos, the sensitivity of the new search, which is not as high as in Ref. [31], is instead aided by the combination with Ref. [30], which is performed in final states with no leptons and is the most sensitive study by ATLAS in that parameter region to date. As a result, the combined sensitivity for models with two-body decays is improved across the full parameter region and supersedes the sensitivities of Refs. [30, 31]. The sensitivity of the new search to spin-0 mediators is also improved across the full parameter space. In addition to enhanced sensitivity, this analysis approach offers the benefit that no dedicated signal region needs to be optimised for specific regions of the parameter space. Moreover, with only one discriminant per category for all signal models under test, the analysis is simpler, since the data and background distributions remain the same while different signal predictions are tested. This makes the validation of the background modelling more straightforward, and the interpretability of results for new signals is likely to be simpler and more effective. Another important development included in this paper is the improved modelling of top quark production in both $t\bar{t}$ and single-top processes.

No statistically significant deviations from the SM expectation are observed and exclusion limits at 95% confidence level are set by combining the new searches with previous analyses performed in similar final states with different lepton multiplicities requirements. In the simplified models considered in this paper, stops are excluded for masses up to 1230 GeV, while neutralinos are excluded for masses up to 570 GeV. These limits are slightly weaker than expected due to the presence of small excesses of data over the predicted background. In the $t\bar{t}$ +DM search, when assuming $g = g_q = g_\chi = 1$ for the strengths of the couplings of the mediator to DM and SM particles, models with scalar (pseudoscalar) mediators with masses up to 350 (370) GeV are excluded. At lower mediator masses, models with production cross-sections as small as 0.15 (0.16) times the nominal predictions are excluded. Results from the analysis presented in this paper are also interpreted in the context of a search for effective vector contact interactions between top quarks and all three generations of left-handed neutrinos. Assuming the Wilson coefficient to satisfy $|V_{ij}| = 4\pi$, lower limits on the energy scale of new physics Λ at 95% confidence level are between 2.12 TeV and 2.23 TeV, depending on the chirality of the top quarks involved in the CI and the sign of the Wilson coefficient.

Acknowledgements

We thank CERN for the very successful operation of the LHC, as well as the support staff from our institutions without whom ATLAS could not be operated efficiently.

We acknowledge the support of ANPCyT, Argentina; YerPhI, Armenia; ARC, Australia; BMWFW and FWF, Austria; ANAS, Azerbaijan; CNPq and FAPESP, Brazil; NSERC, NRC and CFI, Canada; CERN; ANID, Chile; CAS, MOST and NSFC, China; Minciencias, Colombia; MEYS CR, Czech Republic; DNRF and DNSRC, Denmark; IN2P3-CNRS and CEA-DRF/IRFU, France; SRNSFG, Georgia; BMBF, HGF and MPG, Germany; GSRI, Greece; RGC and Hong Kong SAR, China; ISF and Benozziyo Center, Israel; INFN, Italy; MEXT and JSPS, Japan; CNRST, Morocco; NWO, Netherlands; RCN, Norway; MEiN, Poland; FCT, Portugal; MNE/IFA, Romania; MESTD, Serbia; MSSR, Slovakia; ARRS and MIZŠ, Slovenia; DSI/NRF, South Africa; MICINN, Spain; SRC and Wallenberg Foundation, Sweden; SERI, SNSF and Cantons of Bern and Geneva, Switzerland; MOST, Taipei; TENMAK, Türkiye; STFC, United Kingdom; DOE and NSF, United States of America. In addition, individual groups and members have received support from BCKDF, CANARIE, CRC and DRAC, Canada; PRIMUS 21/SCI/017 and UNCE SCI/013, Czech Republic; COST, ERC, ERDF, Horizon 2020, ICSC-NextGenerationEU and Marie Skłodowska-Curie Actions, European Union; Investissements d’Avenir Labex, Investissements d’Avenir IDEX and ANR, France; DFG and AvH Foundation, Germany; Herakleitos, Thales and Aristeia programmes co-financed by EU-ESF and the Greek NSRF, Greece; BSF-NSF and MINERVA, Israel; Norwegian Financial Mechanism 2014-2021, Norway; NCN and NAWA, Poland; La Caixa Banking Foundation, CERCA Programme Generalitat de Catalunya and PROMETEO and GenT Programmes Generalitat Valenciana, Spain; Göran Gustafssons Stiftelse, Sweden; The Royal Society and Leverhulme Trust, United Kingdom.

The crucial computing support from all WLCG partners is acknowledged gratefully, in particular from CERN, the ATLAS Tier-1 facilities at TRIUMF/SFU (Canada), NDGF (Denmark, Norway, Sweden), CC-IN2P3 (France), KIT/GridKA (Germany), INFN-CNAF (Italy), NL-T1 (Netherlands), PIC (Spain), RAL (UK) and BNL (USA), the Tier-2 facilities worldwide and large non-WLCG resource providers. Major contributors of computing resources are listed in Ref. [143].

References

- [1] Y. Golfand and E. Likhtman, *Extension of the Algebra of Poincare Group Generators and Violation of P Invariance*, JETP Lett. **13** (1971) 323, [Pisma Zh. Eksp. Teor. Fiz. **13** (1971) 452].
- [2] D. Volkov and V. Akulov, *Is the neutrino a goldstone particle?*, Phys. Lett. B **46** (1973) 109.
- [3] J. Wess and B. Zumino, *Supergauge transformations in four dimensions*, Nucl. Phys. B **70** (1974) 39.
- [4] J. Wess and B. Zumino, *Supergauge invariant extension of quantum electrodynamics*, Nucl. Phys. B **78** (1974) 1.
- [5] S. Ferrara and B. Zumino, *Supergauge invariant Yang-Mills theories*, Nucl. Phys. B **79** (1974) 413.
- [6] A. Salam and J. Strathdee, *Super-symmetry and non-Abelian gauges*, Phys. Lett. B **51** (1974) 353.
- [7] G. R. Farrar and P. Fayet, *Phenomenology of the production, decay, and detection of new hadronic states associated with supersymmetry*, Phys. Lett. B **76** (1978) 575.

- [8] G. D’Ambrosio, G. Giudice, G. Isidori and A. Strumia, *Minimal flavour violation: an effective field theory approach*, *Nucl. Phys. B* **645** (2002) 155, arXiv: [hep-ph/0207036](#).
- [9] G. Isidori and D. M. Straub, *Minimal flavour violation and beyond*, *Eur. Phys. J. C* **72** (2012), arXiv: [1202.0464 \[hep-ph\]](#).
- [10] ATLAS Collaboration, *Observation of a new particle in the search for the Standard Model Higgs boson with the ATLAS detector at the LHC*, *Phys. Lett. B* **716** (2012) 1, arXiv: [1207.7214 \[hep-ex\]](#).
- [11] CMS Collaboration, *Observation of a new boson at a mass of 125 GeV with the CMS experiment at the LHC*, *Phys. Lett. B* **716** (2012) 30, arXiv: [1207.7235 \[hep-ex\]](#).
- [12] S. Weinberg, *Implications of dynamical symmetry breaking*, *Phys. Rev. D* **13** (1976) 974.
- [13] E. Gildener, *Gauge-symmetry hierarchies*, *Phys. Rev. D* **14** (1976) 1667.
- [14] S. Weinberg, *Implications of dynamical symmetry breaking: An addendum*, *Phys. Rev. D* **19** (1979) 1277.
- [15] L. Susskind, *Dynamics of spontaneous symmetry breaking in the Weinberg-Salam theory*, *Phys. Rev. D* **20** (1979) 2619.
- [16] S. Dimopoulos and H. Georgi, *Softly broken supersymmetry and SU(5)*, *Nucl. Phys. B* **193** (1981) 150.
- [17] E. Witten, *Dynamical breaking of supersymmetry*, *Nucl. Phys. B* **188** (1981) 513.
- [18] M. Dine, W. Fischler and M. Srednicki, *Supersymmetric technicolor*, *Nucl. Phys. B* **189** (1981) 575.
- [19] S. Dimopoulos and S. Raby, *Supercolor*, *Nucl. Phys. B* **192** (1981) 353.
- [20] N. Sakai, *Naturalnes in supersymmetric GUTS*, *Z. Phys. C* **11** (1981) 153.
- [21] R. K. Kaul and P. Majumdar, *Cancellation of quadratically divergent mass corrections in globally supersymmetric spontaneously broken gauge theories*, *Nucl. Phys. B* **199** (1982) 36.
- [22] R. Barbieri and G. Giudice, *Upper bounds on supersymmetric particle masses*, *Nucl. Phys. B* **306** (1988) 63.
- [23] B. de Carlos and J. Casas, *One-loop analysis of the electroweak breaking in supersymmetric models and the fine-tuning problem*, *Phys. Lett. B* **309** (1993) 320.
- [24] P. Fayet, *Supersymmetry and weak, electromagnetic and strong interactions*, *Phys. Lett. B* **64** (1976) 159.
- [25] P. Fayet, *Spontaneously broken supersymmetric theories of weak, electromagnetic and strong interactions*, *Phys. Lett. B* **69** (1977) 489.
- [26] P. Fayet, *Relations between the masses of the superpartners of leptons and quarks, the goldstino coupling and the neutral currents*, *Phys. Lett. B* **84** (1979) 416.
- [27] H. Goldberg, *Constraint on the Photino Mass from Cosmology*, *Phys. Rev. Lett.* **50** (1983) 1419, Erratum: *Phys. Rev. Lett.* **103** (2009) 099905.
- [28] J. Ellis, J. Hagelin, D. V. Nanopoulos, K. A. Olive and M. Srednicki, *Supersymmetric relics from the big bang*, *Nucl. Phys. B* **238** (1984) 453.

- [29] D. Abercrombie et al., *Dark Matter benchmark models for early LHC Run-2 Searches: Report of the ATLAS/CMS Dark Matter Forum*, *Physics of the Dark Universe* **27** (2020) 100371.
- [30] ATLAS Collaboration, *Search for a scalar partner of the top quark in the all-hadronic $t\bar{t}$ plus missing transverse momentum final state at $\sqrt{s} = 13$ TeV with the ATLAS detector*, *Eur. Phys. J. C* **80** (2020) 737, arXiv: 2004.14060 [hep-ex].
- [31] ATLAS Collaboration, *Search for new phenomena with top quark pairs in final states with one lepton, jets, and missing transverse momentum in pp collisions at $\sqrt{s} = 13$ TeV with the ATLAS detector*, *JHEP* **04** (2021) 174, arXiv: 2012.03799 [hep-ex].
- [32] ATLAS Collaboration, *Search for new phenomena in events with two opposite-charge leptons, jets and missing transverse momentum in pp collisions at $\sqrt{s} = 13$ TeV with the ATLAS detector*, *JHEP* **04** (2021) 165, arXiv: 2102.01444 [hep-ex].
- [33] ATLAS Collaboration, *Constraints on spin-0 dark matter mediators and invisible Higgs decays using ATLAS 13 TeV pp collision data with two top quarks and missing transverse momentum in the final state*, *Eur. Phys. J. C* **83** (2023) 503, arXiv: 2211.05426 [hep-ex].
- [34] CMS Collaboration, *Search for top squark production in fully-hadronic final states in proton–proton collisions at $\sqrt{s} = 13$ TeV*, *Phys. Rev. D* **104** (2021) 052001, arXiv: 2103.01290 [hep-ex].
- [35] CMS Collaboration, *Search for direct top squark pair production in events with one lepton, jets, and missing transverse momentum at 13 TeV with the CMS experiment*, *JHEP* **05** (2020) 032, arXiv: 1912.08887 [hep-ex].
- [36] CMS Collaboration, *Search for top squark pair production using dilepton final states in pp collision data collected at $\sqrt{s} = 13$ TeV*, *Eur. Phys. J. C* **81** (2021) 3, arXiv: 2008.05936 [hep-ex].
- [37] CMS Collaboration, *Combined searches for the production of supersymmetric top quark partners in proton–proton collisions at $\sqrt{s} = 13$ TeV*, *Eur. Phys. J. C* **81** (2021) 970, arXiv: 2107.10892 [hep-ex].
- [38] J. Alwall, M.-P. Le, M. Lisanti and J. G. Wacker, *Searching for directly decaying gluinos at the Tevatron*, *Phys. Lett. B* **666** (2008) 34, arXiv: 0803.0019 [hep-ph].
- [39] J. Alwall, P. Schuster and N. Toro, *Simplified models for a first characterization of new physics at the LHC*, *Phys. Rev. D* **79** (2009) 075020, arXiv: 0810.3921 [hep-ph].
- [40] ATLAS Collaboration, *Search for dark matter produced in association with bottom or top quarks in $\sqrt{s} = 13$ TeV pp collisions with the ATLAS detector*, *Eur. Phys. J. C* **78** (2018) 18, arXiv: 1710.11412 [hep-ex].
- [41] Y. Afik, S. Bar-Shalom, K. Pal, A. Soni and J. Wudka, *Multi-lepton probes of new physics and lepton-universality in top-quark interactions*, *Nucl. Phys. B* **980** (2022) 115849.
- [42] Y. Afik, S. Bar-Shalom, J. Cohen, A. Soni and J. Wudka, *High p_T correlated tests of lepton universality in lepton(s) + jet(s) processes; An EFT analysis*, *Phys. Lett. B* **811** (2020) 135908, arXiv: 2005.06457 [hep-ph].

- [43] Y. Afik, S. Bar-Shalom, J. Cohen and Y. Rozen, *Searching for New Physics with $b\bar{b}\ell^+\ell^-$ contact interactions*, *Phys. Lett. B* **807** (2020) 135541, arXiv: [1912.00425 \[hep-ex\]](#).
- [44] Y. Afik, S. Bar-Shalom, A. Soni and J. Wudka, *New flavor physics in di- and trilepton events from single-top production at the LHC and beyond*, *Phys. Rev. D* **103** (2021) 075031, arXiv: [2101.05286 \[hep-ph\]](#).
- [45] W. Buchmüller and D. Wyler, *Effective lagrangian analysis of new interactions and flavour conservation*, *Nucl. Phys. B* **268** (1986) 621.
- [46] C. Arzt, M. B. Einhorn and J. Wudka, *Patterns of deviation from the standard model*, *Nucl. Phys. B* **433** (1995) 41, arXiv: [hep-ph/9405214](#).
- [47] M. B. Einhorn and J. Wudka, *The Bases of Effective Field Theories*, *Nucl. Phys. B* **876** (2013) 556, arXiv: [1307.0478 \[hep-ph\]](#).
- [48] B. Grzadkowski, M. Iskrzyński, M. Misiak and J. Rosiek, *Dimension-Six Terms in the Standard Model Lagrangian*, *JHEP* **10** (2010) 085, arXiv: [1008.4884 \[hep-ph\]](#).
- [49] I. Brivio and M. Trott, *The Standard Model as an Effective Field Theory*, *Phys. Rept.* **793** (2019) 1, arXiv: [1706.08945 \[hep-ph\]](#).
- [50] ATLAS Collaboration, *The ATLAS Experiment at the CERN Large Hadron Collider*, *JINST* **3** (2008) S08003.
- [51] ATLAS Collaboration, *ATLAS Insertable B-Layer: Technical Design Report*, ATLAS-TDR-19; CERN-LHCC-2010-013, 2010, URL: <https://cds.cern.ch/record/1291633>, Addendum: ATLAS-TDR-19-ADD-1; CERN-LHCC-2012-009, 2012, URL: <https://cds.cern.ch/record/1451888>.
- [52] B. Abbott et al., *Production and integration of the ATLAS Insertable B-Layer*, *JINST* **13** (2018) T05008, arXiv: [1803.00844 \[physics.ins-det\]](#).
- [53] ATLAS Collaboration, *Performance of the ATLAS trigger system in 2015*, *Eur. Phys. J. C* **77** (2017) 317, arXiv: [1611.09661 \[hep-ex\]](#).
- [54] ATLAS Collaboration, *The ATLAS Collaboration Software and Firmware*, ATL-SOFT-PUB-2021-001, 2021, URL: <https://cds.cern.ch/record/2767187>.
- [55] ATLAS Collaboration, *ATLAS data quality operations and performance for 2015–2018 data-taking*, *JINST* **15** (2020) P04003, arXiv: [1911.04632 \[physics.ins-det\]](#).
- [56] ATLAS Collaboration, *Luminosity determination in pp collisions at $\sqrt{s} = 13$ TeV using the ATLAS detector at the LHC*, *Eur. Phys. J. C* **83** (2023) 982, arXiv: [2212.09379 \[hep-ex\]](#).
- [57] G. Avoni et al., *The new LUCID-2 detector for luminosity measurement and monitoring in ATLAS*, *JINST* **13** (2018) P07017.
- [58] ATLAS Collaboration, *Performance of the missing transverse momentum triggers for the ATLAS detector during Run-2 data taking*, *JHEP* **08** (2020) 080, arXiv: [2005.09554 \[hep-ex\]](#).
- [59] ATLAS Collaboration, *Performance of electron and photon triggers in ATLAS during LHC Run 2*, *Eur. Phys. J. C* **80** (2020) 47, arXiv: [1909.00761 \[hep-ex\]](#).

- [60] ATLAS Collaboration, *Performance of the ATLAS muon triggers in Run 2*, [JINST **15** \(2020\) P09015](#), arXiv: [2004.13447 \[physics.ins-det\]](#).
- [61] J. Alwall et al., *The automated computation of tree-level and next-to-leading order differential cross sections, and their matching to parton shower simulations*, [JHEP **07** \(2014\) 079](#), arXiv: [1405.0301 \[hep-ph\]](#).
- [62] M. Beneke, M. Czakon, P. Falgari, A. Mitov and C. Schwinn, *Threshold expansion of the $gg(q\bar{q}) \rightarrow Q\bar{Q} + X$ cross section at $O(\alpha_s^4)$* , [Phys. Lett. B **690** \(2010\) 483](#), arXiv: [0911.5166 \[hep-ph\]](#),
Erratum: [Phys. Lett. B **778** \(2018\) 464](#).
- [63] W. Beenakker, C. Borschensky, M. Krämer, A. Kulesza and E. Laenen, *NNLL-fast: predictions for coloured supersymmetric particle production at the LHC with threshold and Coulomb resummation*, [JHEP **12** \(2016\) 133](#), arXiv: [1607.07741 \[hep-ph\]](#).
- [64] W. Beenakker, M. Krämer, T. Plehn, M. Spira and P. Zerwas, *Stop production at hadron colliders*, [Nucl. Phys. B **515** \(1998\) 3](#), arXiv: [hep-ph/9710451](#).
- [65] W. Beenakker et al., *Supersymmetric top and bottom squark production at hadron colliders*, [JHEP **08** \(2010\) 098](#), arXiv: [1006.4771 \[hep-ph\]](#).
- [66] W. Beenakker et al., *NNLL resummation for stop pair-production at the LHC*, [JHEP **05** \(2016\) 153](#), arXiv: [1601.02954 \[hep-ph\]](#).
- [67] O. Mattelaer and E. Vryonidou, *Dark-matter production through loop-induced processes at the LHC: the s-channel mediator case*, [Eur. Phys. J. C **75** \(2015\) 436](#).
- [68] M. Backović et al., *Higher-order QCD predictions for dark matter production at the LHC in simplified models with s-channel mediators*, [Eur. Phys. J. C **75** \(2015\) 482](#).
- [69] E. Bothmann et al., *Event generation with Sherpa 2.2*, [SciPost Phys. **7** \(2019\) 034](#), arXiv: [1905.09127 \[hep-ph\]](#).
- [70] NNPDF Collaboration, R. D. Ball et al., *Parton distributions for the LHC run II*, [JHEP **04** \(2015\) 040](#), arXiv: [1410.8849 \[hep-ph\]](#).
- [71] S. Schumann and F. Krauss, *A parton shower algorithm based on Catani–Seymour dipole factorisation*, [JHEP **03** \(2008\) 038](#), arXiv: [0709.1027 \[hep-ph\]](#).
- [72] S. Höche, F. Krauss, M. Schönherr and F. Siegert, *A critical appraisal of NLO+PS matching methods*, [JHEP **09** \(2012\) 049](#), arXiv: [1111.1220 \[hep-ph\]](#).
- [73] S. Höche, F. Krauss, M. Schönherr and F. Siegert, *QCD matrix elements + parton showers. The NLO case*, [JHEP **04** \(2013\) 027](#), arXiv: [1207.5030 \[hep-ph\]](#).
- [74] S. Catani, F. Krauss, B. R. Webber and R. Kuhn, *QCD Matrix Elements + Parton Showers*, [JHEP **11** \(2001\) 063](#), arXiv: [hep-ph/0109231](#).
- [75] S. Höche, F. Krauss, S. Schumann and F. Siegert, *QCD matrix elements and truncated showers*, [JHEP **05** \(2009\) 053](#), arXiv: [0903.1219 \[hep-ph\]](#).

- [76] M. Beneke, P. Falgari, S. Klein and C. Schwinn, *Hadronic top-quark pair production with NNLL threshold resummation*, *Nucl. Phys. B* **855** (2012) 695, arXiv: [1109.1536 \[hep-ph\]](#).
- [77] M. Cacciari, M. Czakon, M. Mangano, A. Mitov and P. Nason, *Top-pair production at hadron colliders with next-to-next-to-leading logarithmic soft-gluon resummation*, *Phys. Lett. B* **710** (2012) 612, arXiv: [1111.5869 \[hep-ph\]](#).
- [78] P. Bärnreuther, M. Czakon and A. Mitov, *Percent-Level-Precision Physics at the Tevatron: Next-to-Next-to-Leading Order QCD Corrections to $q\bar{q} \rightarrow t\bar{t} + X$* , *Phys. Rev. Lett.* **109** (2012) 132001, arXiv: [1204.5201 \[hep-ph\]](#).
- [79] M. Czakon and A. Mitov, *NNLO corrections to top-pair production at hadron colliders: the all-fermionic scattering channels*, *JHEP* **12** (2012) 054, arXiv: [1207.0236 \[hep-ph\]](#).
- [80] M. Czakon and A. Mitov, *NNLO corrections to top pair production at hadron colliders: the quark-gluon reaction*, *JHEP* **01** (2013) 080, arXiv: [1210.6832 \[hep-ph\]](#).
- [81] M. Czakon, P. Fiedler and A. Mitov, *Total Top-Quark Pair-Production Cross Section at Hadron Colliders Through $O(\alpha_S^4)$* , *Phys. Rev. Lett.* **110** (2013) 252004, arXiv: [1303.6254 \[hep-ph\]](#).
- [82] M. Czakon and A. Mitov, *Top++: A program for the calculation of the top-pair cross-section at hadron colliders*, *Comput. Phys. Commun.* **185** (2014) 2930, arXiv: [1112.5675 \[hep-ph\]](#).
- [83] T. Gleisberg and S. Höche, *Comix, a new matrix element generator*, *JHEP* **12** (2008) 039, arXiv: [0808.3674 \[hep-ph\]](#).
- [84] F. Buccioni et al., *OpenLoops 2*, *Eur. Phys. J. C* **79** (2019) 866, arXiv: [1907.13071 \[hep-ph\]](#).
- [85] F. Cascioli, P. Maierhöfer and S. Pozzorini, *Scattering Amplitudes with Open Loops*, *Phys. Rev. Lett.* **108** (2012) 111601, arXiv: [1111.5206 \[hep-ph\]](#).
- [86] A. Denner, S. Dittmaier and L. Hofer, *COLLIER: A fortran-based complex one-loop library in extended regularizations*, *Comput. Phys. Commun.* **212** (2017) 220, arXiv: [1604.06792 \[hep-ph\]](#).
- [87] E. Re, *Single-top Wt -channel production matched with parton showers using the POWHEG method*, *Eur. Phys. J. C* **71** (2011) 1547, arXiv: [1009.2450 \[hep-ph\]](#).
- [88] P. Nason, *A new method for combining NLO QCD with shower Monte Carlo algorithms*, *JHEP* **11** (2004) 040, arXiv: [hep-ph/0409146](#).
- [89] S. Frixione, P. Nason and C. Oleari, *Matching NLO QCD computations with parton shower simulations: the POWHEG method*, *JHEP* **11** (2007) 070, arXiv: [0709.2092 \[hep-ph\]](#).
- [90] S. Alioli, P. Nason, C. Oleari and E. Re, *A general framework for implementing NLO calculations in shower Monte Carlo programs: the POWHEG BOX*, *JHEP* **06** (2010) 043, arXiv: [1002.2581 \[hep-ph\]](#).
- [91] T. Sjöstrand et al., *An introduction to PYTHIA 8.2*, *Comput. Phys. Commun.* **191** (2015) 159, arXiv: [1410.3012 \[hep-ph\]](#).

- [92] N. Kidonakis, *Two-loop soft anomalous dimensions for single top quark associated production with a W^- or H^-* , *Phys. Rev. D* **82** (2010) 054018, arXiv: [1005.4451 \[hep-ph\]](#).
- [93] N. Kidonakis, ‘Top Quark Production’, *Proceedings, Helmholtz International Summer School on Physics of Heavy Quarks and Hadrons (HQ 2013)* (JINR, Dubna, Russia, 15th–28th July 2013) 139, arXiv: [1311.0283 \[hep-ph\]](#).
- [94] M. Aliev et al., *HATHOR – HAdronic Top and Heavy quarks crOss section calculator*, *Comput. Phys. Commun.* **182** (2011) 1034, arXiv: [1007.1327 \[hep-ph\]](#).
- [95] P. Kant et al., *HatHor for single top-quark production: Updated predictions and uncertainty estimates for single top-quark production in hadronic collisions*, *Comput. Phys. Commun.* **191** (2015) 74, arXiv: [1406.4403 \[hep-ph\]](#).
- [96] C. Anastasiou, L. Dixon, K. Melnikov and F. Petriello, *High-precision QCD at hadron colliders: Electroweak gauge boson rapidity distributions at next-to-next-to leading order*, *Phys. Rev. D* **69** (2004) 094008, arXiv: [hep-ph/0312266](#).
- [97] D. de Florian et al., *Handbook of LHC Higgs Cross Sections: 4. Deciphering the Nature of the Higgs Sector*, (2016), arXiv: [1610.07922 \[hep-ph\]](#).
- [98] D. J. Lange, *The EvtGen particle decay simulation package*, *Nucl. Instrum. Meth. A* **462** (2001) 152.
- [99] ATLAS Collaboration, *ATLAS Pythia 8 tunes to 7 TeV data*, ATL-PHYS-PUB-2014-021, 2014, URL: <https://cds.cern.ch/record/1966419>.
- [100] NNPDF Collaboration, R. D. Ball et al., *Parton distributions with LHC data*, *Nucl. Phys. B* **867** (2013) 244, arXiv: [1207.1303 \[hep-ph\]](#).
- [101] T. Sjöstrand, S. Mrenna and P. Skands, *A brief introduction to PYTHIA 8.1*, *Comput. Phys. Commun.* **178** (2008) 852, arXiv: [0710.3820 \[hep-ph\]](#).
- [102] ATLAS Collaboration, *The Pythia 8 A3 tune description of ATLAS minimum bias and inelastic measurements incorporating the Donnachie–Landshoff diffractive model*, ATL-PHYS-PUB-2016-017, 2016, URL: <https://cds.cern.ch/record/2206965>.
- [103] ATLAS Collaboration, *The ATLAS Simulation Infrastructure*, *Eur. Phys. J. C* **70** (2010) 823, arXiv: [1005.4568 \[physics.ins-det\]](#).
- [104] S. Agostinelli et al., *GEANT4 – a simulation toolkit*, *Nucl. Instrum. Meth. A* **506** (2003) 250.
- [105] P. Artoisenet, R. Frederix, O. Mattelaer and R. Rietkerk, *Automatic spin-entangled decays of heavy resonances in Monte Carlo simulations*, *JHEP* **03** (2013) 015, arXiv: [1212.3460 \[hep-ph\]](#).
- [106] J. Butterworth et al., *PDF4LHC recommendations for LHC Run II*, *J. Phys. G* **43** (2016) 023001, arXiv: [1510.03865 \[hep-ph\]](#).
- [107] S. Frixione, E. Laenen, P. Motylinski, C. White and B. R. Webber, *Single-top hadroproduction in association with a W boson*, *JHEP* **07** (2008) 029, arXiv: [0805.3067 \[hep-ph\]](#).
- [108] ATLAS Collaboration, *Studies on top-quark Monte Carlo modelling for Top2016*, ATL-PHYS-PUB-2016-020, 2016, URL: <https://cds.cern.ch/record/2216168>.

- [109] ATLAS Collaboration, *Electron and photon performance measurements with the ATLAS detector using the 2015–2017 LHC proton–proton collision data*, *JINST* **14** (2019) P12006, arXiv: [1908.00005 \[hep-ex\]](#).
- [110] ATLAS Collaboration, *Muon reconstruction performance of the ATLAS detector in proton–proton collision data at $\sqrt{s} = 13$ TeV*, *Eur. Phys. J. C* **76** (2016) 292, arXiv: [1603.05598 \[hep-ex\]](#).
- [111] ATLAS Collaboration, *Muon reconstruction and identification efficiency in ATLAS using the full Run 2 pp collision data set at $\sqrt{s} = 13$ TeV*, *Eur. Phys. J. C* **81** (2021) 578, arXiv: [2012.00578 \[hep-ex\]](#).
- [112] M. Cacciari, G. P. Salam and G. Soyez, *The anti- k_t jet clustering algorithm*, *JHEP* **04** (2008) 063, arXiv: [0802.1189 \[hep-ph\]](#).
- [113] M. Cacciari, G. P. Salam and G. Soyez, *FastJet user manual*, *Eur. Phys. J. C* **72** (2012) 1896, arXiv: [1111.6097 \[hep-ph\]](#).
- [114] ATLAS Collaboration, *Jet reconstruction and performance using particle flow with the ATLAS Detector*, *Eur. Phys. J. C* **77** (2017) 466, arXiv: [1703.10485 \[hep-ex\]](#).
- [115] ATLAS Collaboration, *Jet energy scale and resolution measured in proton–proton collisions at $\sqrt{s} = 13$ TeV with the ATLAS detector*, *Eur. Phys. J. C* **81** (2021) 689, arXiv: [2007.02645 \[hep-ex\]](#).
- [116] ATLAS Collaboration, *Performance of pile-up mitigation techniques for jets in pp collisions at $\sqrt{s} = 8$ TeV using the ATLAS detector*, *Eur. Phys. J. C* **76** (2016) 581, arXiv: [1510.03823 \[hep-ex\]](#).
- [117] ATLAS Collaboration, *Forward jet vertex tagging using the particle flow algorithm*, ATL-PHYS-PUB-2019-026, 2019, URL: <https://cds.cern.ch/record/2683100>.
- [118] ATLAS Collaboration, *ATLAS b -jet identification performance and efficiency measurement with $t\bar{t}$ events in pp collisions at $\sqrt{s} = 13$ TeV*, *Eur. Phys. J. C* **79** (2019) 970, arXiv: [1907.05120 \[hep-ex\]](#).
- [119] ATLAS Collaboration, *ATLAS flavour-tagging algorithms for the LHC Run 2 pp collision dataset*, *Eur. Phys. J. C* **83** (2023) 681, arXiv: [2211.16345 \[physics.data-an\]](#).
- [120] ATLAS Collaboration, *Optimisation of large-radius jet reconstruction for the ATLAS detector in 13 TeV proton–proton collisions*, *Eur. Phys. J. C* **81** (2021) 334, arXiv: [2009.04986 \[hep-ex\]](#).
- [121] T. Barillari et al., *Local Hadronic Calibration*, ATL-LARG-PUB-2009-001-2, 2008, URL: <https://cds.cern.ch/record/1112035>.
- [122] D. Krohn, J. Thaler and L.-T. Wang, *Jet Trimming*, *JHEP* **02** (2010) 084, arXiv: [0912.1342 \[hep-ph\]](#).
- [123] ATLAS Collaboration, *In situ calibration of large-radius jet energy and mass in 13 TeV proton–proton collisions with the ATLAS detector*, *Eur. Phys. J. C* **79** (2019) 135, arXiv: [1807.09477 \[hep-ex\]](#).
- [124] ATLAS Collaboration, *Measurement of the ATLAS Detector Jet Mass Response using Forward Folding with 80fb^{-1} of $\sqrt{s} = 13$ TeV pp data*, ATLAS-CONF-2020-022, 2020, URL: <https://cds.cern.ch/record/2724442>.

- [125] ATLAS Collaboration, *Performance of top-quark and W-boson tagging with ATLAS in Run 2 of the LHC*, *Eur. Phys. J. C* **79** (2019) 375, arXiv: [1808.07858 \[hep-ex\]](#).
- [126] ATLAS Collaboration, *Boosted hadronic vector boson and top quark tagging with ATLAS using Run 2 data*, ATL-PHYS-PUB-2020-017, 2020, URL: <https://cds.cern.ch/record/2724149>.
- [127] D. Krohn, J. Thaler and L.-T. Wang, *Jets with Variable R*, *JHEP* **06** (2009) 059, arXiv: [0903.0392 \[hep-ph\]](#).
- [128] ATLAS Collaboration, *Reconstruction, Identification, and Calibration of hadronically decaying tau leptons with the ATLAS detector for the LHC Run 3 and reprocessed Run 2 data*, ATL-PHYS-PUB-2022-044, 2022, URL: <https://cds.cern.ch/record/2827111>.
- [129] ATLAS Collaboration, *Measurement of the tau lepton reconstruction and identification performance in the ATLAS experiment using pp collisions at $\sqrt{s} = 13$ TeV*, ATLAS-CONF-2017-029, 2017, URL: <https://cds.cern.ch/record/2261772>.
- [130] ATLAS Collaboration, *E_T^{miss} performance in the ATLAS detector using 2015–2016 LHC pp collisions*, ATLAS-CONF-2018-023, 2018, URL: <https://cds.cern.ch/record/2625233>.
- [131] ATLAS Collaboration, *Object-based missing transverse momentum significance in the ATLAS Detector*, ATLAS-CONF-2018-038, 2018, URL: <https://cds.cern.ch/record/2630948>.
- [132] M. Cacciari, G. P. Salam and G. Soyez, *The Catchment Area of Jets*, *JHEP* **04** (2008) 005, arXiv: [0802.1188 \[hep-ph\]](#).
- [133] F. Chollet et al., *Keras*, 2015, URL: <https://keras.io>.
- [134] H.-C. Cheng and Z. Han, *Minimal Kinematic Constraints and $m(T2)$* , *JHEP* **12** (2008) 063, arXiv: [0810.5178 \[hep-ph\]](#).
- [135] W. Verkerke and D. Kirkby, *The RooFit toolkit for data modeling*, 2003, arXiv: [physics/0306116 \[physics.data-an\]](#).
- [136] L. Moneta et al., *The RooStats Project*, PoS **ACAT2010** (2011) 057, arXiv: [1009.1003 \[physics.data-an\]](#).
- [137] M. Baak et al., *HistFitter software framework for statistical data analysis*, *Eur. Phys. J. C* **75** (2015) 153, arXiv: [1410.1280 \[hep-ex\]](#).
- [138] ATLAS Collaboration, *ATLAS simulation of boson plus jets processes in Run 2*, ATL-PHYS-PUB-2017-006, 2017, URL: <https://cds.cern.ch/record/2261937>.
- [139] ATLAS Collaboration, *Multi-boson simulation for 13 TeV ATLAS analyses*, ATL-PHYS-PUB-2016-002, 2016, URL: <https://cds.cern.ch/record/2119986>.
- [140] ATLAS Collaboration, *Modelling of the $t\bar{t}H$ and $t\bar{t}V$ ($V = W, Z$) processes for $\sqrt{s} = 13$ TeV ATLAS analyses*, ATL-PHYS-PUB-2016-005, 2016, URL: <https://cds.cern.ch/record/2120826>.
- [141] G. Cowan, K. Cranmer, E. Gross and O. Vitells, *Asymptotic formulae for likelihood-based tests of new physics*, *Eur. Phys. J. C* **71** (2011) 1554, arXiv: [1007.1727 \[physics.data-an\]](#), Erratum: *Eur. Phys. J. C* **73** (2013) 2501.

- [142] A. L. Read, *Presentation of search results: the CL_S technique*, *J. Phys. G* **28** (2002) 2693.
- [143] ATLAS Collaboration, *ATLAS Computing Acknowledgements*, ATL-SOFT-PUB-2023-001, 2023, URL: <https://cds.cern.ch/record/2869272>.

The ATLAS Collaboration

G. Aad ¹⁰³, E. Aakvaag ¹⁶, B. Abbott ¹²¹, K. Abeling ⁵⁵, N.J. Abicht ⁴⁹, S.H. Abidi ²⁹, M. Aboeela ⁴⁴, A. Aboulhorma ^{35e}, H. Abramowicz ¹⁵², H. Abreu ¹⁵¹, Y. Abulaiti ¹¹⁸, B.S. Acharya ^{69a,69b,1}, A. Ackermann ^{63a}, C. Adam Bourdarios ⁴, L. Adamczyk ^{86a}, S.V. Addepalli ²⁶, M.J. Addison ¹⁰², J. Adelman ¹¹⁶, A. Adiguzel ^{21c}, T. Adye ¹³⁵, A.A. Affolder ¹³⁷, Y. Afik ³⁹, M.N. Agaras ¹³, J. Agarwala ^{73a,73b}, A. Aggarwal ¹⁰¹, C. Agheorghiesei ^{27c}, A. Ahmad ³⁶, F. Ahmadov ^{38,y}, W.S. Ahmed ¹⁰⁵, S. Ahuja ⁹⁶, X. Ai ^{62e}, G. Aielli ^{76a,76b}, A. Aikot ¹⁶⁴, M. Ait Tamlihat ^{35e}, B. Aitbenchikh ^{35a}, I. Aizenberg ¹⁷⁰, M. Akbiyik ¹⁰¹, T.P.A. Åkesson ⁹⁹, A.V. Akimov ³⁷, D. Akiyama ¹⁶⁹, N.N. Akolkar ²⁴, S. Aktas ^{21a}, K. Al Khoury ⁴¹, G.L. Alberghi ^{23b}, J. Albert ¹⁶⁶, P. Albicocco ⁵³, G.L. Albouy ⁶⁰, S. Alderweireldt ⁵², Z.L. Alegria ¹²², M. Aleksa ³⁶, I.N. Aleksandrov ³⁸, C. Alexa ^{27b}, T. Alexopoulos ¹⁰, F. Alfonsi ^{23b}, M. Algren ⁵⁶, M. Alhroob ¹⁴², B. Ali ¹³³, H.M.J. Ali ⁹², S. Ali ¹⁴⁹, S.W. Alibocus ⁹³, M. Aliev ^{33c}, G. Alimonti ^{71a}, W. Alkakhki ⁵⁵, C. Allaire ⁶⁶, B.M.M. Allbrooke ¹⁴⁷, J.F. Allen ⁵², C.A. Allendes Flores ^{138f}, P.P. Allport ²⁰, A. Aloisio ^{72a,72b}, F. Alonso ⁹¹, C. Alpigiani ¹³⁹, M. Alvarez Estevez ¹⁰⁰, A. Alvarez Fernandez ¹⁰¹, M. Alves Cardoso ⁵⁶, M.G. Alviggi ^{72a,72b}, M. Aly ¹⁰², Y. Amaral Coutinho ^{83b}, A. Ambler ¹⁰⁵, C. Amelung ³⁶, M. Amerl ¹⁰², C.G. Ames ¹¹⁰, D. Amidei ¹⁰⁷, K.J. Amirie ¹⁵⁶, S.P. Amor Dos Santos ^{131a}, K.R. Amos ¹⁶⁴, V. Ananiev ¹²⁶, C. Anastopoulos ¹⁴⁰, T. Andeen ¹¹, J.K. Anders ³⁶, S.Y. Andrean ^{47a,47b}, A. Andreazza ^{71a,71b}, S. Angelidakis ⁹, A. Angerami ^{41,aa}, A.V. Anisenkov ³⁷, A. Annovi ^{74a}, C. Antel ⁵⁶, M.T. Anthony ¹⁴⁰, E. Antipov ¹⁴⁶, M. Antonelli ⁵³, F. Anulli ^{75a}, M. Aoki ⁸⁴, T. Aoki ¹⁵⁴, J.A. Aparisi Pozo ¹⁶⁴, M.A. Aparo ¹⁴⁷, L. Aperio Bella ⁴⁸, C. Appelt ¹⁸, A. Apyan ²⁶, S.J. Arbiol Val ⁸⁷, C. Arcangeletti ⁵³, A.T.H. Arce ⁵¹, E. Arena ⁹³, J-F. Arguin ¹⁰⁹, S. Argyropoulos ⁵⁴, J.-H. Arling ⁴⁸, O. Arnaez ⁴, H. Arnold ¹¹⁵, G. Artoni ^{75a,75b}, H. Asada ¹¹², K. Asai ¹¹⁹, S. Asai ¹⁵⁴, N.A. Asbah ³⁶, K. Assamagan ²⁹, R. Astalos ^{28a}, K.S.V. Astrand ⁹⁹, S. Atashi ¹⁶⁰, R.J. Atkin ^{33a}, M. Atkinson ¹⁶³, H. Atmani ^{35f}, P.A. Atlasiddha ¹²⁹, K. Augsten ¹³³, S. Auricchio ^{72a,72b}, A.D. Auriol ²⁰, V.A. Austrup ¹⁰², G. Avolio ³⁶, K. Axiotis ⁵⁶, G. Azuelos ^{109,ae}, D. Babal ^{28b}, H. Bachacou ¹³⁶, K. Bachas ^{153,p}, A. Bachi ³⁴, F. Backman ^{47a,47b}, A. Badae ³⁹, T.M. Baer ¹⁰⁷, P. Bagnaia ^{75a,75b}, M. Bahmani ¹⁸, D. Bahner ⁵⁴, K. Bai ¹²⁴, A.J. Bailey ¹⁶⁴, J.T. Baines ¹³⁵, L. Baines ⁹⁵, O.K. Baker ¹⁷³, E. Bakos ¹⁵, D. Bakshi Gupta ⁸, V. Balakrishnan ¹²¹, R. Balasubramanian ¹¹⁵, E.M. Baldin ³⁷, P. Balek ^{86a}, E. Ballabene ^{23b,23a}, F. Balli ¹³⁶, L.M. Baltes ^{63a}, W.K. Balunas ³², J. Balz ¹⁰¹, E. Banas ⁸⁷, M. Bandieramonte ¹³⁰, A. Bandyopadhyay ²⁴, S. Bansal ²⁴, L. Barak ¹⁵², M. Barakat ⁴⁸, E.L. Barberio ¹⁰⁶, D. Barberis ^{57b,57a}, M. Barbero ¹⁰³, M.Z. Barel ¹¹⁵, K.N. Barends ^{33a}, T. Barillari ¹¹¹, M-S. Barisits ³⁶, T. Barklow ¹⁴⁴, P. Baron ¹²³, D.A. Baron Moreno ¹⁰², A. Baroncelli ^{62a}, G. Barone ²⁹, A.J. Barr ¹²⁷, J.D. Barr ⁹⁷, F. Barreiro ¹⁰⁰, J. Barreiro Guimarães da Costa ^{14a}, U. Barron ¹⁵², M.G. Barros Teixeira ^{131a}, S. Barsov ³⁷, F. Bartels ^{63a}, R. Bartoldus ¹⁴⁴, A.E. Barton ⁹², P. Bartos ^{28a}, A. Basan ¹⁰¹, M. Baselga ⁴⁹, A. Bassalat ^{66,b}, M.J. Basso ^{157a}, R.L. Bates ⁵⁹, S. Batlamous ^{35e}, B. Batool ¹⁴², M. Battaglia ¹³⁷, D. Battulga ¹⁸, M. Bauce ^{75a,75b}, M. Bauer ³⁶, P. Bauer ²⁴, L.T. Bazzano Hurrell ³⁰, J.B. Beacham ⁵¹, T. Beau ¹²⁸, J.Y. Beauchamp ⁹¹, P.H. Beauchemin ¹⁵⁹, P. Bechtle ²⁴, H.P. Beck ^{19,o}, K. Becker ¹⁶⁸, A.J. Beddall ⁸², V.A. Bednyakov ³⁸, C.P. Bee ¹⁴⁶, L.J. Beemster ¹⁵, T.A. Beermann ³⁶, M. Begalli ^{83d}, M. Begel ²⁹, A. Behera ¹⁴⁶, J.K. Behr ⁴⁸, J.F. Beirer ³⁶, F. Beisiegel ²⁴, M. Belfkir ^{117b}, G. Bella ¹⁵², L. Bellagamba ^{23b}, A. Bellerive ³⁴, P. Bellos ²⁰, K. Beloborodov ³⁷, D. Bencheikroun ^{35a}, F. Bendebba ^{35a}, Y. Benhammou ¹⁵², K.C. Benkendorfer ⁶¹, L. Beresford ⁴⁸, M. Beretta ⁵³, E. Bergeaas Kuutmann ¹⁶², N. Berger ⁴,

B. Bergmann ¹³³, J. Beringer ^{17a}, G. Bernardi ⁵, C. Bernius ¹⁴⁴, F.U. Bernlochner ²⁴,
 F. Bernon ^{36,103}, A. Berrocal Guardia ¹³, T. Berry ⁹⁶, P. Berta ¹³⁴, A. Berthold ⁵⁰, S. Bethke ¹¹¹,
 A. Betti ^{75a,75b}, A.J. Bevan ⁹⁵, N.K. Bhalla ⁵⁴, M. Bhamjee ^{33c}, S. Bhatta ¹⁴⁶,
 D.S. Bhattacharya ¹⁶⁷, P. Bhattarai ¹⁴⁴, K.D. Bhide ⁵⁴, V.S. Bhopatkar ¹²², R.M. Bianchi ¹³⁰,
 G. Bianco ^{23b,23a}, O. Biebel ¹¹⁰, R. Bielski ¹²⁴, M. Biglietti ^{77a}, C.S. Billingsley ⁴⁴, M. Bindi ⁵⁵,
 A. Bingul ^{21b}, C. Bini ^{75a,75b}, A. Biondini ⁹³, C.J. Birch-sykes ¹⁰², G.A. Bird ³², M. Birman ¹⁷⁰,
 M. Biros ¹³⁴, S. Biryukov ¹⁴⁷, T. Bisanz ⁴⁹, E. Bisceglie ^{43b,43a}, J.P. Biswal ¹³⁵, D. Biswas ¹⁴²,
 K. Bjørke ¹²⁶, I. Bloch ⁴⁸, A. Blue ⁵⁹, U. Blumenschein ⁹⁵, J. Blumenthal ¹⁰¹,
 V.S. Bobrovnikov ³⁷, M. Boehler ⁵⁴, B. Boehm ¹⁶⁷, D. Bogavac ³⁶, A.G. Bogdanchikov ³⁷,
 C. Bohm ^{47a}, V. Boisvert ⁹⁶, P. Bokan ³⁶, T. Bold ^{86a}, M. Bomben ⁵, M. Bona ⁹⁵,
 M. Boonekamp ¹³⁶, C.D. Booth ⁹⁶, A.G. Borbély ⁵⁹, I.S. Bordulev ³⁷, H.M. Borecka-Bielska ¹⁰⁹,
 G. Borissov ⁹², D. Bortoletto ¹²⁷, D. Boscherini ^{23b}, M. Bosman ¹³, J.D. Bossio Sola ³⁶,
 K. Bouaouda ^{35a}, N. Bouchhar ¹⁶⁴, J. Boudreau ¹³⁰, E.V. Bouhova-Thacker ⁹², D. Boumediene ⁴⁰,
 R. Bouquet ^{57b,57a}, A. Boveia ¹²⁰, J. Boyd ³⁶, D. Boye ²⁹, I.R. Boyko ³⁸, J. Bracinik ²⁰,
 N. Brahimy ⁴, G. Brandt ¹⁷², O. Brandt ³², F. Braren ⁴⁸, B. Brau ¹⁰⁴, J.E. Brau ¹²⁴,
 R. Brenner ¹⁷⁰, L. Brenner ¹¹⁵, R. Brenner ¹⁶², S. Bressler ¹⁷⁰, D. Britton ⁵⁹, D. Britzger ¹¹¹,
 I. Brock ²⁴, G. Brooijmans ⁴¹, E. Brost ²⁹, L.M. Brown ¹⁶⁶, L.E. Bruce ⁶¹, T.L. Bruckler ¹²⁷,
 P.A. Bruckman de Renstrom ⁸⁷, B. Brüers ⁴⁸, A. Bruni ^{23b}, G. Bruni ^{23b}, M. Bruschi ^{23b},
 N. Bruscino ^{75a,75b}, T. Buanes ¹⁶, Q. Buat ¹³⁹, D. Buchin ¹¹¹, A.G. Buckley ⁵⁹, O. Bulekov ³⁷,
 B.A. Bullard ¹⁴⁴, S. Burdin ⁹³, C.D. Burgard ⁴⁹, A.M. Burger ³⁶, B. Burghgrave ⁸,
 O. Burlayenko ⁵⁴, J.T.P. Burr ³², C.D. Burton ¹¹, J.C. Burzynski ¹⁴³, E.L. Busch ⁴¹,
 V. Büscher ¹⁰¹, P.J. Bussey ⁵⁹, J.M. Butler ²⁵, C.M. Buttar ⁵⁹, J.M. Butterworth ⁹⁷,
 W. Buttinger ¹³⁵, C.J. Buxo Vazquez ¹⁰⁸, A.R. Buzykaev ³⁷, S. Cabrera Urbán ¹⁶⁴,
 L. Cadamuro ⁶⁶, D. Caforio ⁵⁸, H. Cai ¹³⁰, Y. Cai ^{14a,14e}, Y. Cai ^{14c}, V.M.M. Cairo ³⁶,
 O. Cakir ^{3a}, N. Calace ³⁶, P. Calafiura ^{17a}, G. Calderini ¹²⁸, P. Calfayan ⁶⁸, G. Callea ⁵⁹,
 L.P. Caloba ^{83b}, D. Calvet ⁴⁰, S. Calvet ⁴⁰, M. Calvetti ^{74a,74b}, R. Camacho Toro ¹²⁸,
 S. Camarda ³⁶, D. Camarero Munoz ²⁶, P. Camarri ^{76a,76b}, M.T. Camerlingo ^{72a,72b},
 D. Cameron ³⁶, C. Camincher ¹⁶⁶, M. Campanelli ⁹⁷, A. Camplani ⁴², V. Canale ^{72a,72b},
 A.C. Canbay ^{3a}, E. Canonero ⁹⁶, J. Cantero ¹⁶⁴, Y. Cao ¹⁶³, F. Capocasa ²⁶, M. Capua ^{43b,43a},
 A. Carbone ^{71a,71b}, R. Cardarelli ^{76a}, J.C.J. Cardenas ⁸, F. Cardillo ¹⁶⁴, G. Carducci ^{43b,43a},
 T. Carli ³⁶, G. Carlino ^{72a}, J.I. Carlotto ¹³, B.T. Carlson ^{130,q}, E.M. Carlson ^{166,157a},
 L. Carminati ^{71a,71b}, A. Carnelli ¹³⁶, M. Carnesale ^{75a,75b}, S. Caron ¹¹⁴, E. Carquin ^{138f},
 S. Carrá ^{71a}, G. Carratta ^{23b,23a}, A.M. Carroll ¹²⁴, T.M. Carter ⁵², M.P. Casado ^{13,i},
 M. Caspar ⁴⁸, F.L. Castillo ⁴, L. Castillo Garcia ¹³, V. Castillo Gimenez ¹⁶⁴, N.F. Castro ^{131a,131e},
 A. Catinaccio ³⁶, J.R. Catmore ¹²⁶, T. Cavaliere ⁴, V. Cavaliere ²⁹, N. Cavalli ^{23b,23a},
 Y.C. Cekmecelioglu ⁴⁸, E. Celebi ^{21a}, S. Cella ³⁶, F. Celli ¹²⁷, M.S. Centonze ^{70a,70b},
 V. Cepaitis ⁵⁶, K. Cerny ¹²³, A.S. Cerqueira ^{83a}, A. Cerri ¹⁴⁷, L. Cerrito ^{76a,76b}, F. Cerutti ^{17a},
 B. Cervato ¹⁴², A. Cervelli ^{23b}, G. Cesarini ⁵³, S.A. Cetin ⁸², D. Chakraborty ¹¹⁶, J. Chan ¹⁷¹,
 W.Y. Chan ¹⁵⁴, J.D. Chapman ³², E. Chapon ¹³⁶, B. Chargeishvili ^{150b}, D.G. Charlton ²⁰,
 M. Chatterjee ¹⁹, C. Chauhan ¹³⁴, Y. Che ^{14c}, S. Chekanov ⁶, S.V. Chekulaev ^{157a},
 G.A. Chelkov ^{38,a}, A. Chen ¹⁰⁷, B. Chen ¹⁵², B. Chen ¹⁶⁶, H. Chen ^{14c}, H. Chen ²⁹,
 J. Chen ^{62c}, J. Chen ¹⁴³, M. Chen ¹²⁷, S. Chen ¹⁵⁴, S.J. Chen ^{14c}, X. Chen ^{62c,136},
 X. Chen ^{14b,ad}, Y. Chen ^{62a}, C.L. Cheng ¹⁷¹, H.C. Cheng ^{64a}, S. Cheong ¹⁴⁴, A. Cheplakov ³⁸,
 E. Cheremushkina ⁴⁸, E. Cherepanova ¹¹⁵, R. Cherkaoui El Moursli ^{35e}, E. Cheu ⁷, K. Cheung ⁶⁵,
 L. Chevalier ¹³⁶, V. Chiarella ⁵³, G. Chiarelli ^{74a}, N. Chiedde ¹⁰³, G. Chiodini ^{70a},
 A.S. Chisholm ²⁰, A. Chitan ^{27b}, M. Chitishvili ¹⁶⁴, M.V. Chizhov ³⁸, K. Choi ¹¹, Y. Chou ¹³⁹,
 E.Y.S. Chow ¹¹⁴, K.L. Chu ¹⁷⁰, M.C. Chu ^{64a}, X. Chu ^{14a,14e}, J. Chudoba ¹³²,

J.J. Chwastowski ⁸⁷, D. Cieri ¹¹¹, K.M. Ciesla ^{86a}, V. Cindro ⁹⁴, A. Ciocio ^{17a}, F. Cirotto ^{72a,72b}, Z.H. Citron ¹⁷⁰, M. Citterio ^{71a}, D.A. Ciubotaru ^{27b}, A. Clark ⁵⁶, P.J. Clark ⁵², C. Clarry ¹⁵⁶, J.M. Clavijo Columbie ⁴⁸, S.E. Clawson ⁴⁸, C. Clement ^{47a,47b}, J. Clercx ⁴⁸, Y. Coadou ¹⁰³, M. Cobal ^{69a,69c}, A. Coccaro ^{57b}, R.F. Coelho Barrue ^{131a}, R. Coelho Lopes De Sa ¹⁰⁴, S. Coelli ^{71a}, B. Cole ⁴¹, J. Collot ⁶⁰, P. Conde Muiño ^{131a,131g}, M.P. Connell ^{33c}, S.H. Connell ^{33c}, E.I. Conroy ¹²⁷, F. Conventi ^{72a,af}, H.G. Cooke ²⁰, A.M. Cooper-Sarkar ¹²⁷, A. Cordeiro Oudot Choi ¹²⁸, L.D. Corpe ⁴⁰, M. Corradi ^{75a,75b}, F. Corriveau ^{105,w}, A. Cortes-Gonzalez ¹⁸, M.J. Costa ¹⁶⁴, F. Costanza ⁴, D. Costanzo ¹⁴⁰, B.M. Cote ¹²⁰, G. Cowan ⁹⁶, K. Cranmer ¹⁷¹, D. Cremonini ^{23b,23a}, S. Crépe-Renaudin ⁶⁰, F. Crescioli ¹²⁸, M. Cristinziani ¹⁴², M. Cristoforetti ^{78a,78b}, V. Croft ¹¹⁵, J.E. Crosby ¹²², G. Crosetti ^{43b,43a}, A. Cueto ¹⁰⁰, T. Cuhadar Donszelmann ¹⁶⁰, H. Cui ^{14a,14e}, Z. Cui ⁷, W.R. Cunningham ⁵⁹, F. Curcio ¹⁶⁴, J.R. Curran ⁵², P. Czodrowski ³⁶, M.M. Czurylo ³⁶, M.J. Da Cunha Sargedas De Sousa ^{57b,57a}, J.V. Da Fonseca Pinto ^{83b}, C. Da Via ¹⁰², W. Dabrowski ^{86a}, T. Dado ⁴⁹, S. Dahbi ¹⁴⁹, T. Dai ¹⁰⁷, D. Dal Santo ¹⁹, C. Dallapiccola ¹⁰⁴, M. Dam ⁴², G. D'amen ²⁹, V. D'Amico ¹¹⁰, J. Damp ¹⁰¹, J.R. Dandoy ³⁴, M. Danninger ¹⁴³, V. Dao ³⁶, G. Darbo ^{57b}, S. Darmora ⁶, S.J. Das ^{29,ag}, S. D'Auria ^{71a,71b}, A. D'avanzo ^{72a,72b}, C. David ^{33a}, T. Davidek ¹³⁴, B. Davis-Purcell ³⁴, I. Dawson ⁹⁵, H.A. Day-hall ¹³³, K. De ⁸, R. De Asmundis ^{72a}, N. De Biase ⁴⁸, S. De Castro ^{23b,23a}, N. De Groot ¹¹⁴, P. de Jong ¹¹⁵, H. De la Torre ¹¹⁶, A. De Maria ^{14c}, A. De Salvo ^{75a}, U. De Sanctis ^{76a,76b}, F. De Santis ^{70a,70b}, A. De Santo ¹⁴⁷, J.B. De Vivie De Regie ⁶⁰, D.V. Dedovich ³⁸, J. Degens ⁹³, A.M. Deiana ⁴⁴, F. Del Corso ^{23b,23a}, J. Del Peso ¹⁰⁰, F. Del Rio ^{63a}, L. Delagrangé ¹²⁸, F. Deliot ¹³⁶, C.M. Delitzsch ⁴⁹, M. Della Pietra ^{72a,72b}, D. Della Volpe ⁵⁶, A. Dell'Acqua ³⁶, L. Dell'Asta ^{71a,71b}, M. Delmastro ⁴, P.A. Delsart ⁶⁰, S. Demers ¹⁷³, M. Demichev ³⁸, S.P. Denisov ³⁷, L. D'Eramo ⁴⁰, D. Derendarz ⁸⁷, F. Derue ¹²⁸, P. Dervan ⁹³, K. Desch ²⁴, C. Deutsch ²⁴, F.A. Di Bello ^{57b,57a}, A. Di Ciaccio ^{76a,76b}, L. Di Ciaccio ⁴, A. Di Domenico ^{75a,75b}, C. Di Donato ^{72a,72b}, A. Di Girolamo ³⁶, G. Di Gregorio ³⁶, A. Di Luca ^{78a,78b}, B. Di Micco ^{77a,77b}, R. Di Nardo ^{77a,77b}, M. Diamantopoulou ³⁴, F.A. Dias ¹¹⁵, T. Dias Do Vale ¹⁴³, M.A. Diaz ^{138a,138b}, F.G. Diaz Capriles ²⁴, M. Didenko ¹⁶⁴, E.B. Diehl ¹⁰⁷, S. Díez Cornell ⁴⁸, C. Diez Pardos ¹⁴², C. Dimitriadi ^{162,24}, A. Dimitrievska ^{17a}, J. Dingfelder ²⁴, I-M. Dinu ^{27b}, S.J. Dittmeier ^{63b}, F. Dittus ³⁶, M. Divisek ¹³⁴, F. Djama ¹⁰³, T. Djobava ^{150b}, C. Doglioni ^{102,99}, A. Dohnalova ^{28a}, J. Dolejsi ¹³⁴, Z. Dolezal ¹³⁴, K.M. Dona ³⁹, M. Donadelli ^{83c}, B. Dong ¹⁰⁸, J. Donini ⁴⁰, A. D'Onofrio ^{72a,72b}, M. D'Onofrio ⁹³, J. Dopke ¹³⁵, A. Doria ^{72a}, N. Dos Santos Fernandes ^{131a}, P. Dougan ¹⁰², M.T. Dova ⁹¹, A.T. Doyle ⁵⁹, M.A. Draguet ¹²⁷, E. Dreyer ¹⁷⁰, I. Drivas-koulouris ¹⁰, M. Drnevich ¹¹⁸, M. Drozdova ⁵⁶, D. Du ^{62a}, T.A. du Pree ¹¹⁵, F. Dubinin ³⁷, M. Dubovsky ^{28a}, E. Duchovni ¹⁷⁰, G. Duckeck ¹¹⁰, O.A. Ducu ^{27b}, D. Duda ⁵², A. Dudarev ³⁶, E.R. Duden ²⁶, M. D'uffizi ¹⁰², L. DufLOT ⁶⁶, M. Dührssen ³⁶, A.E. Dumitriu ^{27b}, M. Dunford ^{63a}, S. Dungs ⁴⁹, K. Dunne ^{47a,47b}, A. Duperrin ¹⁰³, H. Duran Yildiz ^{3a}, M. Düren ⁵⁸, A. Durglishvili ^{150b}, B.L. Dwyer ¹¹⁶, G.I. Dyckes ^{17a}, M. Dyndal ^{86a}, B.S. Dziedzic ⁸⁷, Z.O. Earnshaw ¹⁴⁷, G.H. Eberwein ¹²⁷, B. Eckerova ^{28a}, S. Eggebrecht ⁵⁵, E. Egidio Purcino De Souza ¹²⁸, L.F. Ehrke ⁵⁶, G. Eigen ¹⁶, K. Einsweiler ^{17a}, T. Ekelof ¹⁶², P.A. Ekman ⁹⁹, S. El Farkh ^{35b}, Y. El Ghazali ^{35b}, H. El Jarrari ³⁶, A. El Moussaouy ¹⁰⁹, V. Ellajosyula ¹⁶², M. Ellert ¹⁶², F. Ellinghaus ¹⁷², N. Ellis ³⁶, J. Elmsheuser ²⁹, M. Elsayy ^{117a}, M. Elsing ³⁶, D. Emeliyanov ¹³⁵, Y. Enari ¹⁵⁴, I. Ene ^{17a}, S. Epari ¹³, P.A. Erland ⁸⁷, M. Errenst ¹⁷², M. Escalier ⁶⁶, C. Escobar ¹⁶⁴, E. Etzion ¹⁵², G. Evans ^{131a}, H. Evans ⁶⁸, L.S. Evans ⁹⁶, A. Ezhilov ³⁷, S. Ezzarqtouni ^{35a}, F. Fabbri ^{23b,23a}, L. Fabbri ^{23b,23a}, G. Facini ⁹⁷, V. Fadeyev ¹³⁷, R.M. Fakhruddinov ³⁷, D. Fakoudis ¹⁰¹, S. Falciano ^{75a}, L.F. Falda Ulhoa Coelho ³⁶, P.J. Falke ²⁴, J. Faltova ¹³⁴,

C. Fan ¹⁶³, Y. Fan ^{14a}, Y. Fang ^{14a,14e}, M. Fanti ^{71a,71b}, M. Faraj ^{69a,69b}, Z. Farazpay ⁹⁸,
 A. Farbin ⁸, A. Farilla ^{77a}, T. Farooque ¹⁰⁸, S.M. Farrington ⁵², F. Fassi ^{35e}, D. Fassouliotis ⁹,
 M. Faucci Giannelli ^{76a,76b}, W.J. Fawcett ³², L. Fayard ⁵⁶, P. Federic ¹³⁴, P. Federicova ¹³²,
 O.L. Fedin ^{37,a}, M. Feickert ¹⁷¹, L. Feligioni ¹⁰³, D.E. Fellers ¹²⁴, C. Feng ^{62b}, M. Feng ^{14b},
 Z. Feng ¹¹⁵, M.J. Fenton ¹⁶⁰, L. Ferencz ⁴⁸, R.A.M. Ferguson ⁹², S.I. Fernandez Luengo ^{138f},
 P. Fernandez Martinez ¹³, M.J.V. Fernoux ¹⁰³, J. Ferrando ⁹², A. Ferrari ¹⁶², P. Ferrari ^{115,114},
 R. Ferrari ^{73a}, D. Ferrere ⁵⁶, C. Ferretti ¹⁰⁷, F. Fiedler ¹⁰¹, P. Fiedler ¹³³, A. Filipčić ⁹⁴,
 E.K. Filmer ¹, F. Filthaut ¹¹⁴, M.C.N. Fiolhais ^{131a,131c,c}, L. Fiorini ¹⁶⁴, W.C. Fisher ¹⁰⁸,
 T. Fitschen ¹⁰², P.M. Fitzhugh ¹³⁶, I. Fleck ¹⁴², P. Fleischmann ¹⁰⁷, T. Flick ¹⁷², M. Flores ^{33d,ab},
 L.R. Flores Castillo ^{64a}, L. Flores Sanz De Acedo ³⁶, F.M. Follega ^{78a,78b}, N. Fomin ¹⁶,
 J.H. Foo ¹⁵⁶, A. Formica ¹³⁶, A.C. Forti ¹⁰², E. Fortin ³⁶, A.W. Fortman ^{17a}, M.G. Foti ^{17a},
 L. Fountas ^{9j}, D. Fournier ⁶⁶, H. Fox ⁹², P. Francavilla ^{74a,74b}, S. Francescato ⁶¹,
 S. Franchellucci ⁵⁶, M. Franchini ^{23b,23a}, S. Franchino ^{63a}, D. Francis ³⁶, L. Franco ¹¹⁴,
 V. Franco Lima ³⁶, L. Franconi ⁴⁸, M. Franklin ⁶¹, G. Frattari ²⁶, W.S. Freund ^{83b}, Y.Y. Frid ¹⁵²,
 J. Friend ⁵⁹, N. Fritzsche ⁵⁰, A. Froch ⁵⁴, D. Froidevaux ³⁶, J.A. Frost ¹²⁷, Y. Fu ^{62a},
 S. Fuenzalida Garrido ^{138f}, M. Fujimoto ¹⁰³, K.Y. Fung ^{64a}, E. Furtado De Simas Filho ^{83e},
 M. Furukawa ¹⁵⁴, J. Fuster ¹⁶⁴, A. Gabrielli ^{23b,23a}, A. Gabrielli ¹⁵⁶, P. Gadow ³⁶,
 G. Gagliardi ^{57b,57a}, L.G. Gagnon ^{17a}, S. Galantzan ¹⁵², E.J. Gallas ¹²⁷, B.J. Gallop ¹³⁵,
 K.K. Gan ¹²⁰, S. Ganguly ¹⁵⁴, Y. Gao ⁵², F.M. Garay Walls ^{138a,138b}, B. Garcia ²⁹, C. García ¹⁶⁴,
 A. Garcia Alonso ¹¹⁵, A.G. Garcia Caffaro ¹⁷³, J.E. García Navarro ¹⁶⁴, M. Garcia-Sciveres ^{17a},
 G.L. Gardner ¹²⁹, R.W. Gardner ³⁹, N. Garelli ¹⁵⁹, D. Garg ⁸⁰, R.B. Garg ^{144,m}, J.M. Gargan ⁵²,
 C.A. Garner ¹⁵⁶, C.M. Garvey ^{33a}, P. Gaspar ^{83b}, V.K. Gassmann ¹⁵⁹, G. Gaudio ^{73a}, V. Gautam ¹³,
 P. Gauzzi ^{75a,75b}, I.L. Gavrilenko ³⁷, A. Gavriilyuk ³⁷, C. Gay ¹⁶⁵, G. Gaycken ⁴⁸, E.N. Gazis ¹⁰,
 A.A. Geanta ^{27b}, C.M. Gee ¹³⁷, A. Gekow ¹²⁰, C. Gemme ^{57b}, M.H. Genest ⁶⁰, A.D. Gentry ¹¹³,
 S. George ⁹⁶, W.F. George ²⁰, T. Geralis ⁴⁶, P. Gessinger-Befurt ³⁶, M.E. Geyik ¹⁷²,
 M. Ghani ¹⁶⁸, K. Ghorbanian ⁹⁵, A. Ghosal ¹⁴², A. Ghosh ¹⁶⁰, A. Ghosh ⁷, B. Giacobbe ^{23b},
 S. Giagu ^{75a,75b}, T. Giani ¹¹⁵, P. Giannetti ^{74a}, A. Giannini ^{62a}, S.M. Gibson ⁹⁶, M. Gignac ¹³⁷,
 D.T. Gil ^{86b}, A.K. Gilbert ^{86a}, B.J. Gilbert ⁴¹, D. Gillberg ³⁴, G. Gilles ¹¹⁵, L. Ginabat ¹²⁸,
 D.M. Gingrich ^{2,ae}, M.P. Giordani ^{69a,69c}, P.F. Giraud ¹³⁶, G. Giugliarelli ^{69a,69c}, D. Giugni ^{71a},
 F. Giuli ³⁶, I. Gkialas ^{9j}, L.K. Gladilin ³⁷, C. Glasman ¹⁰⁰, G.R. Gledhill ¹²⁴, G. Glemža ⁴⁸,
 M. Glisic ¹²⁴, I. Gnesi ^{43b,f}, Y. Go ²⁹, M. Goblirsch-Kolb ³⁶, B. Gocke ⁴⁹, D. Godin ¹⁰⁹,
 B. Gokturk ^{21a}, S. Goldfarb ¹⁰⁶, T. Golling ⁵⁶, M.G.D. Gololo ^{33g}, D. Golubkov ³⁷,
 J.P. Gombas ¹⁰⁸, A. Gomes ^{131a,131b}, G. Gomes Da Silva ¹⁴², A.J. Gomez Delegido ¹⁶⁴,
 R. Gonçalves ^{131a,131c}, L. Gonella ²⁰, A. Gongadze ^{150c}, F. Gonnella ²⁰, J.L. Gonski ¹⁴⁴,
 R.Y. González Andana ⁵², S. González de la Hoz ¹⁶⁴, R. Gonzalez Lopez ⁹³,
 C. Gonzalez Renteria ^{17a}, M.V. Gonzalez Rodrigues ⁴⁸, R. Gonzalez Suarez ¹⁶²,
 S. Gonzalez-Sevilla ⁵⁶, L. Goossens ³⁶, B. Gorini ³⁶, E. Gorini ^{70a,70b}, A. Gorišek ⁹⁴,
 T.C. Gosart ¹²⁹, A.T. Goshaw ⁵¹, M.I. Gostkin ³⁸, S. Goswami ¹²², C.A. Gottardo ³⁶,
 S.A. Gotz ¹¹⁰, M. Gouighri ^{35b}, V. Goumarre ⁴⁸, A.G. Goussiou ¹³⁹, N. Govender ^{33c},
 I. Grabowska-Bold ^{86a}, K. Graham ³⁴, E. Gramstad ¹²⁶, S. Grancagnolo ^{70a,70b}, C.M. Grant ^{1,136},
 P.M. Gravila ^{27f}, F.G. Gravili ^{70a,70b}, H.M. Gray ^{17a}, M. Greco ^{70a,70b}, C. Grefe ²⁴,
 I.M. Gregor ⁴⁸, P. Grenier ¹⁴⁴, S.G. Grewe ¹¹¹, A.A. Grillo ¹³⁷, K. Grimm ³¹, S. Grinstein ^{13,s},
 J.-F. Grivaz ⁶⁶, E. Gross ¹⁷⁰, J. Grosse-Knetter ⁵⁵, J.C. Grundy ¹²⁷, L. Guan ¹⁰⁷, C. Gubbels ¹⁶⁵,
 J.G.R. Guerrero Rojas ¹⁶⁴, G. Guerrieri ^{69a,69c}, F. Guescini ¹¹¹, R. Gugel ¹⁰¹, J.A.M. Guhit ¹⁰⁷,
 A. Guida ¹⁸, E. Guilloton ¹⁶⁸, S. Guindon ³⁶, F. Guo ^{14a,14e}, J. Guo ^{62c}, L. Guo ⁴⁸, Y. Guo ¹⁰⁷,
 R. Gupta ⁴⁸, R. Gupta ¹³⁰, S. Gurbuz ²⁴, S.S. Gurdasani ⁵⁴, G. Gustavino ³⁶, M. Guth ⁵⁶,
 P. Gutierrez ¹²¹, L.F. Gutierrez Zagazeta ¹²⁹, M. Gutsche ⁵⁰, C. Gutschow ⁹⁷, C. Gwenlan ¹²⁷,

C.B. Gwilliam ⁹³, E.S. Haaland ¹²⁶, A. Haas ¹¹⁸, M. Habedank ⁴⁸, C. Haber ^{17a},
 H.K. Hadavand ⁸, A. Hadeef ⁵⁰, S. Hadzic ¹¹¹, A.I. Hagan ⁹², J.J. Hahn ¹⁴², E.H. Haines ⁹⁷,
 M. Haleem ¹⁶⁷, J. Haley ¹²², J.J. Hall ¹⁴⁰, G.D. Hallelwell ¹⁰³, L. Halser ¹⁹, K. Hamano ¹⁶⁶,
 M. Hamer ²⁴, G.N. Hamity ⁵², E.J. Hampshire ⁹⁶, J. Han ^{62b}, K. Han ^{62a}, L. Han ^{14c},
 L. Han ^{62a}, S. Han ^{17a}, Y.F. Han ¹⁵⁶, K. Hanagaki ⁸⁴, M. Hance ¹³⁷, D.A. Hangal ⁴¹,
 H. Hanif ¹⁴³, M.D. Hank ¹²⁹, J.B. Hansen ⁴², P.H. Hansen ⁴², K. Hara ¹⁵⁸, D. Harada ⁵⁶,
 T. Harenberg ¹⁷², S. Harkusha ³⁷, M.L. Harris ¹⁰⁴, Y.T. Harris ¹²⁷, J. Harrison ¹³,
 N.M. Harrison ¹²⁰, P.F. Harrison ¹⁶⁸, N.M. Hartman ¹¹¹, N.M. Hartmann ¹¹⁰, Y. Hasegawa ¹⁴¹,
 S. Hassan ¹⁶, R. Hauser ¹⁰⁸, C.M. Hawkes ²⁰, R.J. Hawkings ³⁶, Y. Hayashi ¹⁵⁴,
 S. Hayashida ¹¹², D. Hayden ¹⁰⁸, C. Hayes ¹⁰⁷, R.L. Hayes ¹¹⁵, C.P. Hays ¹²⁷, J.M. Hays ⁹⁵,
 H.S. Hayward ⁹³, F. He ^{62a}, M. He ^{14a,14e}, Y. He ¹⁵⁵, Y. He ⁴⁸, Y. He ⁹⁷, N.B. Heatley ⁹⁵,
 V. Hedberg ⁹⁹, A.L. Heggelund ¹²⁶, N.D. Hehir ^{95,*}, C. Heidegger ⁵⁴, K.K. Heidegger ⁵⁴,
 W.D. Heidorn ⁸¹, J. Heilman ³⁴, S. Heim ⁴⁸, T. Heim ^{17a}, J.G. Heinlein ¹²⁹, J.J. Heinrich ¹²⁴,
 L. Heinrich ^{111,ac}, J. Hejbal ¹³², A. Held ¹⁷¹, S. Hellesund ¹⁶, C.M. Helling ¹⁶⁵,
 S. Hellman ^{47a,47b}, R.C.W. Henderson ⁹², L. Henkelmann ³², A.M. Henriques Correia ³⁶, H. Herde ⁹⁹,
 Y. Hernández Jiménez ¹⁴⁶, L.M. Herrmann ²⁴, T. Herrmann ⁵⁰, G. Herten ⁵⁴, R. Hertenberger ¹¹⁰,
 L. Hervas ³⁶, M.E. Hesping ¹⁰¹, N.P. Hessey ^{157a}, E. Hill ¹⁵⁶, S.J. Hillier ²⁰, J.R. Hinds ¹⁰⁸,
 F. Hinterkeuser ²⁴, M. Hirose ¹²⁵, S. Hirose ¹⁵⁸, D. Hirschbuehl ¹⁷², T.G. Hitchings ¹⁰²,
 B. Hiti ⁹⁴, J. Hobbs ¹⁴⁶, R. Hobincu ^{27e}, N. Hod ¹⁷⁰, M.C. Hodgkinson ¹⁴⁰,
 B.H. Hodgkinson ¹²⁷, A. Hoecker ³⁶, D.D. Hofer ¹⁰⁷, J. Hofer ⁴⁸, T. Holm ²⁴, M. Holzbock ¹¹¹,
 L.B.A.H. Hommels ³², B.P. Honan ¹⁰², J. Hong ^{62c}, T.M. Hong ¹³⁰, B.H. Hooberman ¹⁶³,
 W.H. Hopkins ⁶, Y. Horii ¹¹², S. Hou ¹⁴⁹, A.S. Howard ⁹⁴, J. Howarth ⁵⁹, J. Hoya ⁶,
 M. Hrabovsky ¹²³, A. Hrynevich ⁴⁸, T. Hryn'ova ⁴, P.J. Hsu ⁶⁵, S.-C. Hsu ¹³⁹, Q. Hu ^{62a},
 S. Huang ^{64b}, X. Huang ^{14a,14e}, Y. Huang ¹⁴⁰, Y. Huang ^{14a}, Z. Huang ¹⁰², Z. Hubacek ¹³³,
 M. Huebner ²⁴, F. Huegging ²⁴, T.B. Huffman ¹²⁷, C.A. Hugli ⁴⁸, M. Huhtinen ³⁶,
 S.K. Huiberts ¹⁶, R. Hulsken ¹⁰⁵, N. Huseynov ¹², J. Huston ¹⁰⁸, J. Huth ⁶¹, R. Hyneman ¹⁴⁴,
 G. Iacobucci ⁵⁶, G. Iakovidis ²⁹, I. Ibragimov ¹⁴², L. Iconomidou-Fayard ⁶⁶, J.P. Iddon ³⁶,
 P. Iengo ^{72a,72b}, R. Iguchi ¹⁵⁴, T. Iizawa ¹²⁷, Y. Ikegami ⁸⁴, N. Ilic ¹⁵⁶, H. Imam ^{35a},
 M. Ince Lezki ⁵⁶, T. Ingebretsen Carlson ^{47a,47b}, G. Introzzi ^{73a,73b}, M. Iodice ^{77a},
 V. Ippolito ^{75a,75b}, R.K. Irwin ⁹³, M. Ishino ¹⁵⁴, W. Islam ¹⁷¹, C. Issever ^{18,48}, S. Istin ^{21a,ai},
 H. Ito ¹⁶⁹, R. Iuppa ^{78a,78b}, A. Ivina ¹⁷⁰, J.M. Izen ⁴⁵, V. Izzo ^{72a}, P. Jacka ^{132,133}, P. Jackson ¹,
 B.P. Jaeger ¹⁴³, C.S. Jagfeld ¹¹⁰, G. Jain ^{157a}, P. Jain ⁵⁴, K. Jakobs ⁵⁴, T. Jakoubek ¹⁷⁰,
 J. Jamieson ⁵⁹, K.W. Janas ^{86a}, M. Javurkova ¹⁰⁴, L. Jeanty ¹²⁴, J. Jejelava ^{150a,z}, P. Jenni ^{54,g},
 C.E. Jessiman ³⁴, C. Jia ^{62b}, J. Jia ¹⁴⁶, X. Jia ⁶¹, X. Jia ^{14a,14e}, Z. Jia ^{14c}, S. Jiggins ⁴⁸,
 J. Jimenez Pena ¹³, S. Jin ^{14c}, A. Jinaru ^{27b}, O. Jinnouchi ¹⁵⁵, P. Johansson ¹⁴⁰, K.A. Johns ⁷,
 J.W. Johnson ¹³⁷, D.M. Jones ¹⁴⁷, E. Jones ⁴⁸, P. Jones ³², R.W.L. Jones ⁹², T.J. Jones ⁹³,
 H.L. Joos ^{55,36}, R. Joshi ¹²⁰, J. Jovicevic ¹⁵, X. Ju ^{17a}, J.J. Junggeburth ¹⁰⁴, T. Junkermann ^{63a},
 A. Juste Rozas ^{13,s}, M.K. Juzek ⁸⁷, S. Kabana ^{138e}, A. Kaczmarska ⁸⁷, M. Kado ¹¹¹,
 H. Kagan ¹²⁰, M. Kagan ¹⁴⁴, A. Kahn ⁴¹, A. Kahn ¹²⁹, C. Kahra ¹⁰¹, T. Kaji ¹⁵⁴,
 E. Kajomovitz ¹⁵¹, N. Kakati ¹⁷⁰, I. Kalaitzidou ⁵⁴, C.W. Kalderon ²⁹, N.J. Kang ¹³⁷,
 D. Kar ^{33g}, K. Karava ¹²⁷, M.J. Kareem ^{157b}, E. Karentzos ⁵⁴, I. Karknias ¹⁵³, O. Karkout ¹¹⁵,
 S.N. Karpov ³⁸, Z.M. Karpova ³⁸, V. Kartvelishvili ⁹², A.N. Karyukhin ³⁷, E. Kasimi ¹⁵³,
 J. Katzy ⁴⁸, S. Kaur ³⁴, K. Kawade ¹⁴¹, M.P. Kawale ¹²¹, C. Kawamoto ⁸⁸, T. Kawamoto ^{62a},
 E.F. Kay ³⁶, F.I. Kaya ¹⁵⁹, S. Kazakos ¹⁰⁸, V.F. Kazanin ³⁷, Y. Ke ¹⁴⁶, J.M. Keaveney ^{33a},
 R. Keeler ¹⁶⁶, G.V. Kehris ⁶¹, J.S. Keller ³⁴, A.S. Kelly ⁹⁷, J.J. Kempster ¹⁴⁷, P.D. Kennedy ¹⁰¹,
 O. Kepka ¹³², B.P. Kerridge ¹³⁵, S. Kersten ¹⁷², B.P. Kerševan ⁹⁴, L. Keszeghova ^{28a},
 S. Ketabchi Haghghat ¹⁵⁶, R.A. Khan ¹³⁰, A. Khanov ¹²², A.G. Kharlamov ³⁷, T. Kharlamova ³⁷,

E.E. Khoda ¹³⁹, M. Kholodenko ³⁷, T.J. Khoo ¹⁸, G. Khoriauli ¹⁶⁷, J. Khubua ^{150b},
 Y.A.R. Khwaira ⁶⁶, B. Kibirige^{33g}, A. Kilgallon ¹²⁴, D.W. Kim ^{47a,47b}, Y.K. Kim ³⁹,
 N. Kimura ⁹⁷, M.K. Kingston ⁵⁵, A. Kirchhoff ⁵⁵, C. Kirfel ²⁴, F. Kirfel ²⁴, J. Kirk ¹³⁵,
 A.E. Kiryunin ¹¹¹, C. Kitsaki ¹⁰, O. Kivernyk ²⁴, M. Klassen ^{63a}, C. Klein ³⁴, L. Klein ¹⁶⁷,
 M.H. Klein ⁴⁴, S.B. Klein ⁵⁶, U. Klein ⁹³, P. Klimek ³⁶, A. Klimentov ²⁹, T. Klioutchnikova ³⁶,
 P. Kluit ¹¹⁵, S. Kluth ¹¹¹, E. Kneringer ⁷⁹, T.M. Knight ¹⁵⁶, A. Knue ⁴⁹, R. Kobayashi ⁸⁸,
 D. Kobylanski ¹⁷⁰, S.F. Koch ¹²⁷, M. Kocian ¹⁴⁴, P. Kodyš ¹³⁴, D.M. Koeck ¹²⁴,
 P.T. Koenig ²⁴, T. Koffas ³⁴, O. Kolay ⁵⁰, I. Koletsou ⁴, T. Komarek ¹²³, K. Köneke ⁵⁴,
 A.X.Y. Kong ¹, T. Kono ¹¹⁹, N. Konstantinidis ⁹⁷, P. Kontaxakis ⁵⁶, B. Konya ⁹⁹,
 R. Kopeliński ⁴¹, S. Koperny ^{86a}, K. Korcyl ⁸⁷, K. Kordas ^{153,e}, A. Korn ⁹⁷, S. Korn ⁵⁵,
 I. Korolkov ¹³, N. Korotkova ³⁷, B. Kortman ¹¹⁵, O. Kortner ¹¹¹, S. Kortner ¹¹¹,
 W.H. Kostecka ¹¹⁶, V.V. Kostyukhin ¹⁴², A. Kotsokhechagia ¹³⁶, A. Kotwal ⁵¹, A. Koulouris ³⁶,
 A. Kourkoumeli-Charalampidi ^{73a,73b}, C. Kourkoumelis ⁹, E. Kourlitis ^{111,ac}, O. Kovanda ¹²⁴,
 R. Kowalewski ¹⁶⁶, W. Kozanecki ¹³⁶, A.S. Kozhin ³⁷, V.A. Kramarenko ³⁷, G. Kramberger ⁹⁴,
 P. Kramer ¹⁰¹, M.W. Krasny ¹²⁸, A. Krasznahorkay ³⁶, J.W. Kraus ¹⁷², J.A. Kremer ⁴⁸,
 T. Kresse ⁵⁰, J. Kretschmar ⁹³, K. Kreul ¹⁸, P. Krieger ¹⁵⁶, S. Krishnamurthy ¹⁰⁴,
 M. Krivos ¹³⁴, K. Krizka ²⁰, K. Kroeninger ⁴⁹, H. Kroha ¹¹¹, J. Kroll ¹³², J. Kroll ¹²⁹,
 K.S. Krowpman ¹⁰⁸, U. Kruchonak ³⁸, H. Krüger ²⁴, N. Krumnack ⁸¹, M.C. Kruse ⁵¹,
 O. Kuchinskaia ³⁷, S. Kuday ^{3a}, S. Kuehn ³⁶, R. Kuesters ⁵⁴, T. Kuhl ⁴⁸, V. Kukhtin ³⁸,
 Y. Kulchitsky ^{37,a}, S. Kuleshov ^{138d,138b}, M. Kumar ^{33g}, N. Kumari ⁴⁸, P. Kumari ^{157b},
 A. Kupco ¹³², T. Kupfer ⁴⁹, A. Kupich ³⁷, O. Kuprash ⁵⁴, H. Kurashige ⁸⁵, L.L. Kurchaninov ^{157a},
 O. Kurdysh ⁶⁶, Y.A. Kurochkin ³⁷, A. Kurova ³⁷, M. Kuze ¹⁵⁵, A.K. Kvam ¹⁰⁴, J. Kvita ¹²³,
 T. Kwan ¹⁰⁵, N.G. Kyriacou ¹⁰⁷, L.A.O. Laatu ¹⁰³, C. Lacasta ¹⁶⁴, F. Lacava ^{75a,75b},
 H. Lacker ¹⁸, D. Lacour ¹²⁸, N.N. Lad ⁹⁷, E. Ladygin ³⁸, A. Lafarge ⁴⁰, B. Laforge ¹²⁸,
 T. Lagouri ¹⁷³, F.Z. Lahbabi ^{35a}, S. Lai ⁵⁵, I.K. Lakomic ^{86a}, N. Lalloue ⁶⁰, J.E. Lambert ¹⁶⁶,
 S. Lammers ⁶⁸, W. Lampl ⁷, C. Lampoudis ^{153,e}, G. Lamprinoudis ¹⁰¹, A.N. Lancaster ¹¹⁶,
 E. Lançon ²⁹, U. Landgraf ⁵⁴, M.P.J. Landon ⁹⁵, V.S. Lang ⁵⁴, O.K.B. Langrekken ¹²⁶,
 A.J. Lankford ¹⁶⁰, F. Lanni ³⁶, K. Lantzsch ²⁴, A. Lanza ^{73a}, A. Lapertosa ^{57b,57a},
 J.F. Laporte ¹³⁶, T. Lari ^{71a}, F. Lasagni Manghi ^{23b}, M. Lassnig ³⁶, V. Latonova ¹³²,
 A. Laudrain ¹⁰¹, A. Laurier ¹⁵¹, S.D. Lawlor ¹⁴⁰, Z. Lawrence ¹⁰², R. Lazaridou ¹⁶⁸,
 M. Lazzaroni ^{71a,71b}, B. Le ¹⁰², E.M. Le Boulicaut ⁵¹, B. Leban ^{23b,23a}, A. Lebedev ⁸¹,
 M. LeBlanc ¹⁰², F. Ledroit-Guillon ⁶⁰, A.C.A. Lee ⁹⁷, S.C. Lee ¹⁴⁹, S. Lee ^{47a,47b}, T.F. Lee ⁹³,
 L.L. Leeuw ^{33c}, H.P. Lefebvre ⁹⁶, M. Lefebvre ¹⁶⁶, C. Leggett ^{17a}, G. Lehmann Miotto ³⁶,
 M. Leigh ⁵⁶, W.A. Leight ¹⁰⁴, W. Leinonen ¹¹⁴, A. Leisos ^{153,r}, M.A.L. Leite ^{83c},
 C.E. Leitgeb ¹⁸, R. Leitner ¹³⁴, K.J.C. Leney ⁴⁴, T. Lenz ²⁴, S. Leone ^{74a}, C. Leonidopoulos ⁵²,
 A. Leopold ¹⁴⁵, C. Leroy ¹⁰⁹, R. Les ¹⁰⁸, C.G. Lester ³², M. Levchenko ³⁷, J. Levêque ⁴,
 L.J. Levinson ¹⁷⁰, G. Levrini ^{23b,23a}, M.P. Lewicki ⁸⁷, D.J. Lewis ⁴, A. Li ⁵, B. Li ^{62b}, C. Li ^{62a},
 C-Q. Li ¹¹¹, H. Li ^{62a}, H. Li ^{62b}, H. Li ^{14c}, H. Li ^{14b}, H. Li ^{62b}, J. Li ^{62c}, K. Li ¹³⁹,
 L. Li ^{62c}, M. Li ^{14a,14e}, Q.Y. Li ^{62a}, S. Li ^{14a,14e}, S. Li ^{62d,62c,d}, T. Li ⁵, X. Li ¹⁰⁵, Z. Li ¹²⁷,
 Z. Li ¹⁰⁵, Z. Li ^{14a,14e}, S. Liang ^{14a,14e}, Z. Liang ^{14a}, M. Liberatore ¹³⁶, B. Liberti ^{76a}, K. Lie ^{64c},
 J. Lieber Marin ^{83b}, H. Lien ⁶⁸, K. Lin ¹⁰⁸, R.E. Lindley ⁷, J.H. Lindon ², E. Lipeles ¹²⁹,
 A. Lipniacka ¹⁶, A. Lister ¹⁶⁵, J.D. Little ⁴, B. Liu ^{14a}, B.X. Liu ¹⁴³, D. Liu ^{62d,62c},
 E.H.L. Liu ²⁰, J.B. Liu ^{62a}, J.K.K. Liu ³², K. Liu ^{62d}, K. Liu ^{62d,62c}, M. Liu ^{62a}, M.Y. Liu ^{62a},
 P. Liu ^{14a}, Q. Liu ^{62d,139,62c}, X. Liu ^{62a}, X. Liu ^{62b}, Y. Liu ^{14d,14e}, Y.L. Liu ^{62b}, Y.W. Liu ^{62a},
 J. Llorente Merino ¹⁴³, S.L. Lloyd ⁹⁵, E.M. Lobodzinska ⁴⁸, P. Loch ⁷, T. Lohse ¹⁸,
 K. Lohwasser ¹⁴⁰, E. Loiacono ⁴⁸, M. Lokajicek ^{132,*}, J.D. Lomas ²⁰, J.D. Long ¹⁶³,
 I. Longarini ¹⁶⁰, L. Longo ^{70a,70b}, R. Longo ¹⁶³, I. Lopez Paz ⁶⁷, A. Lopez Solis ⁴⁸,

N. Lorenzo Martinez ⁴, A.M. Lory ¹¹⁰, G. Löschcke Centeno ¹⁴⁷, O. Loseva ³⁷, X. Lou ^{47a,47b},
 X. Lou ^{14a,14e}, A. Lounis ⁶⁶, P.A. Love ⁹², G. Lu ^{14a,14e}, M. Lu ⁸⁰, S. Lu ¹²⁹, Y.J. Lu ⁶⁵,
 H.J. Lubatti ¹³⁹, C. Luci ^{75a,75b}, F.L. Lucio Alves ^{14c}, F. Luehring ⁶⁸, I. Luise ¹⁴⁶,
 O. Lukianchuk ⁶⁶, O. Lundberg ¹⁴⁵, B. Lund-Jensen ¹⁴⁵, N.A. Luongo ⁶, M.S. Lutz ³⁶,
 A.B. Lux ²⁵, D. Lynn ²⁹, R. Lysak ¹³², E. Lytken ⁹⁹, V. Lyubushkin ³⁸, T. Lyubushkina ³⁸,
 M.M. Lyukova ¹⁴⁶, H. Ma ²⁹, K. Ma ^{62a}, L.L. Ma ^{62b}, W. Ma ^{62a}, Y. Ma ¹²²,
 D.M. Mac Donell ¹⁶⁶, G. Maccarrone ⁵³, J.C. MacDonald ¹⁰¹, P.C. Machado De Abreu Farias ^{83b},
 R. Madar ⁴⁰, T. Madula ⁹⁷, J. Maeda ⁸⁵, T. Maeno ²⁹, H. Maguire ¹⁴⁰, V. Maiboroda ¹³⁶,
 A. Maio ^{131a,131b,131d}, K. Maj ^{86a}, O. Majersky ⁴⁸, S. Majewski ¹²⁴, N. Makovec ⁶⁶,
 V. Maksimovic ¹⁵, B. Malaescu ¹²⁸, Pa. Malecki ⁸⁷, V.P. Maleev ³⁷, F. Malek ^{60,n}, M. Mali ⁹⁴,
 D. Malito ⁹⁶, U. Mallik ⁸⁰, S. Maltezos ¹⁰, S. Malyukov ³⁸, J. Mamuzic ¹³, G. Mancini ⁵³,
 M.N. Mancini ²⁶, G. Manco ^{73a,73b}, J.P. Mandalia ⁹⁵, I. Mandić ⁹⁴,
 L. Manhaes de Andrade Filho ^{83a}, I.M. Maniatis ¹⁷⁰, J. Manjarres Ramos ⁹⁰, D.C. Mankad ¹⁷⁰,
 A. Mann ¹¹⁰, S. Manzoni ³⁶, L. Mao ^{62c}, X. Mapekula ^{33c}, A. Marantis ^{153,r}, G. Marchiori ⁵,
 M. Marcisovsky ¹³², C. Marcon ^{71a}, M. Marinescu ²⁰, S. Marium ⁴⁸, M. Marjanovic ¹²¹,
 M. Markovitch ⁶⁶, E.J. Marshall ⁹², Z. Marshall ^{17a}, S. Marti-Garcia ¹⁶⁴, T.A. Martin ¹⁶⁸,
 V.J. Martin ⁵², B. Martin dit Latour ¹⁶, L. Martinelli ^{75a,75b}, M. Martinez ^{13,s},
 P. Martinez Agullo ¹⁶⁴, V.I. Martinez Outschoorn ¹⁰⁴, P. Martinez Suarez ¹³, S. Martin-Haugh ¹³⁵,
 G. Martinovicova ¹³⁴, V.S. Martoiu ^{27b}, A.C. Martyniuk ⁹⁷, A. Marzin ³⁶, D. Mascione ^{78a,78b},
 L. Masetti ¹⁰¹, T. Mashimo ¹⁵⁴, J. Masik ¹⁰², A.L. Maslennikov ³⁷, P. Massarotti ^{72a,72b},
 P. Mastrandrea ^{74a,74b}, A. Mastroberardino ^{43b,43a}, T. Masubuchi ¹⁵⁴, T. Mathisen ¹⁶²,
 J. Matousek ¹³⁴, N. Matsuzawa ¹⁵⁴, J. Maurer ^{27b}, A.J. Maury ⁶⁶, B. Maček ⁹⁴, D.A. Maximov ³⁷,
 R. Mazini ¹⁴⁹, I. Maznas ¹¹⁶, M. Mazza ¹⁰⁸, S.M. Mazza ¹³⁷, E. Mazzeo ^{71a,71b}, C. Mc Ginn ²⁹,
 J.P. Mc Gowan ¹⁶⁶, S.P. Mc Kee ¹⁰⁷, C.C. McCracken ¹⁶⁵, E.F. McDonald ¹⁰⁶,
 A.E. McDougall ¹¹⁵, J.A. Mcfayden ¹⁴⁷, R.P. McGovern ¹²⁹, G. Mchedlidze ^{150b},
 R.P. Mckenzie ^{33g}, T.C. Mclachlan ⁴⁸, D.J. Mclaughlin ⁹⁷, S.J. McMahon ¹³⁵,
 C.M. Mcpartland ⁹³, R.A. McPherson ^{166,w}, S. Mehlhase ¹¹⁰, A. Mehta ⁹³, D. Melini ¹⁶⁴,
 B.R. Mellado Garcia ^{33g}, A.H. Melo ⁵⁵, F. Meloni ⁴⁸, A.M. Mendes Jacques Da Costa ¹⁰²,
 H.Y. Meng ¹⁵⁶, L. Meng ⁹², S. Menke ¹¹¹, M. Mentink ³⁶, E. Meoni ^{43b,43a}, G. Mercado ¹¹⁶,
 C. Merlassino ^{69a,69c}, L. Merola ^{72a,72b}, C. Meroni ^{71a,71b}, J. Metcalfe ⁶, A.S. Mete ⁶,
 C. Meyer ⁶⁸, J-P. Meyer ¹³⁶, R.P. Middleton ¹³⁵, L. Mijović ⁵², G. Mikenberg ¹⁷⁰,
 M. Mikestikova ¹³², M. Mikuž ⁹⁴, H. Mildner ¹⁰¹, A. Milic ³⁶, D.W. Miller ³⁹, E.H. Miller ¹⁴⁴,
 L.S. Miller ³⁴, A. Milov ¹⁷⁰, D.A. Milstead ^{47a,47b}, T. Min ^{14c}, A.A. Minaenko ³⁷,
 I.A. Minashvili ^{150b}, L. Mince ⁵⁹, A.I. Mincer ¹¹⁸, B. Mindur ^{86a}, M. Mineev ³⁸, Y. Mino ⁸⁸,
 L.M. Mir ¹³, M. Miralles Lopez ⁵⁹, M. Mironova ^{17a}, A. Mishima ¹⁵⁴, M.C. Missio ¹¹⁴,
 A. Mitra ¹⁶⁸, V.A. Mitsou ¹⁶⁴, Y. Mitsumori ¹¹², O. Miu ¹⁵⁶, P.S. Miyagawa ⁹⁵,
 T. Mkrtchyan ^{63a}, M. Mlinarevic ⁹⁷, T. Mlinarevic ⁹⁷, M. Mlynarikova ³⁶, S. Mobius ¹⁹,
 P. Mogg ¹¹⁰, M.H. Mohamed Farook ¹¹³, A.F. Mohammed ^{14a,14e}, S. Mohapatra ⁴¹,
 G. Mokgatitwane ^{33g}, L. Moleri ¹⁷⁰, B. Mondal ¹⁴², S. Mondal ¹³³, K. Mönig ⁴⁸,
 E. Monnier ¹⁰³, L. Monsonis Romero ¹⁶⁴, J. Montejo Berlingen ¹³, M. Montella ¹²⁰,
 F. Montereali ^{77a,77b}, F. Monticelli ⁹¹, S. Monzani ^{69a,69c}, N. Morange ⁶⁶,
 A.L. Moreira De Carvalho ^{131a}, M. Moreno Llácer ¹⁶⁴, C. Moreno Martinez ⁵⁶, P. Morettini ^{57b},
 S. Morgenstern ³⁶, M. Morii ⁶¹, M. Morinaga ¹⁵⁴, F. Morodei ^{75a,75b}, L. Morvaj ³⁶,
 P. Moschovakos ³⁶, B. Moser ³⁶, M. Mosidze ^{150b}, T. Moskalets ⁵⁴, P. Moskvitina ¹¹⁴,
 J. Moss ^{31,k}, A. Moussa ^{35d}, E.J.W. Moyse ¹⁰⁴, O. Mtintsilana ^{33g}, S. Muanza ¹⁰³,
 J. Mueller ¹³⁰, D. Muenstermann ⁹², R. Müller ¹⁹, G.A. Mullier ¹⁶², A.J. Mullin ³², J.J. Mullin ¹²⁹,
 D.P. Mungo ¹⁵⁶, D. Munoz Perez ¹⁶⁴, F.J. Munoz Sanchez ¹⁰², M. Murin ¹⁰², W.J. Murray ^{168,135},

M. Muškinja ⁹⁴, C. Mwewa ²⁹, A.G. Myagkov ^{37,a}, A.J. Myers ⁸, G. Myers ¹⁰⁷, M. Myska ¹³³,
B.P. Nachman ^{17a}, O. Nackenhorst ⁴⁹, K. Nagai ¹²⁷, K. Nagano ⁸⁴, J.L. Nagle ^{29,ag}, E. Nagy ¹⁰³,
A.M. Nairz ³⁶, Y. Nakahama ⁸⁴, K. Nakamura ⁸⁴, K. Nakkalil ⁵, H. Nanjo ¹²⁵, R. Narayan ⁴⁴,
E.A. Narayanan ¹¹³, I. Naryshkin ³⁷, M. Naseri ³⁴, S. Nasri ^{117b}, C. Nass ²⁴, G. Navarro ^{22a},
J. Navarro-Gonzalez ¹⁶⁴, R. Nayak ¹⁵², A. Nayaz ¹⁸, P.Y. Nechaeva ³⁷, F. Nechansky ⁴⁸,
L. Nedic ¹²⁷, T.J. Neep ²⁰, A. Negri ^{73a,73b}, M. Negrini ^{23b}, C. Nellist ¹¹⁵, C. Nelson ¹⁰⁵,
K. Nelson ¹⁰⁷, S. Nemecek ¹³², M. Nessi ^{36,h}, M.S. Neubauer ¹⁶³, F. Neuhaus ¹⁰¹,
J. Neundorf ⁴⁸, R. Newhouse ¹⁶⁵, P.R. Newman ²⁰, C.W. Ng ¹³⁰, Y.W.Y. Ng ⁴⁸, B. Ngair ^{117a},
H.D.N. Nguyen ¹⁰⁹, R.B. Nickerson ¹²⁷, R. Nicolaidou ¹³⁶, J. Nielsen ¹³⁷, M. Niemeyer ⁵⁵,
J. Niermann ⁵⁵, N. Nikiforou ³⁶, V. Nikolaenko ^{37,a}, I. Nikolic-Audit ¹²⁸, K. Nikolopoulos ²⁰,
P. Nilsson ²⁹, I. Ninca ⁴⁸, H.R. Nindhito ⁵⁶, G. Ninio ¹⁵², A. Nisati ^{75a}, N. Nishu ²,
R. Nisius ¹¹¹, J.-E. Nitschke ⁵⁰, E.K. Nkadimeng ^{33g}, T. Nobe ¹⁵⁴, D.L. Noel ³²,
T. Nommensen ¹⁴⁸, M.B. Norfolk ¹⁴⁰, R.R.B. Norisam ⁹⁷, B.J. Norman ³⁴, M. Noury ^{35a},
J. Novak ⁹⁴, T. Novak ⁴⁸, L. Novotny ¹³³, R. Novotny ¹¹³, L. Nozka ¹²³, K. Ntekas ¹⁶⁰,
N.M.J. Nunes De Moura Junior ^{83b}, J. Ocariz ¹²⁸, A. Ochi ⁸⁵, I. Ochoa ^{131a}, S. Oerdek ⁴⁸,
J.T. Offermann ³⁹, A. Ogrodnik ¹³⁴, A. Oh ¹⁰², C.C. Ohm ¹⁴⁵, H. Oide ⁸⁴, R. Oishi ¹⁵⁴,
M.L. Ojeda ⁴⁸, Y. Okumura ¹⁵⁴, L.F. Oleiro Seabra ^{131a}, S.A. Olivares Pino ^{138d},
G. Oliveira Correa ¹³, D. Oliveira Damazio ²⁹, D. Oliveira Goncalves ^{83a}, J.L. Oliver ¹⁶⁰,
Ö.O. Öncel ⁵⁴, A.P. O'Neill ¹⁹, A. Onofre ^{131a,131e}, P.U.E. Onyisi ¹¹, M.J. Oreglia ³⁹,
G.E. Orellana ⁹¹, D. Orestano ^{77a,77b}, N. Orlando ¹³, R.S. Orr ¹⁵⁶, V. O'Shea ⁵⁹,
L.M. Osojnak ¹²⁹, R. Ospanov ^{62a}, G. Otero y Garzon ³⁰, H. Otono ⁸⁹, P.S. Ott ^{63a},
G.J. Ottino ^{17a}, M. Ouchrif ^{35d}, F. Ould-Saada ¹²⁶, T. Ovsianikova ¹³⁹, M. Owen ⁵⁹,
R.E. Owen ¹³⁵, K.Y. Oyulmaz ^{21a}, V.E. Ozcan ^{21a}, F. Ozturk ⁸⁷, N. Ozturk ⁸, S. Ozturk ⁸²,
H.A. Pacey ¹²⁷, A. Pacheco Pages ¹³, C. Padilla Aranda ¹³, G. Padovano ^{75a,75b},
S. Pagan Griso ^{17a}, G. Palacino ⁶⁸, A. Palazzo ^{70a,70b}, J. Pampel ²⁴, J. Pan ¹⁷³, T. Pan ^{64a},
D.K. Panchal ¹¹, C.E. Pandini ¹¹⁵, J.G. Panduro Vazquez ⁹⁶, H.D. Pandya ¹, H. Pang ^{14b},
P. Pani ⁴⁸, G. Panizzo ^{69a,69c}, L. Panwar ¹²⁸, L. Paolozzi ⁵⁶, S. Parajuli ¹⁶³, A. Paramonov ⁶,
C. Paraskevopoulos ⁵³, D. Paredes Hernandez ^{64b}, A. Pareti ^{73a,73b}, K.R. Park ⁴¹, T.H. Park ¹⁵⁶,
M.A. Parker ³², F. Parodi ^{57b,57a}, E.W. Parrish ¹¹⁶, V.A. Parrish ⁵², J.A. Parsons ⁴¹,
U. Parzefall ⁵⁴, B. Pascual Dias ¹⁰⁹, L. Pascual Dominguez ¹⁵², E. Pasqualucci ^{75a},
S. Passaggio ^{57b}, F. Pastore ⁹⁶, P. Patel ⁸⁷, U.M. Patel ⁵¹, J.R. Pater ¹⁰², T. Pauly ³⁶,
C.I. Pazos ¹⁵⁹, J. Pearkes ¹⁴⁴, M. Pedersen ¹²⁶, R. Pedro ^{131a}, S.V. Peleganchuk ³⁷, O. Penc ³⁶,
E.A. Pender ⁵², G.D. Penn ¹⁷³, K.E. Pensi ¹¹⁰, M. Penzin ³⁷, B.S. Peralva ^{83d},
A.P. Pereira Peixoto ¹³⁹, L. Pereira Sanchez ¹⁴⁴, D.V. Perpelitsa ^{29,ag}, E. Perez Codina ^{157a},
M. Perganti ¹⁰, H. Pernegger ³⁶, O. Perrin ⁴⁰, K. Peters ⁴⁸, R.F.Y. Peters ¹⁰², B.A. Petersen ³⁶,
T.C. Petersen ⁴², E. Petit ¹⁰³, V. Petousis ¹³³, C. Petridou ^{153,e}, T. Petru ¹³⁴, A. Petrukhin ¹⁴²,
M. Pettee ^{17a}, N.E. Pettersson ³⁶, A. Petukhov ³⁷, K. Petukhova ¹³⁴, R. Pezoa ^{138f},
L. Pezzotti ³⁶, G. Pezzullo ¹⁷³, T.M. Pham ¹⁷¹, T. Pham ¹⁰⁶, P.W. Phillips ¹³⁵, G. Piacquadio ¹⁴⁶,
E. Pianori ^{17a}, F. Piazza ¹²⁴, R. Piegai ³⁰, D. Pietreanu ^{27b}, A.D. Pilkington ¹⁰²,
M. Pinamonti ^{69a,69c}, J.L. Pinfeld ², B.C. Pinheiro Pereira ^{131a}, A.E. Pinto Pinoargote ^{101,136},
L. Pintucci ^{69a,69c}, K.M. Piper ¹⁴⁷, A. Pirttikoski ⁵⁶, D.A. Pizzi ³⁴, L. Pizzimento ^{64b},
A. Pizzini ¹¹⁵, M.-A. Pleier ²⁹, V. Plesanovs ⁵⁴, V. Pleskot ¹³⁴, E. Plotnikova ³⁸, G. Poddar ⁹⁵,
R. Poettgen ⁹⁹, L. Poggioli ¹²⁸, I. Pokharel ⁵⁵, S. Polacek ¹³⁴, G. Polesello ^{73a}, A. Poley ^{143,157a},
A. Polini ^{23b}, C.S. Pollard ¹⁶⁸, Z.B. Pollock ¹²⁰, E. Pompa Pacchi ^{75a,75b}, D. Ponomarenko ¹¹⁴,
L. Pontecorvo ³⁶, S. Popa ^{27a}, G.A. Popeneciu ^{27d}, A. Poreba ³⁶, D.M. Portillo Quintero ^{157a},
S. Pospisil ¹³³, M.A. Postill ¹⁴⁰, P. Postolache ^{27c}, K. Potamianos ¹⁶⁸, P.A. Potepa ^{86a},
I.N. Potrap ³⁸, C.J. Potter ³², H. Potti ¹, J. Poveda ¹⁶⁴, M.E. Pozo Astigarraga ³⁶,

A. Prades Ibanez ¹⁶⁴, J. Pretel ⁵⁴, D. Price ¹⁰², M. Primavera ^{70a}, M.A. Principe Martin ¹⁰⁰,
 R. Privara ¹²³, T. Procter ⁵⁹, M.L. Proffitt ¹³⁹, N. Proklova ¹²⁹, K. Prokofiev ^{64c}, G. Proto ¹¹¹,
 J. Proudfoot ⁶, M. Przybycien ^{86a}, W.W. Przygoda ^{86b}, A. Psallidas ⁴⁶, J.E. Puddefoot ¹⁴⁰,
 D. Pudzha ³⁷, D. Pyatiizbyantseva ³⁷, J. Qian ¹⁰⁷, D. Qichen ¹⁰², Y. Qin ¹³, T. Qiu ⁵²,
 A. Quadt ⁵⁵, M. Queitsch-Maitland ¹⁰², G. Quetant ⁵⁶, R.P. Quinn ¹⁶⁵, G. Rabanal Bolanos ⁶¹,
 D. Rafanoharana ⁵⁴, F. Ragusa ^{71a,71b}, J.L. Rainbolt ³⁹, J.A. Raine ⁵⁶, S. Rajagopalan ²⁹,
 E. Ramakoti ³⁷, I.A. Ramirez-Berend ³⁴, K. Ran ^{48,14e}, N.P. Rapheeha ^{33g}, H. Rasheed ^{27b},
 V. Raskina ¹²⁸, D.F. Rassloff ^{63a}, A. Rastogi ^{17a}, S. Rave ¹⁰¹, B. Ravina ⁵⁵, I. Ravinovich ¹⁷⁰,
 M. Raymond ³⁶, A.L. Read ¹²⁶, N.P. Readioff ¹⁴⁰, D.M. Rebuzzi ^{73a,73b}, G. Redlinger ²⁹,
 A.S. Reed ¹¹¹, K. Reeves ²⁶, J.A. Reidelsturz ¹⁷², D. Reikher ¹⁵², A. Rej ⁴⁹, C. Rembser ³⁶,
 M. Renda ^{27b}, M.B. Rendel ¹¹¹, F. Renner ⁴⁸, A.G. Rennie ¹⁶⁰, A.L. Rescia ⁴⁸, S. Resconi ^{71a},
 M. Ressegotti ^{57b,57a}, S. Rettie ³⁶, J.G. Reyes Rivera ¹⁰⁸, E. Reynolds ^{17a}, O.L. Rezanova ³⁷,
 P. Reznicek ¹³⁴, H. Riani ^{35d}, N. Ribaric ⁹², E. Ricci ^{78a,78b}, R. Richter ¹¹¹, S. Richter ^{47a,47b},
 E. Richter-Was ^{86b}, M. Ridel ¹²⁸, S. Ridouani ^{35d}, P. Rieck ¹¹⁸, P. Riedler ³⁶, E.M. Riefel ^{47a,47b},
 J.O. Rieger ¹¹⁵, M. Rijssenbeek ¹⁴⁶, M. Rimoldi ³⁶, L. Rinaldi ^{23b,23a}, T.T. Rinn ²⁹,
 M.P. Rinnagel ¹¹⁰, G. Ripellino ¹⁶², I. Riu ¹³, J.C. Rivera Vergara ¹⁶⁶, F. Rizatdinova ¹²²,
 E. Rizvi ⁹⁵, B.R. Roberts ^{17a}, S.H. Robertson ^{105,w}, D. Robinson ³², C.M. Robles Gajardo ^{138f},
 M. Robles Manzano ¹⁰¹, A. Robson ⁵⁹, A. Rocchi ^{76a,76b}, C. Roda ^{74a,74b}, S. Rodriguez Bosca ³⁶,
 Y. Rodriguez Garcia ^{22a}, A. Rodriguez Rodriguez ⁵⁴, A.M. Rodríguez Vera ¹¹⁶, S. Roe ³⁶,
 J.T. Roemer ¹⁶⁰, A.R. Roepe-Gier ¹³⁷, J. Roggel ¹⁷², O. Røhne ¹²⁶, R.A. Rojas ¹⁰⁴,
 C.P.A. Roland ¹²⁸, J. Roloff ²⁹, A. Romaniouk ³⁷, E. Romano ^{73a,73b}, M. Romano ^{23b},
 A.C. Romero Hernandez ¹⁶³, N. Rompotis ⁹³, L. Roos ¹²⁸, S. Rosati ^{75a}, B.J. Rosser ³⁹,
 E. Rossi ¹²⁷, E. Rossi ^{72a,72b}, L.P. Rossi ⁶¹, L. Rossini ⁵⁴, R. Rosten ¹²⁰, M. Rotaru ^{27b},
 B. Rottler ⁵⁴, C. Rougier ⁹⁰, D. Rousseau ⁶⁶, D. Rousso ³², A. Roy ¹⁶³, S. Roy-Garand ¹⁵⁶,
 A. Rozanov ¹⁰³, Z.M.A. Rozario ⁵⁹, Y. Rozen ¹⁵¹, A. Rubio Jimenez ¹⁶⁴, A.J. Ruby ⁹³,
 V.H. Ruelas Rivera ¹⁸, T.A. Ruggeri ¹, A. Ruggiero ¹²⁷, A. Ruiz-Martinez ¹⁶⁴, A. Rummler ³⁶,
 Z. Rurikova ⁵⁴, N.A. Rusakovich ³⁸, H.L. Russell ¹⁶⁶, G. Russo ^{75a,75b}, J.P. Rutherford ⁷,
 S. Rutherford Colmenares ³², K. Rybacki ⁹², M. Rybar ¹³⁴, E.B. Rye ¹²⁶, A. Ryzhov ⁴⁴,
 J.A. Sabater Iglesias ⁵⁶, P. Sabatini ¹⁶⁴, H.F-W. Sadrozinski ¹³⁷, F. Safai Tehrani ^{75a},
 B. Safarzadeh Samani ¹³⁵, M. Safdari ¹⁴⁴, S. Saha ¹, M. Sahinsoy ¹¹¹, A. Saibel ¹⁶⁴,
 M. Saimpert ¹³⁶, M. Saito ¹⁵⁴, T. Saito ¹⁵⁴, A. Sala ^{71a,71b}, D. Salamani ³⁶, A. Salnikov ¹⁴⁴,
 J. Salt ¹⁶⁴, A. Salvador Salas ¹⁵², D. Salvatore ^{43b,43a}, F. Salvatore ¹⁴⁷, A. Salzburger ³⁶,
 D. Sammel ⁵⁴, E. Sampson ⁹², D. Sampsonidis ^{153,e}, D. Sampsonidou ¹²⁴, J. Sánchez ¹⁶⁴,
 V. Sanchez Sebastian ¹⁶⁴, H. Sandaker ¹²⁶, C.O. Sander ⁴⁸, J.A. Sandesara ¹⁰⁴, M. Sandhoff ¹⁷²,
 C. Sandoval ^{22b}, D.P.C. Sankey ¹³⁵, T. Sano ⁸⁸, A. Sansoni ⁵³, L. Santi ^{75a,75b}, C. Santoni ⁴⁰,
 H. Santos ^{131a,131b}, A. Santra ¹⁷⁰, K.A. Saoucha ¹⁶¹, J.G. Saraiva ^{131a,131d}, J. Sardain ⁷,
 O. Sasaki ⁸⁴, K. Sato ¹⁵⁸, C. Sauer ^{63b}, F. Sauerburger ⁵⁴, E. Sauvan ⁴, P. Savard ^{156,ae},
 R. Sawada ¹⁵⁴, C. Sawyer ¹³⁵, L. Sawyer ⁹⁸, I. Sayago Galvan ¹⁶⁴, C. Sbarra ^{23b}, A. Sbrizzi ^{23b,23a},
 T. Scanlon ⁹⁷, J. Schaarschmidt ¹³⁹, U. Schäfer ¹⁰¹, A.C. Schaffer ^{66,44}, D. Schaile ¹¹⁰,
 R.D. Schamberger ¹⁴⁶, C. Scharf ¹⁸, M.M. Schefer ¹⁹, V.A. Schegelsky ³⁷, D. Scheirich ¹³⁴,
 F. Schenck ¹⁸, M. Schernau ¹⁶⁰, C. Scheulen ⁵⁵, C. Schiavi ^{57b,57a}, M. Schioppa ^{43b,43a},
 B. Schlag ^{144,m}, K.E. Schleicher ⁵⁴, S. Schlenker ³⁶, J. Schmeing ¹⁷², M.A. Schmidt ¹⁷²,
 K. Schmieden ¹⁰¹, C. Schmitt ¹⁰¹, N. Schmitt ¹⁰¹, S. Schmitt ⁴⁸, L. Schoeffel ¹³⁶,
 A. Schoening ^{63b}, P.G. Scholer ³⁴, E. Schopf ¹²⁷, M. Schott ¹⁰¹, J. Schovancova ³⁶,
 S. Schramm ⁵⁶, T. Schroer ⁵⁶, H-C. Schultz-Coulon ^{63a}, M. Schumacher ⁵⁴, B.A. Schumm ¹³⁷,
 Ph. Schune ¹³⁶, A.J. Schuy ¹³⁹, H.R. Schwartz ¹³⁷, A. Schwartzman ¹⁴⁴, T.A. Schwarz ¹⁰⁷,
 Ph. Schwemling ¹³⁶, R. Schwienhorst ¹⁰⁸, A. Sciandra ¹³⁷, G. Sciolla ²⁶, F. Scuri ^{74a},

C.D. Sebastiani [id](#)⁹³, K. Sedlaczek [id](#)¹¹⁶, P. Seema [id](#)¹⁸, S.C. Seidel [id](#)¹¹³, A. Seiden [id](#)¹³⁷,
 B.D. Seidlitz [id](#)⁴¹, C. Seitz [id](#)⁴⁸, J.M. Seixas [id](#)^{83b}, G. Sekhniaidze [id](#)^{72a}, L. Selem [id](#)⁶⁰,
 N. Semprini-Cesari [id](#)^{23b,23a}, D. Sengupta [id](#)⁵⁶, V. Senthilkumar [id](#)¹⁶⁴, L. Serin [id](#)⁶⁶, L. Serkin [id](#)^{69a,69b},
 M. Sessa [id](#)^{76a,76b}, H. Severini [id](#)¹²¹, F. Sforza [id](#)^{57b,57a}, A. Sfyrla [id](#)⁵⁶, Q. Sha [id](#)^{14a}, E. Shabalina [id](#)⁵⁵,
 R. Shaheen [id](#)¹⁴⁵, J.D. Shahinian [id](#)¹²⁹, D. Shaked Renous [id](#)¹⁷⁰, L.Y. Shan [id](#)^{14a}, M. Shapiro [id](#)^{17a},
 A. Sharma [id](#)³⁶, A.S. Sharma [id](#)¹⁶⁵, P. Sharma [id](#)⁸⁰, P.B. Shatalov [id](#)³⁷, K. Shaw [id](#)¹⁴⁷, S.M. Shaw [id](#)¹⁰²,
 A. Shcherbakova [id](#)³⁷, Q. Shen [id](#)^{62c,5}, D.J. Sheppard [id](#)¹⁴³, P. Sherwood [id](#)⁹⁷, L. Shi [id](#)⁹⁷, X. Shi [id](#)^{14a},
 C.O. Shimmin [id](#)¹⁷³, J.D. Shinner [id](#)⁹⁶, I.P.J. Shipsey [id](#)¹²⁷, S. Shirabe [id](#)⁸⁹, M. Shiyakova [id](#)^{38,u},
 J. Shlomi [id](#)¹⁷⁰, M.J. Shochet [id](#)³⁹, J. Shojaii [id](#)¹⁰⁶, D.R. Shope [id](#)¹²⁶, B. Shrestha [id](#)¹²¹, S. Shrestha [id](#)^{120,ah},
 E.M. Shrif [id](#)^{33g}, M.J. Shroff [id](#)¹⁶⁶, P. Sicho [id](#)¹³², A.M. Sickles [id](#)¹⁶³, E. Sideras Haddad [id](#)^{33g},
 A. Sidoti [id](#)^{23b}, F. Siegert [id](#)⁵⁰, Dj. Sijacki [id](#)¹⁵, F. Sili [id](#)⁹¹, J.M. Silva [id](#)⁵², M.V. Silva Oliveira [id](#)²⁹,
 S.B. Silverstein [id](#)^{47a}, S. Simion [id](#)⁶⁶, R. Simoniello [id](#)³⁶, E.L. Simpson [id](#)⁵⁹, H. Simpson [id](#)¹⁴⁷,
 L.R. Simpson [id](#)¹⁰⁷, N.D. Simpson [id](#)⁹⁹, S. Simsek [id](#)⁸², S. Sindhu [id](#)⁵⁵, P. Sinervo [id](#)¹⁵⁶, S. Singh [id](#)¹⁵⁶,
 S. Sinha [id](#)⁴⁸, S. Sinha [id](#)¹⁰², M. Sioli [id](#)^{23b,23a}, I. Siral [id](#)³⁶, E. Sitnikova [id](#)⁴⁸, J. Sjölin [id](#)^{47a,47b},
 A. Skaf [id](#)⁵⁵, E. Skorda [id](#)²⁰, P. Skubic [id](#)¹²¹, M. Slawinska [id](#)⁸⁷, V. Smakhtin [id](#)¹⁷⁰, B.H. Smart [id](#)¹³⁵,
 S.Yu. Smirnov [id](#)³⁷, Y. Smirnov [id](#)³⁷, L.N. Smirnova [id](#)^{37,a}, O. Smirnova [id](#)⁹⁹, A.C. Smith [id](#)⁴¹,
 E.A. Smith [id](#)³⁹, H.A. Smith [id](#)¹²⁷, J.L. Smith [id](#)¹⁰², R. Smith [id](#)¹⁴⁴, M. Smizanska [id](#)⁹², K. Smolek [id](#)¹³³,
 A.A. Snesarev [id](#)³⁷, S.R. Snider [id](#)¹⁵⁶, H.L. Snoek [id](#)¹¹⁵, S. Snyder [id](#)²⁹, R. Sobie [id](#)^{166,w}, A. Soffer [id](#)¹⁵²,
 C.A. Solans Sanchez [id](#)³⁶, E.Yu. Soldatov [id](#)³⁷, U. Soldevila [id](#)¹⁶⁴, A.A. Solodkov [id](#)³⁷, S. Solomon [id](#)²⁶,
 A. Soloshenko [id](#)³⁸, K. Solovieva [id](#)⁵⁴, O.V. Solovyanov [id](#)⁴⁰, V. Solovyev [id](#)³⁷, P. Sommer [id](#)³⁶,
 A. Sonay [id](#)¹³, W.Y. Song [id](#)^{157b}, A. Sopczak [id](#)¹³³, A.L. Soppio [id](#)⁹⁷, F. Sopkova [id](#)^{28b}, J.D. Sorenson [id](#)¹¹³,
 I.R. Sotarriva Alvarez [id](#)¹⁵⁵, V. Sothilingam [id](#)^{63a}, O.J. Soto Sandoval [id](#)^{138c,138b}, S. Sottocornola [id](#)⁶⁸,
 R. Soualah [id](#)¹⁶¹, Z. Soumami [id](#)^{35e}, D. South [id](#)⁴⁸, N. Soybelman [id](#)¹⁷⁰, S. Spagnolo [id](#)^{70a,70b},
 M. Spalla [id](#)¹¹¹, D. Sperlich [id](#)⁵⁴, G. Spigo [id](#)³⁶, S. Spinali [id](#)⁹², D.P. Spiteri [id](#)⁵⁹, M. Spousta [id](#)¹³⁴,
 E.J. Staats [id](#)³⁴, R. Stamen [id](#)^{63a}, A. Stampeki [id](#)²⁰, M. Standke [id](#)²⁴, E. Stanecka [id](#)⁸⁷, M.V. Stange [id](#)⁵⁰,
 B. Stanislaus [id](#)^{17a}, M.M. Stanitzki [id](#)⁴⁸, B. Stapf [id](#)⁴⁸, E.A. Starchenko [id](#)³⁷, G.H. Stark [id](#)¹³⁷, J. Stark [id](#)⁹⁰,
 P. Staroba [id](#)¹³², P. Starovoitov [id](#)^{63a}, S. Stärz [id](#)¹⁰⁵, R. Staszewski [id](#)⁸⁷, G. Stavropoulos [id](#)⁴⁶,
 J. Steentoft [id](#)¹⁶², P. Steinberg [id](#)²⁹, B. Stelzer [id](#)^{143,157a}, H.J. Stelzer [id](#)¹³⁰, O. Stelzer-Chilton [id](#)^{157a},
 H. Stenzel [id](#)⁵⁸, T.J. Stevenson [id](#)¹⁴⁷, G.A. Stewart [id](#)³⁶, J.R. Stewart [id](#)¹²², M.C. Stockton [id](#)³⁶,
 G. Stoicea [id](#)^{27b}, M. Stolarski [id](#)^{131a}, S. Stonjek [id](#)¹¹¹, A. Straessner [id](#)⁵⁰, J. Strandberg [id](#)¹⁴⁵,
 S. Strandberg [id](#)^{47a,47b}, M. Stratmann [id](#)¹⁷², M. Strauss [id](#)¹²¹, T. Strebler [id](#)¹⁰³, P. Strizenec [id](#)^{28b},
 R. Ströhmer [id](#)¹⁶⁷, D.M. Strom [id](#)¹²⁴, R. Stroynowski [id](#)⁴⁴, A. Strubig [id](#)^{47a,47b}, S.A. Stucci [id](#)²⁹,
 B. Stugu [id](#)¹⁶, J. Stupak [id](#)¹²¹, N.A. Styles [id](#)⁴⁸, D. Su [id](#)¹⁴⁴, S. Su [id](#)^{62a}, W. Su [id](#)^{62d}, X. Su [id](#)^{62a},
 D. Suchy [id](#)^{28a}, K. Sugizaki [id](#)¹⁵⁴, V.V. Sulin [id](#)³⁷, M.J. Sullivan [id](#)⁹³, D.M.S. Sultan [id](#)¹²⁷,
 L. Sultanaliyeva [id](#)³⁷, S. Sultansoy [id](#)^{3b}, T. Sumida [id](#)⁸⁸, S. Sun [id](#)¹⁰⁷, S. Sun [id](#)¹⁷¹,
 O. Sunneborn Gudnadottir [id](#)¹⁶², N. Sur [id](#)¹⁰³, M.R. Sutton [id](#)¹⁴⁷, H. Suzuki [id](#)¹⁵⁸, M. Svatos [id](#)¹³²,
 M. Swiatlowski [id](#)^{157a}, T. Swirski [id](#)¹⁶⁷, I. Sykora [id](#)^{28a}, M. Sykora [id](#)¹³⁴, T. Sykora [id](#)¹³⁴, D. Ta [id](#)¹⁰¹,
 K. Tackmann [id](#)^{48,t}, A. Taffard [id](#)¹⁶⁰, R. Tafirout [id](#)^{157a}, J.S. Tafoya Vargas [id](#)⁶⁶, Y. Takubo [id](#)⁸⁴,
 M. Talby [id](#)¹⁰³, A.A. Talyshev [id](#)³⁷, K.C. Tam [id](#)^{64b}, N.M. Tamir [id](#)¹⁵², A. Tanaka [id](#)¹⁵⁴, J. Tanaka [id](#)¹⁵⁴,
 R. Tanaka [id](#)⁶⁶, M. Tanasini [id](#)^{57b,57a}, Z. Tao [id](#)¹⁶⁵, S. Tapia Araya [id](#)^{138f}, S. Tapprogge [id](#)¹⁰¹,
 A. Tarek Abouelfadl Mohamed [id](#)¹⁰⁸, S. Tarem [id](#)¹⁵¹, K. Tariq [id](#)^{14a}, G. Tarna [id](#)^{103,27b}, G.F. Tartarelli [id](#)^{71a},
 P. Tas [id](#)¹³⁴, M. Tasevsky [id](#)¹³², E. Tassi [id](#)^{43b,43a}, A.C. Tate [id](#)¹⁶³, G. Tateno [id](#)¹⁵⁴, Y. Tayalati [id](#)^{35e,v},
 G.N. Taylor [id](#)¹⁰⁶, W. Taylor [id](#)^{157b}, A.S. Tee [id](#)¹⁷¹, R. Teixeira De Lima [id](#)¹⁴⁴, P. Teixeira-Dias [id](#)⁹⁶,
 J.J. Teoh [id](#)¹⁵⁶, K. Terashi [id](#)¹⁵⁴, J. Terron [id](#)¹⁰⁰, S. Terzo [id](#)¹³, M. Testa [id](#)⁵³, R.J. Teuscher [id](#)^{156,w},
 A. Thaler [id](#)⁷⁹, O. Theiner [id](#)⁵⁶, N. Themistokleous [id](#)⁵², T. Thevenaux-Pelzer [id](#)¹⁰³, O. Thielmann [id](#)¹⁷²,
 D.W. Thomas [id](#)⁹⁶, J.P. Thomas [id](#)²⁰, E.A. Thompson [id](#)^{17a}, P.D. Thompson [id](#)²⁰, E. Thomson [id](#)¹²⁹,
 R.E. Thornberry [id](#)⁴⁴, Y. Tian [id](#)⁵⁵, V. Tikhomirov [id](#)^{37,a}, Yu.A. Tikhonov [id](#)³⁷, S. Timoshenko [id](#)³⁷,

D. Timoshyn ¹³⁴, E.X.L. Ting ¹, P. Tipton ¹⁷³, S.H. Tlou ^{33g}, K. Todome ¹⁵⁵,
 S. Todorova-Nova ¹³⁴, S. Todt ⁵⁰, M. Togawa ⁸⁴, J. Tojo ⁸⁹, S. Tokár ^{28a}, K. Tokushuku ⁸⁴,
 O. Toldaiev ⁶⁸, R. Tombs ³², M. Tomoto ^{84,112}, L. Tompkins ^{144,m}, K.W. Topolnicki ^{86b},
 E. Torrence ¹²⁴, H. Torres ⁹⁰, E. Torró Pastor ¹⁶⁴, M. Toscani ³⁰, C. Tosciri ³⁹, M. Tost ¹¹,
 D.R. Tovey ¹⁴⁰, A. Traeet ¹⁶, I.S. Trandafir ^{27b}, T. Trefzger ¹⁶⁷, A. Tricoli ²⁹, I.M. Trigger ^{157a},
 S. Trincaz-Duvoid ¹²⁸, D.A. Trischuk ²⁶, B. Trocmé ⁶⁰, L. Truong ^{33c}, M. Trzebinski ⁸⁷,
 A. Trzupek ⁸⁷, F. Tsai ¹⁴⁶, M. Tsai ¹⁰⁷, A. Tsiamis ^{153,e}, P.V. Tsiarehka ³⁷, S. Tsigaridas ^{157a},
 A. Tsirigotis ^{153,r}, V. Tsiskaridze ¹⁵⁶, E.G. Tskhadadze ^{150a}, M. Tsopoulou ¹⁵³, Y. Tsujikawa ⁸⁸,
 I.I. Tsukerman ³⁷, V. Tsulaia ^{17a}, S. Tsuno ⁸⁴, K. Tsuru ¹¹⁹, D. Tsybychev ¹⁴⁶, Y. Tu ^{64b},
 A. Tudorache ^{27b}, V. Tudorache ^{27b}, A.N. Tuna ⁶¹, S. Turchikhin ^{57b,57a}, I. Turk Cakir ^{3a},
 R. Turra ^{71a}, T. Turtuvshin ^{38,x}, P.M. Tuts ⁴¹, S. Tzamarias ^{153,e}, E. Tzovara ¹⁰¹, F. Ukegawa ¹⁵⁸,
 P.A. Ulloa Poblete ^{138c,138b}, E.N. Umaka ²⁹, G. Unal ³⁶, A. Undrus ²⁹, G. Unel ¹⁶⁰, J. Urban ^{28b},
 P. Urquijo ¹⁰⁶, P. Urrejola ^{138a}, G. Usai ⁸, R. Ushioda ¹⁵⁵, M. Usman ¹⁰⁹, Z. Uysal ⁸²,
 V. Vacek ¹³³, B. Vachon ¹⁰⁵, K.O.H. Vadla ¹²⁶, T. Vafeiadis ³⁶, A. Vaitkus ⁹⁷, C. Valderanis ¹¹⁰,
 E. Valdes Santurio ^{47a,47b}, M. Valente ^{157a}, S. Valentinetti ^{23b,23a}, A. Valero ¹⁶⁴,
 E. Valiente Moreno ¹⁶⁴, A. Vallier ⁹⁰, J.A. Valls Ferrer ¹⁶⁴, D.R. Van Arneman ¹¹⁵,
 T.R. Van Daalen ¹³⁹, A. Van Der Graaf ⁴⁹, P. Van Gemmeren ⁶, M. Van Rijnbach ¹²⁶,
 S. Van Stroud ⁹⁷, I. Van Vulpen ¹¹⁵, P. Vana ¹³⁴, M. Vanadia ^{76a,76b}, W. Vandelli ³⁶,
 E.R. Vandewall ¹²², D. Vannicola ¹⁵², L. Vannoli ⁵³, R. Vari ^{75a}, E.W. Varnes ⁷, C. Varni ^{17b},
 T. Varol ¹⁴⁹, D. Varouchas ⁶⁶, L. Varriale ¹⁶⁴, K.E. Varvell ¹⁴⁸, M.E. Vasile ^{27b}, L. Vaslin ⁸⁴,
 G.A. Vasquez ¹⁶⁶, A. Vasyukov ³⁸, R. Vavricka ¹⁰¹, F. Vazeille ⁴⁰, T. Vazquez Schroeder ³⁶,
 J. Veatch ³¹, V. Vecchio ¹⁰², M.J. Veen ¹⁰⁴, I. Veliscek ²⁹, L.M. Veloce ¹⁵⁶, F. Veloso ^{131a,131c},
 S. Veneziano ^{75a}, A. Ventura ^{70a,70b}, S. Ventura Gonzalez ¹³⁶, A. Verbytskyi ¹¹¹,
 M. Verducci ^{74a,74b}, C. Vergis ²⁴, M. Verissimo De Araujo ^{83b}, W. Verkerke ¹¹⁵,
 J.C. Vermeulen ¹¹⁵, C. Vernieri ¹⁴⁴, M. Vessella ¹⁰⁴, M.C. Vetterli ^{143,ae}, A. Vgenopoulos ^{153,e},
 N. Viaux Maira ^{138f}, T. Vickey ¹⁴⁰, O.E. Vickey Boeriu ¹⁴⁰, G.H.A. Viehhauser ¹²⁷, L. Viganì ^{63b},
 M. Villa ^{23b,23a}, M. Villaplana Perez ¹⁶⁴, E.M. Villhauer ⁵², E. Vilucchi ⁵³, M.G. Vinciter ³⁴,
 G.S. Virdee ²⁰, A. Vishwakarma ⁵², A. Visibile ¹¹⁵, C. Vittori ³⁶, I. Vivarelli ^{23b,23a},
 E. Voevodina ¹¹¹, F. Vogel ¹¹⁰, J.C. Voigt ⁵⁰, P. Vokac ¹³³, Yu. Volkotrub ^{86b}, J. Von Ahnen ⁴⁸,
 E. Von Toerne ²⁴, B. Vormwald ³⁶, V. Vorobel ¹³⁴, K. Vorobev ³⁷, M. Vos ¹⁶⁴, K. Voss ¹⁴²,
 M. Vozak ¹¹⁵, L. Vozdecky ¹²¹, N. Vranjes ¹⁵, M. Vranjes Milosavljevic ¹⁵, M. Vreeswijk ¹¹⁵,
 N.K. Vu ^{62d,62c}, R. Vuillermet ³⁶, O. Vujanovic ¹⁰¹, I. Vukotic ³⁹, S. Wada ¹⁵⁸, C. Wagner ¹⁰⁴,
 J.M. Wagner ^{17a}, W. Wagner ¹⁷², S. Wahdan ¹⁷², H. Wahlberg ⁹¹, M. Wakida ¹¹², J. Walder ¹³⁵,
 R. Walker ¹¹⁰, W. Walkowiak ¹⁴², A. Wall ¹²⁹, E.J. Wallin ⁹⁹, T. Wamorkar ⁶, A.Z. Wang ¹³⁷,
 C. Wang ¹⁰¹, C. Wang ¹¹, H. Wang ^{17a}, J. Wang ^{64c}, R.-J. Wang ¹⁰¹, R. Wang ⁶¹, R. Wang ⁶,
 S.M. Wang ¹⁴⁹, S. Wang ^{62b}, T. Wang ^{62a}, W.T. Wang ⁸⁰, W. Wang ^{14a}, X. Wang ^{14c},
 X. Wang ¹⁶³, X. Wang ^{62c}, Y. Wang ^{62d}, Y. Wang ^{14c}, Z. Wang ¹⁰⁷, Z. Wang ^{62d,51,62c},
 Z. Wang ¹⁰⁷, A. Warburton ¹⁰⁵, R.J. Ward ²⁰, N. Warrack ⁵⁹, S. Waterhouse ⁹⁶, A.T. Watson ²⁰,
 H. Watson ⁵⁹, M.F. Watson ²⁰, E. Watton ^{59,135}, G. Watts ¹³⁹, B.M. Waugh ⁹⁷, C. Weber ²⁹,
 H.A. Weber ¹⁸, M.S. Weber ¹⁹, S.M. Weber ^{63a}, C. Wei ^{62a}, Y. Wei ¹²⁷, A.R. Weidberg ¹²⁷,
 E.J. Weik ¹¹⁸, J. Weingarten ⁴⁹, M. Weirich ¹⁰¹, C. Weiser ⁵⁴, C.J. Wells ⁴⁸, T. Wenaus ²⁹,
 B. Wendland ⁴⁹, T. Wengler ³⁶, N.S. Wenke ¹¹¹, N. Wermes ²⁴, M. Wessels ^{63a}, A.M. Wharton ⁹²,
 A.S. White ⁶¹, A. White ⁸, M.J. White ¹, D. Whiteson ¹⁶⁰, L. Wickremasinghe ¹²⁵,
 W. Wiedenmann ¹⁷¹, M. Wielers ¹³⁵, C. Wiglesworth ⁴², D.J. Wilbern ¹²¹, H.G. Wilkens ³⁶,
 D.M. Williams ⁴¹, H.H. Williams ¹²⁹, S. Williams ³², S. Willocq ¹⁰⁴, B.J. Wilson ¹⁰²,
 P.J. Windischhofer ³⁹, F.I. Winkel ³⁰, F. Winklmeier ¹²⁴, B.T. Winter ⁵⁴, J.K. Winter ¹⁰²,
 M. Wittgen ¹⁴⁴, M. Wobisch ⁹⁸, Z. Wolffs ¹¹⁵, J. Wollrath ¹⁶⁰, M.W. Wolter ⁸⁷, H. Wolters ^{131a,131c},

M.C. Wong¹³⁷, E.L. Woodward⁴¹, S.D. Worm⁴⁸, B.K. Wosiek⁸⁷, K.W. Woźniak⁸⁷, S. Wozniowski⁵⁵, K. Wraight⁵⁹, C. Wu²⁰, M. Wu^{14d}, M. Wu¹¹⁴, S.L. Wu¹⁷¹, X. Wu⁵⁶, Y. Wu^{62a}, Z. Wu⁴, J. Wuerzinger^{111,ac}, T.R. Wyatt¹⁰², B.M. Wynne⁵², S. Xella⁴², L. Xia^{14c}, M. Xia^{14b}, J. Xiang^{64c}, M. Xie^{62a}, X. Xie^{62a}, S. Xin^{14a,14e}, A. Xiong¹²⁴, J. Xiong^{17a}, D. Xu^{14a}, H. Xu^{62a}, L. Xu^{62a}, R. Xu¹²⁹, T. Xu¹⁰⁷, Y. Xu^{14b}, Z. Xu⁵², Z. Xu^{14c}, B. Yabsley¹⁴⁸, S. Yacoob^{33a}, Y. Yamaguchi¹⁵⁵, E. Yamashita¹⁵⁴, H. Yamauchi¹⁵⁸, T. Yamazaki^{17a}, Y. Yamazaki⁸⁵, J. Yan^{62c}, S. Yan⁵⁹, Z. Yan¹⁰⁴, H.J. Yang^{62c,62d}, H.T. Yang^{62a}, S. Yang^{62a}, T. Yang^{64c}, X. Yang³⁶, X. Yang^{14a}, Y. Yang⁴⁴, Y. Yang^{62a}, Z. Yang^{62a}, W-M. Yao^{17a}, H. Ye^{14c}, H. Ye⁵⁵, J. Ye^{14a}, S. Ye²⁹, X. Ye^{62a}, Y. Yeh⁹⁷, I. Yeletsikh³⁸, B.K. Yeo^{17b}, M.R. Yexley⁹⁷, P. Yin⁴¹, K. Yorita¹⁶⁹, S. Younas^{27b}, C.J.S. Young³⁶, C. Young¹⁴⁴, C. Yu^{14a,14e}, Y. Yu^{62a}, M. Yuan¹⁰⁷, R. Yuan^{62b}, L. Yue⁹⁷, M. Zaazoua^{62a}, B. Zabinski⁸⁷, E. Zaid⁵², Z.K. Zak⁸⁷, T. Zakareishvili¹⁶⁴, N. Zakharchuk³⁴, S. Zambito⁵⁶, J.A. Zamora Saa^{138d,138b}, J. Zang¹⁵⁴, D. Zanzi⁵⁴, O. Zaplatilek¹³³, C. Zeitnitz¹⁷², H. Zeng^{14a}, J.C. Zeng¹⁶³, D.T. Zenger Jr²⁶, O. Zenin³⁷, T. Ženiš^{28a}, S. Zenz⁹⁵, S. Zerradi^{35a}, D. Zerwas⁶⁶, M. Zhai^{14a,14e}, D.F. Zhang¹⁴⁰, J. Zhang^{62b}, J. Zhang⁶, K. Zhang^{14a,14e}, L. Zhang^{14c}, P. Zhang^{14a,14e}, R. Zhang¹⁷¹, S. Zhang¹⁰⁷, S. Zhang⁴⁴, T. Zhang¹⁵⁴, X. Zhang^{62c}, X. Zhang^{62b}, Y. Zhang^{62c,5}, Y. Zhang⁹⁷, Y. Zhang^{14c}, Z. Zhang^{17a}, Z. Zhang⁶⁶, H. Zhao¹³⁹, T. Zhao^{62b}, Y. Zhao¹³⁷, Z. Zhao^{62a}, Z. Zhao^{62a}, A. Zhemchugov³⁸, J. Zheng^{14c}, K. Zheng¹⁶³, X. Zheng^{62a}, Z. Zheng¹⁴⁴, D. Zhong¹⁶³, B. Zhou¹⁰⁷, H. Zhou⁷, N. Zhou^{62c}, Y. Zhou^{14c}, Y. Zhou⁷, C.G. Zhu^{62b}, J. Zhu¹⁰⁷, Y. Zhu^{62c}, Y. Zhu^{62a}, X. Zhuang^{14a}, K. Zhukov³⁷, N.I. Zimine³⁸, J. Zinsser^{63b}, M. Ziolkowski¹⁴², L. Živković¹⁵, A. Zoccoli^{23b,23a}, K. Zoch⁶¹, T.G. Zorbas¹⁴⁰, O. Zormpa⁴⁶, W. Zou⁴¹, L. Zwalinski³⁶.

¹Department of Physics, University of Adelaide, Adelaide; Australia.

²Department of Physics, University of Alberta, Edmonton AB; Canada.

³(^a)Department of Physics, Ankara University, Ankara; (^b)Division of Physics, TOBB University of Economics and Technology, Ankara; Türkiye.

⁴LAPP, Université Savoie Mont Blanc, CNRS/IN2P3, Annecy; France.

⁵APC, Université Paris Cité, CNRS/IN2P3, Paris; France.

⁶High Energy Physics Division, Argonne National Laboratory, Argonne IL; United States of America.

⁷Department of Physics, University of Arizona, Tucson AZ; United States of America.

⁸Department of Physics, University of Texas at Arlington, Arlington TX; United States of America.

⁹Physics Department, National and Kapodistrian University of Athens, Athens; Greece.

¹⁰Physics Department, National Technical University of Athens, Zografou; Greece.

¹¹Department of Physics, University of Texas at Austin, Austin TX; United States of America.

¹²Institute of Physics, Azerbaijan Academy of Sciences, Baku; Azerbaijan.

¹³Institut de Física d'Altes Energies (IFAE), Barcelona Institute of Science and Technology, Barcelona; Spain.

¹⁴(^a)Institute of High Energy Physics, Chinese Academy of Sciences, Beijing; (^b)Physics Department, Tsinghua University, Beijing; (^c)Department of Physics, Nanjing University, Nanjing; (^d)School of Science, Shenzhen Campus of Sun Yat-sen University; (^e)University of Chinese Academy of Science (UCAS), Beijing; China.

¹⁵Institute of Physics, University of Belgrade, Belgrade; Serbia.

¹⁶Department for Physics and Technology, University of Bergen, Bergen; Norway.

¹⁷(^a)Physics Division, Lawrence Berkeley National Laboratory, Berkeley CA; (^b)University of California, Berkeley CA; United States of America.

- ¹⁸Institut für Physik, Humboldt Universität zu Berlin, Berlin; Germany.
- ¹⁹Albert Einstein Center for Fundamental Physics and Laboratory for High Energy Physics, University of Bern, Bern; Switzerland.
- ²⁰School of Physics and Astronomy, University of Birmingham, Birmingham; United Kingdom.
- ²¹(^a) Department of Physics, Bogazici University, Istanbul; (^b) Department of Physics Engineering, Gaziantep University, Gaziantep; (^c) Department of Physics, Istanbul University, Istanbul; Türkiye.
- ²²(^a) Facultad de Ciencias y Centro de Investigaciones, Universidad Antonio Nariño, Bogotá; (^b) Departamento de Física, Universidad Nacional de Colombia, Bogotá; Colombia.
- ²³(^a) Dipartimento di Fisica e Astronomia A. Righi, Università di Bologna, Bologna; (^b) INFN Sezione di Bologna; Italy.
- ²⁴Physikalisches Institut, Universität Bonn, Bonn; Germany.
- ²⁵Department of Physics, Boston University, Boston MA; United States of America.
- ²⁶Department of Physics, Brandeis University, Waltham MA; United States of America.
- ²⁷(^a) Transilvania University of Brasov, Brasov; (^b) Horia Hulubei National Institute of Physics and Nuclear Engineering, Bucharest; (^c) Department of Physics, Alexandru Ioan Cuza University of Iasi, Iasi; (^d) National Institute for Research and Development of Isotopic and Molecular Technologies, Physics Department, Cluj-Napoca; (^e) University Politehnica Bucharest, Bucharest; (^f) West University in Timisoara, Timisoara; (^g) Faculty of Physics, University of Bucharest, Bucharest; Romania.
- ²⁸(^a) Faculty of Mathematics, Physics and Informatics, Comenius University, Bratislava; (^b) Department of Subnuclear Physics, Institute of Experimental Physics of the Slovak Academy of Sciences, Kosice; Slovak Republic.
- ²⁹Physics Department, Brookhaven National Laboratory, Upton NY; United States of America.
- ³⁰Universidad de Buenos Aires, Facultad de Ciencias Exactas y Naturales, Departamento de Física, y CONICET, Instituto de Física de Buenos Aires (IFIBA), Buenos Aires; Argentina.
- ³¹California State University, CA; United States of America.
- ³²Cavendish Laboratory, University of Cambridge, Cambridge; United Kingdom.
- ³³(^a) Department of Physics, University of Cape Town, Cape Town; (^b) iThemba Labs, Western Cape; (^c) Department of Mechanical Engineering Science, University of Johannesburg, Johannesburg; (^d) National Institute of Physics, University of the Philippines Diliman (Philippines); (^e) University of South Africa, Department of Physics, Pretoria; (^f) University of Zululand, KwaDlangezwa; (^g) School of Physics, University of the Witwatersrand, Johannesburg; South Africa.
- ³⁴Department of Physics, Carleton University, Ottawa ON; Canada.
- ³⁵(^a) Faculté des Sciences Ain Chock, Réseau Universitaire de Physique des Hautes Energies - Université Hassan II, Casablanca; (^b) Faculté des Sciences, Université Ibn-Tofail, Kénitra; (^c) Faculté des Sciences Semlalia, Université Cadi Ayyad, LPHEA-Marrakech; (^d) LPMR, Faculté des Sciences, Université Mohamed Premier, Oujda; (^e) Faculté des sciences, Université Mohammed V, Rabat; (^f) Institute of Applied Physics, Mohammed VI Polytechnic University, Ben Guerir; Morocco.
- ³⁶CERN, Geneva; Switzerland.
- ³⁷Affiliated with an institute covered by a cooperation agreement with CERN.
- ³⁸Affiliated with an international laboratory covered by a cooperation agreement with CERN.
- ³⁹Enrico Fermi Institute, University of Chicago, Chicago IL; United States of America.
- ⁴⁰LPC, Université Clermont Auvergne, CNRS/IN2P3, Clermont-Ferrand; France.
- ⁴¹Nevis Laboratory, Columbia University, Irvington NY; United States of America.
- ⁴²Niels Bohr Institute, University of Copenhagen, Copenhagen; Denmark.
- ⁴³(^a) Dipartimento di Fisica, Università della Calabria, Rende; (^b) INFN Gruppo Collegato di Cosenza, Laboratori Nazionali di Frascati; Italy.
- ⁴⁴Physics Department, Southern Methodist University, Dallas TX; United States of America.

- ⁴⁵Physics Department, University of Texas at Dallas, Richardson TX; United States of America.
- ⁴⁶National Centre for Scientific Research "Demokritos", Agia Paraskevi; Greece.
- ⁴⁷(^a) Department of Physics, Stockholm University; (^b) Oskar Klein Centre, Stockholm; Sweden.
- ⁴⁸Deutsches Elektronen-Synchrotron DESY, Hamburg and Zeuthen; Germany.
- ⁴⁹Fakultät Physik, Technische Universität Dortmund, Dortmund; Germany.
- ⁵⁰Institut für Kern- und Teilchenphysik, Technische Universität Dresden, Dresden; Germany.
- ⁵¹Department of Physics, Duke University, Durham NC; United States of America.
- ⁵²SUPA - School of Physics and Astronomy, University of Edinburgh, Edinburgh; United Kingdom.
- ⁵³INFN e Laboratori Nazionali di Frascati, Frascati; Italy.
- ⁵⁴Physikalisches Institut, Albert-Ludwigs-Universität Freiburg, Freiburg; Germany.
- ⁵⁵II. Physikalisches Institut, Georg-August-Universität Göttingen, Göttingen; Germany.
- ⁵⁶Département de Physique Nucléaire et Corpusculaire, Université de Genève, Genève; Switzerland.
- ⁵⁷(^a) Dipartimento di Fisica, Università di Genova, Genova; (^b) INFN Sezione di Genova; Italy.
- ⁵⁸II. Physikalisches Institut, Justus-Liebig-Universität Giessen, Giessen; Germany.
- ⁵⁹SUPA - School of Physics and Astronomy, University of Glasgow, Glasgow; United Kingdom.
- ⁶⁰LPSC, Université Grenoble Alpes, CNRS/IN2P3, Grenoble INP, Grenoble; France.
- ⁶¹Laboratory for Particle Physics and Cosmology, Harvard University, Cambridge MA; United States of America.
- ⁶²(^a) Department of Modern Physics and State Key Laboratory of Particle Detection and Electronics, University of Science and Technology of China, Hefei; (^b) Institute of Frontier and Interdisciplinary Science and Key Laboratory of Particle Physics and Particle Irradiation (MOE), Shandong University, Qingdao; (^c) School of Physics and Astronomy, Shanghai Jiao Tong University, Key Laboratory for Particle Astrophysics and Cosmology (MOE), SKLPPC, Shanghai; (^d) Tsung-Dao Lee Institute, Shanghai; (^e) School of Physics and Microelectronics, Zhengzhou University; China.
- ⁶³(^a) Kirchhoff-Institut für Physik, Ruprecht-Karls-Universität Heidelberg, Heidelberg; (^b) Physikalisches Institut, Ruprecht-Karls-Universität Heidelberg, Heidelberg; Germany.
- ⁶⁴(^a) Department of Physics, Chinese University of Hong Kong, Shatin, N.T., Hong Kong; (^b) Department of Physics, University of Hong Kong, Hong Kong; (^c) Department of Physics and Institute for Advanced Study, Hong Kong University of Science and Technology, Clear Water Bay, Kowloon, Hong Kong; China.
- ⁶⁵Department of Physics, National Tsing Hua University, Hsinchu; Taiwan.
- ⁶⁶IJCLab, Université Paris-Saclay, CNRS/IN2P3, 91405, Orsay; France.
- ⁶⁷Centro Nacional de Microelectrónica (IMB-CNM-CSIC), Barcelona; Spain.
- ⁶⁸Department of Physics, Indiana University, Bloomington IN; United States of America.
- ⁶⁹(^a) INFN Gruppo Collegato di Udine, Sezione di Trieste, Udine; (^b) ICTP, Trieste; (^c) Dipartimento Politecnico di Ingegneria e Architettura, Università di Udine, Udine; Italy.
- ⁷⁰(^a) INFN Sezione di Lecce; (^b) Dipartimento di Matematica e Fisica, Università del Salento, Lecce; Italy.
- ⁷¹(^a) INFN Sezione di Milano; (^b) Dipartimento di Fisica, Università di Milano, Milano; Italy.
- ⁷²(^a) INFN Sezione di Napoli; (^b) Dipartimento di Fisica, Università di Napoli, Napoli; Italy.
- ⁷³(^a) INFN Sezione di Pavia; (^b) Dipartimento di Fisica, Università di Pavia, Pavia; Italy.
- ⁷⁴(^a) INFN Sezione di Pisa; (^b) Dipartimento di Fisica E. Fermi, Università di Pisa, Pisa; Italy.
- ⁷⁵(^a) INFN Sezione di Roma; (^b) Dipartimento di Fisica, Sapienza Università di Roma, Roma; Italy.
- ⁷⁶(^a) INFN Sezione di Roma Tor Vergata; (^b) Dipartimento di Fisica, Università di Roma Tor Vergata, Roma; Italy.
- ⁷⁷(^a) INFN Sezione di Roma Tre; (^b) Dipartimento di Matematica e Fisica, Università Roma Tre, Roma; Italy.
- ⁷⁸(^a) INFN-TIFPA; (^b) Università degli Studi di Trento, Trento; Italy.
- ⁷⁹Universität Innsbruck, Department of Astro and Particle Physics, Innsbruck; Austria.

- ⁸⁰University of Iowa, Iowa City IA; United States of America.
- ⁸¹Department of Physics and Astronomy, Iowa State University, Ames IA; United States of America.
- ⁸²Istinye University, Sariyer, Istanbul; Türkiye.
- ⁸³(^a)Departamento de Engenharia Elétrica, Universidade Federal de Juiz de Fora (UFJF), Juiz de Fora; (^b)Universidade Federal do Rio De Janeiro COPPE/EE/IF, Rio de Janeiro; (^c)Instituto de Física, Universidade de São Paulo, São Paulo; (^d)Rio de Janeiro State University, Rio de Janeiro; (^e)Federal University of Bahia, Bahia; Brazil.
- ⁸⁴KEK, High Energy Accelerator Research Organization, Tsukuba; Japan.
- ⁸⁵Graduate School of Science, Kobe University, Kobe; Japan.
- ⁸⁶(^a)AGH University of Krakow, Faculty of Physics and Applied Computer Science, Krakow; (^b)Marian Smoluchowski Institute of Physics, Jagiellonian University, Krakow; Poland.
- ⁸⁷Institute of Nuclear Physics Polish Academy of Sciences, Krakow; Poland.
- ⁸⁸Faculty of Science, Kyoto University, Kyoto; Japan.
- ⁸⁹Research Center for Advanced Particle Physics and Department of Physics, Kyushu University, Fukuoka ; Japan.
- ⁹⁰L2IT, Université de Toulouse, CNRS/IN2P3, UPS, Toulouse; France.
- ⁹¹Instituto de Física La Plata, Universidad Nacional de La Plata and CONICET, La Plata; Argentina.
- ⁹²Physics Department, Lancaster University, Lancaster; United Kingdom.
- ⁹³Oliver Lodge Laboratory, University of Liverpool, Liverpool; United Kingdom.
- ⁹⁴Department of Experimental Particle Physics, Jožef Stefan Institute and Department of Physics, University of Ljubljana, Ljubljana; Slovenia.
- ⁹⁵School of Physics and Astronomy, Queen Mary University of London, London; United Kingdom.
- ⁹⁶Department of Physics, Royal Holloway University of London, Egham; United Kingdom.
- ⁹⁷Department of Physics and Astronomy, University College London, London; United Kingdom.
- ⁹⁸Louisiana Tech University, Ruston LA; United States of America.
- ⁹⁹Fysiska institutionen, Lunds universitet, Lund; Sweden.
- ¹⁰⁰Departamento de Física Teórica C-15 and CIAFF, Universidad Autónoma de Madrid, Madrid; Spain.
- ¹⁰¹Institut für Physik, Universität Mainz, Mainz; Germany.
- ¹⁰²School of Physics and Astronomy, University of Manchester, Manchester; United Kingdom.
- ¹⁰³CPPM, Aix-Marseille Université, CNRS/IN2P3, Marseille; France.
- ¹⁰⁴Department of Physics, University of Massachusetts, Amherst MA; United States of America.
- ¹⁰⁵Department of Physics, McGill University, Montreal QC; Canada.
- ¹⁰⁶School of Physics, University of Melbourne, Victoria; Australia.
- ¹⁰⁷Department of Physics, University of Michigan, Ann Arbor MI; United States of America.
- ¹⁰⁸Department of Physics and Astronomy, Michigan State University, East Lansing MI; United States of America.
- ¹⁰⁹Group of Particle Physics, University of Montreal, Montreal QC; Canada.
- ¹¹⁰Fakultät für Physik, Ludwig-Maximilians-Universität München, München; Germany.
- ¹¹¹Max-Planck-Institut für Physik (Werner-Heisenberg-Institut), München; Germany.
- ¹¹²Graduate School of Science and Kobayashi-Maskawa Institute, Nagoya University, Nagoya; Japan.
- ¹¹³Department of Physics and Astronomy, University of New Mexico, Albuquerque NM; United States of America.
- ¹¹⁴Institute for Mathematics, Astrophysics and Particle Physics, Radboud University/Nikhef, Nijmegen; Netherlands.
- ¹¹⁵Nikhef National Institute for Subatomic Physics and University of Amsterdam, Amsterdam; Netherlands.
- ¹¹⁶Department of Physics, Northern Illinois University, DeKalb IL; United States of America.

- ¹¹⁷(^a)New York University Abu Dhabi, Abu Dhabi;(^b)United Arab Emirates University, Al Ain; United Arab Emirates.
- ¹¹⁸Department of Physics, New York University, New York NY; United States of America.
- ¹¹⁹Ochanomizu University, Otsuka, Bunkyo-ku, Tokyo; Japan.
- ¹²⁰Ohio State University, Columbus OH; United States of America.
- ¹²¹Homer L. Dodge Department of Physics and Astronomy, University of Oklahoma, Norman OK; United States of America.
- ¹²²Department of Physics, Oklahoma State University, Stillwater OK; United States of America.
- ¹²³Palacký University, Joint Laboratory of Optics, Olomouc; Czech Republic.
- ¹²⁴Institute for Fundamental Science, University of Oregon, Eugene, OR; United States of America.
- ¹²⁵Graduate School of Science, Osaka University, Osaka; Japan.
- ¹²⁶Department of Physics, University of Oslo, Oslo; Norway.
- ¹²⁷Department of Physics, Oxford University, Oxford; United Kingdom.
- ¹²⁸LPNHE, Sorbonne Université, Université Paris Cité, CNRS/IN2P3, Paris; France.
- ¹²⁹Department of Physics, University of Pennsylvania, Philadelphia PA; United States of America.
- ¹³⁰Department of Physics and Astronomy, University of Pittsburgh, Pittsburgh PA; United States of America.
- ¹³¹(^a)Laboratório de Instrumentação e Física Experimental de Partículas - LIP, Lisboa;(^b)Departamento de Física, Faculdade de Ciências, Universidade de Lisboa, Lisboa;(^c)Departamento de Física, Universidade de Coimbra, Coimbra;(^d)Centro de Física Nuclear da Universidade de Lisboa, Lisboa;(^e)Departamento de Física, Universidade do Minho, Braga;(^f)Departamento de Física Teórica y del Cosmos, Universidad de Granada, Granada (Spain);(^g)Departamento de Física, Instituto Superior Técnico, Universidade de Lisboa, Lisboa; Portugal.
- ¹³²Institute of Physics of the Czech Academy of Sciences, Prague; Czech Republic.
- ¹³³Czech Technical University in Prague, Prague; Czech Republic.
- ¹³⁴Charles University, Faculty of Mathematics and Physics, Prague; Czech Republic.
- ¹³⁵Particle Physics Department, Rutherford Appleton Laboratory, Didcot; United Kingdom.
- ¹³⁶IRFU, CEA, Université Paris-Saclay, Gif-sur-Yvette; France.
- ¹³⁷Santa Cruz Institute for Particle Physics, University of California Santa Cruz, Santa Cruz CA; United States of America.
- ¹³⁸(^a)Departamento de Física, Pontificia Universidad Católica de Chile, Santiago;(^b)Millennium Institute for Subatomic physics at high energy frontier (SAPHIR), Santiago;(^c)Instituto de Investigación Multidisciplinario en Ciencia y Tecnología, y Departamento de Física, Universidad de La Serena;(^d)Universidad Andres Bello, Department of Physics, Santiago;(^e)Instituto de Alta Investigación, Universidad de Tarapacá, Arica;(^f)Departamento de Física, Universidad Técnica Federico Santa María, Valparaíso; Chile.
- ¹³⁹Department of Physics, University of Washington, Seattle WA; United States of America.
- ¹⁴⁰Department of Physics and Astronomy, University of Sheffield, Sheffield; United Kingdom.
- ¹⁴¹Department of Physics, Shinshu University, Nagano; Japan.
- ¹⁴²Department Physik, Universität Siegen, Siegen; Germany.
- ¹⁴³Department of Physics, Simon Fraser University, Burnaby BC; Canada.
- ¹⁴⁴SLAC National Accelerator Laboratory, Stanford CA; United States of America.
- ¹⁴⁵Department of Physics, Royal Institute of Technology, Stockholm; Sweden.
- ¹⁴⁶Departments of Physics and Astronomy, Stony Brook University, Stony Brook NY; United States of America.
- ¹⁴⁷Department of Physics and Astronomy, University of Sussex, Brighton; United Kingdom.
- ¹⁴⁸School of Physics, University of Sydney, Sydney; Australia.

- ¹⁴⁹Institute of Physics, Academia Sinica, Taipei; Taiwan.
- ¹⁵⁰(^a)E. Andronikashvili Institute of Physics, Iv. Javakhishvili Tbilisi State University, Tbilisi; (^b)High Energy Physics Institute, Tbilisi State University, Tbilisi; (^c)University of Georgia, Tbilisi; Georgia.
- ¹⁵¹Department of Physics, Technion, Israel Institute of Technology, Haifa; Israel.
- ¹⁵²Raymond and Beverly Sackler School of Physics and Astronomy, Tel Aviv University, Tel Aviv; Israel.
- ¹⁵³Department of Physics, Aristotle University of Thessaloniki, Thessaloniki; Greece.
- ¹⁵⁴International Center for Elementary Particle Physics and Department of Physics, University of Tokyo, Tokyo; Japan.
- ¹⁵⁵Department of Physics, Tokyo Institute of Technology, Tokyo; Japan.
- ¹⁵⁶Department of Physics, University of Toronto, Toronto ON; Canada.
- ¹⁵⁷(^a)TRIUMF, Vancouver BC; (^b)Department of Physics and Astronomy, York University, Toronto ON; Canada.
- ¹⁵⁸Division of Physics and Tomonaga Center for the History of the Universe, Faculty of Pure and Applied Sciences, University of Tsukuba, Tsukuba; Japan.
- ¹⁵⁹Department of Physics and Astronomy, Tufts University, Medford MA; United States of America.
- ¹⁶⁰Department of Physics and Astronomy, University of California Irvine, Irvine CA; United States of America.
- ¹⁶¹University of Sharjah, Sharjah; United Arab Emirates.
- ¹⁶²Department of Physics and Astronomy, University of Uppsala, Uppsala; Sweden.
- ¹⁶³Department of Physics, University of Illinois, Urbana IL; United States of America.
- ¹⁶⁴Instituto de Física Corpuscular (IFIC), Centro Mixto Universidad de Valencia - CSIC, Valencia; Spain.
- ¹⁶⁵Department of Physics, University of British Columbia, Vancouver BC; Canada.
- ¹⁶⁶Department of Physics and Astronomy, University of Victoria, Victoria BC; Canada.
- ¹⁶⁷Fakultät für Physik und Astronomie, Julius-Maximilians-Universität Würzburg, Würzburg; Germany.
- ¹⁶⁸Department of Physics, University of Warwick, Coventry; United Kingdom.
- ¹⁶⁹Waseda University, Tokyo; Japan.
- ¹⁷⁰Department of Particle Physics and Astrophysics, Weizmann Institute of Science, Rehovot; Israel.
- ¹⁷¹Department of Physics, University of Wisconsin, Madison WI; United States of America.
- ¹⁷²Fakultät für Mathematik und Naturwissenschaften, Fachgruppe Physik, Bergische Universität Wuppertal, Wuppertal; Germany.
- ¹⁷³Department of Physics, Yale University, New Haven CT; United States of America.
- ^a Also Affiliated with an institute covered by a cooperation agreement with CERN.
- ^b Also at An-Najah National University, Nablus; Palestine.
- ^c Also at Borough of Manhattan Community College, City University of New York, New York NY; United States of America.
- ^d Also at Center for High Energy Physics, Peking University; China.
- ^e Also at Center for Interdisciplinary Research and Innovation (CIRI-AUTH), Thessaloniki; Greece.
- ^f Also at Centro Studi e Ricerche Enrico Fermi; Italy.
- ^g Also at CERN, Geneva; Switzerland.
- ^h Also at Département de Physique Nucléaire et Corpusculaire, Université de Genève, Genève; Switzerland.
- ⁱ Also at Departament de Física de la Universitat Autònoma de Barcelona, Barcelona; Spain.
- ^j Also at Department of Financial and Management Engineering, University of the Aegean, Chios; Greece.
- ^k Also at Department of Physics, California State University, Sacramento; United States of America.
- ^l Also at Department of Physics, King's College London, London; United Kingdom.
- ^m Also at Department of Physics, Stanford University, Stanford CA; United States of America.
- ⁿ Also at Department of Physics, Stellenbosch University; South Africa.

- ^o Also at Department of Physics, University of Fribourg, Fribourg; Switzerland.
- ^p Also at Department of Physics, University of Thessaly; Greece.
- ^q Also at Department of Physics, Westmont College, Santa Barbara; United States of America.
- ^r Also at Hellenic Open University, Patras; Greece.
- ^s Also at Institutio Catalana de Recerca i Estudis Avancats, ICREA, Barcelona; Spain.
- ^t Also at Institut für Experimentalphysik, Universität Hamburg, Hamburg; Germany.
- ^u Also at Institute for Nuclear Research and Nuclear Energy (INRNE) of the Bulgarian Academy of Sciences, Sofia; Bulgaria.
- ^v Also at Institute of Applied Physics, Mohammed VI Polytechnic University, Ben Guerir; Morocco.
- ^w Also at Institute of Particle Physics (IPP); Canada.
- ^x Also at Institute of Physics and Technology, Ulaanbaatar; Mongolia.
- ^y Also at Institute of Physics, Azerbaijan Academy of Sciences, Baku; Azerbaijan.
- ^z Also at Institute of Theoretical Physics, Ilia State University, Tbilisi; Georgia.
- ^{aa} Also at Lawrence Livermore National Laboratory, Livermore; United States of America.
- ^{ab} Also at National Institute of Physics, University of the Philippines Diliman (Philippines); Philippines.
- ^{ac} Also at Technical University of Munich, Munich; Germany.
- ^{ad} Also at The Collaborative Innovation Center of Quantum Matter (CICQM), Beijing; China.
- ^{ae} Also at TRIUMF, Vancouver BC; Canada.
- ^{af} Also at Università di Napoli Parthenope, Napoli; Italy.
- ^{ag} Also at University of Colorado Boulder, Department of Physics, Colorado; United States of America.
- ^{ah} Also at Washington College, Chestertown, MD; United States of America.
- ^{ai} Also at Yeditepe University, Physics Department, Istanbul; Türkiye.
- * Deceased